SANDIA REPORT
SAND2019-1915
Unlimited Release
Printed February 2019

Deep Borehole Disposal Safety Case

Geoff Freeze, Emily Stein, Patrick V. Brady, Carlos Lopez, David Sassani
Sandia National Laboratories

Karl Travis, Fergus Gibb
University of Sheffield

Prepared by
Sandia National Laboratories
Albuquerque, New Mexico 87185 and Livermore, California 94550

Sandia National Laboratories is a multi-mission laboratory managed and operated by National Technology and Engineering Solutions of Sandia, LLC., a wholly owned subsidiary of Honeywell International, Inc., for the U.S. Department of Energy's National Nuclear Security Administration under contract DE-NA-0003525.

Sandia National Laboratories

Issued by Sandia National Laboratories, operated for the United States Department of Energy by Sandia Corporation.

Available to DOE and DOE contractors from
U.S. Department of Energy
Office of Scientific and Technical Information
P.O. Box 62
Oak Ridge, TN 37831

Telephone: (865) 576-8401
Facsimile: (865) 576-5728
E-Mail: reports@osti.gov
Online ordering: http://www.osti.gov/scitech

Available to the public from
U.S. Department of Commerce
National Technical Information Service
5301 Shawnee Rd
Alexandria, VA 22312

Telephone: (800) 553-6847
Facsimile: (703) 605-6900
E-Mail: orders@ntis.gov
Online order: http://www.ntis.gov/search

SAND2019-1915
Unlimited Release
Printed February 2019

Deep Borehole Disposal Safety Case

Geoff Freeze, Emily Stein, Patrick V. Brady, Carlos Lopez, David Sassani[1]
Karl Travis, Fergus Gibb[2]

[1]Sandia National Laboratories,
P.O. Box 5800, Albuquerque, New Mexico 87185-0747

[2]University of Sheffield, Department of Materials Science and Engineering,
Sir Robert Hadfield Building, Sheffield S1 3JD, U.K.

Abstract

This report describes the current status of the safety case for the deep borehole disposal (DBD) concept. It builds on the safety case presented in Freeze et al. (2016), presenting new information and identifying additional information needs for specific safety case elements. At this preliminary phase of development, the DBD safety case focuses on the generic feasibility of the DBD concept. It is based on potential system designs, waste forms, engineering, and geologic conditions; however, no specific site or regulatory framework exists.

Updated information is provided for the following safety case elements:

- pre-closure basis and safety analysis,
- post-closure basis and performance assessment, and
- confidence enhancement.

This research was performed as part of the deep borehole field test (DBFT). Based on revised U.S. Department of Energy (DOE) priorities in mid-2017, the DBFT and other research related to a DBD option was discontinued; ongoing work and documentation were closed out by the end of fiscal year (FY) 2017. This report was initiated as part of the DBFT and documented as an incomplete draft at the end of FY 2017. The report was finalized by Sandia National Laboratories in FY2018 without DOE funding, subsequent to the termination of the DBFT, and published in FY2019.

ACKNOWLEDGMENTS

The authors would like to thank Mark Rigali for his technical review of the document and Laura Connolly for her help with document production and formatting.

CONTENTS

FIGURES

TABLES

NOMENCLATURE

2D	two-dimensional
3D	three-dimensional
BSC	Bechtel-SAIC Company
CB	Characterization Borehole
CFC	chlorofluorocarbon
CFR	Code of Federal Regulations
DBD	deep borehole disposal
DBFT	Deep Borehole Field Test
DFN	discrete fracture network
DOE	U.S. Department of Energy
DOE-NE	DOE Office of Nuclear Energy
DRZ	disturbed rock zone
ECPM	equivalent continuous porous medium
EPA	U.S. Environmental Protection Agency
EZ	emplacement zone
FEPs	features, events, and processes
FTB	Field Test Borehole
FY	fiscal year
GDSA	geologic disposal safety assessment
HLW	high-level radioactive waste
IAEA	International Atomic Energy Agency
MLD	master logic diagram
NEA	Nuclear Energy Agency
NWPA	Nuclear Waste Policy Act
NRC	Nuclear Regulatory Commission
NWTRB	U.S. Nuclear Waste Technical Review Board
PA	performance assessment
PCSA	pre-closure safety analysis
PFD	process flow diagram
PRA	probabilistic risk assessment
R&D	research and development

RD&D	research, development, and demonstration
RFP	Request for Proposal
SFWD	DOE-NE Spent Fuel and Waste Disposition Program
SFWST	DOE-NE Office of Spent Fuel and Waste Science and Technology
SNF	spent nuclear fuel
SNL	Sandia National Laboratories
SSCs	structures, systems, and components
SSMs	sealing and support matrices
SZ	seal zone
TDS	total dissolved solids
THCM	thermal, hydrologic, chemical, and mechanical
UBZ	upper borehole zone
UFD	DOE-NE Office of Used Nuclear Fuel Disposition Research and Development
WESF	Waste Encapsulation and Storage Facility
WIPP	Waste Isolation Pilot Plant
WF	waste form
WP	waste package

1 INTRODUCTION

This report supports the development of a preliminary safety case for the deep borehole disposal (DBD) concept. A safety case is an integrated collection of qualitative and quantitative arguments, evidence, and analyses that substantiate the safety, and the level of confidence in the safety, of a geologic repository (Freeze et al. 2012, Section 1.1). At this early phase of development, the DBD safety case focuses on the generic feasibility of the DBD concept. It is based on potential system designs, waste forms, engineering, and geologic conditions; however, no specific site or regulatory framework exists.

Prior documentation (Freeze et al. 2016) outlines a preliminary, generic DBD safety case. The elements of a safety case were identified and existing technical information was synthesized to identify open issues and information gaps relevant to disposal of radioactive waste in deep boreholes. This report provides additional information and analyses that address some of the open issues and further augments the DBD safety case. Additional information is provided for the following safety case elements:

- pre-closure basis and safety analysis,
- post-closure basis and performance assessment, and
- confidence enhancement.

An overview of DBD is presented in Section 1.1. An overview of the elements of a safety case is presented in Section 1.2. Regulatory considerations are summarized in Section 1.3. The DBD reference design is summarized in Section 1.4. The new information and analyses are summarized in Section 1.5.

The remainder of the report, Sections 2 through 5, presents the details of the new information and analyses and discusses how each addresses specific elements of the DBD safety case.

1.1 Deep Borehole Disposal Overview

DBD for the geologic isolation of spent nuclear fuel (SNF) and high-level radioactive waste (HLW) has been considered for many years, beginning with evaluations of nuclear waste disposal options by the National Academy of Sciences in 1957 (NAS 1957). Efforts by the United States and the international community over the last half-century toward disposal of SNF and HLW (collectively referred to as high-activity waste[1]) have primarily focused on mined geological repositories. Nonetheless, evaluations of DBD have periodically continued in several countries (Freeze et al. 2016, Table 1-1).

[1] The Nuclear Waste Policy Act (NWPA) defines "spent nuclear fuel" as "fuel that has been withdrawn from a nuclear reactor following irradiation, the constituent elements of which have not been separated by reprocessing" (NWPA 1983, Sec. 2(23)) and defines "high-level radioactive waste" as "(A) the highly radioactive material resulting from the reprocessing of spent nuclear fuel, including liquid waste produced directly in reprocessing and any solid material derived from such liquid waste that contains fission products in sufficient concentrations; and (B) other highly radioactive material that the Commission, consistent with existing law, determines by rule requires permanent isolation" (NWPA 1983, Sec. 2(12)).

In the U.S., the Department of Energy Office of Nuclear Energy (DOE-NE) investigated DBD between 2014 and 2017 as one alternative for the disposal of high-activity waste, along with research and development (R&D) for mined repositories in salt, granite, and clay/shale, as part of the Spent Fuel and Waste Disposition (SFWD) Program, Office of Spent Fuel and Waste Science and Technology (SFWST). Prior to 2016, SFWST was known as the Office of Used Nuclear Fuel Disposition (UFD) R&D.

The DBD concept, illustrated in Figure 1-1, consists of drilling a large-diameter borehole into crystalline basement rock to a depth of about 5,000 m, placing waste packages in the lower, waste emplacement zone portion of the borehole, and sealing and plugging the upper portion of the borehole with a combination of bentonite, cement plugs, and sand/crushed rock backfill. As shown in Figure 1-1, waste in a DBD system is several times deeper than typical mined repositories (e.g., Onkalo and Waste Isolation Pilot Plant (WIPP)) and is well below the typical maximum depth of fresh groundwater resources, indicated by the dashed blue line.

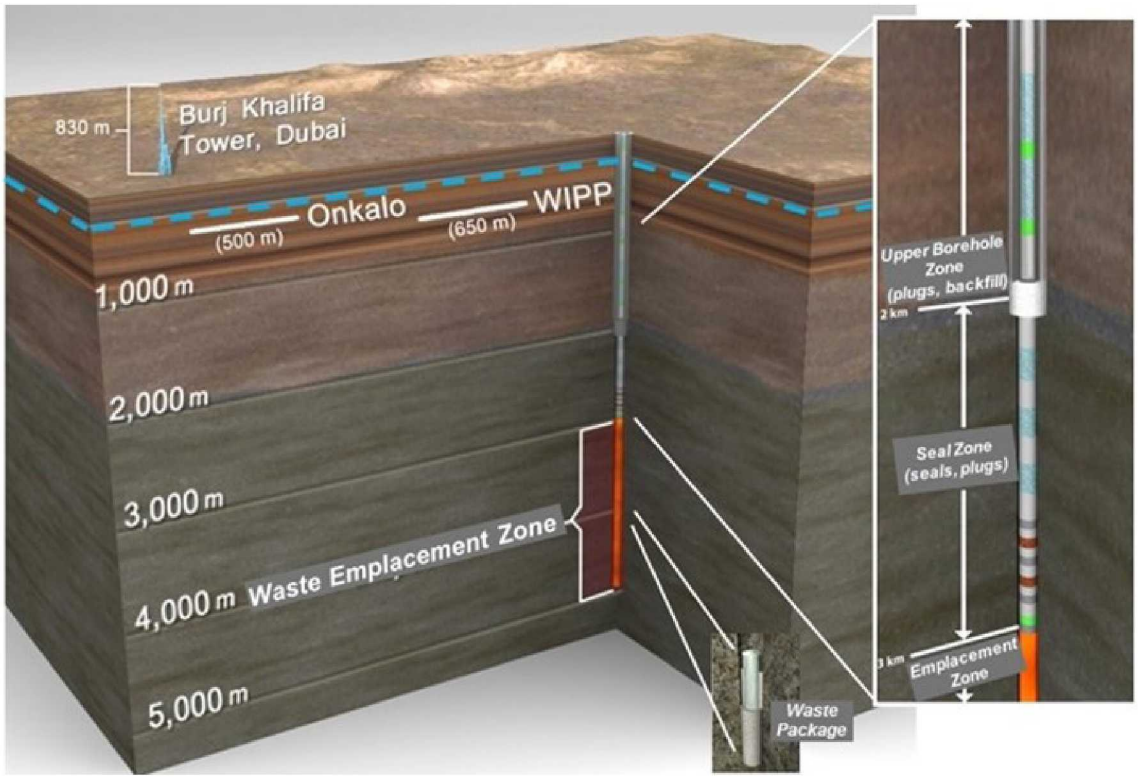

Figure 1-1. Generalized Schematic of the Deep Borehole Disposal Concept

Several design alternatives exist that satisfy the basic DBD concept, depending on a variety of factors, most notably the size and characteristics of the waste form and packaging. Initial DBD studies (e.g., Brady et al. 2009; Arnold et al. 2011; Arnold et al. 2012) proposed waste packages that contained commercial SNF. Specifically, the waste package was designed to encapsulate a single pressurized water reactor assembly, requiring a borehole with a bottom-hole diameter of approximately 0.43 m (17 in). In 2014, DOE recommended "a focused RD&D program addressing

technologies relevant to deep borehole disposal of smaller DOE-managed waste forms" (DOE 2014). For example, the smallest DOE-managed waste forms, cesium (Cs) and strontium (Sr) capsules, are all less than 0.09 m (3.5 in) in diameter (DOE 2014), and could be emplaced in a borehole with a bottom-hole diameter on the order of 0.22 m (8.5 in).

Factors suggesting that the DBD concept is viable and safe have been summarized previously in Brady et al. (2009), Arnold et al. (2011), SNL (2016a), and Freeze et al. (2016). Safety of the concept relies primarily on the natural barriers (the great depth of burial and the isolation provided by the deep natural geological environment), and, to a lesser extent, on the engineered barriers (the durability of the waste packages and waste forms and the integrity of the borehole seals). In contrast, mined geological repositories, with the possible exception of those located in extensive salt or argillaceous formations, rely on engineered barriers such as waste packages and/or buffer/backfill material to a greater degree.

Safe borehole disposal is possible at shallower depths, over a range of borehole diameters, depending on the target geologies and waste forms. Viable options range from low-level waste and sealed sources in "shallow" boreholes (< hundreds of meters deep) to intermediate-level radioactive waste and HLW in "deeper" boreholes (< ~2,000 m). For these shallower borehole concepts, demonstration of post-closure safety relies on a combination of engineered and natural system performance, much like a mined repository; and the reliance on the engineered seals may be greater. The remainder of this report focuses on the "very deep" DBD concept, with waste emplacement at a depth of about 5,000 m.

DOE-NE initiated R&D for a Deep Borehole Field Test (DBFT) in 2014. The overall goal of the DBFT was to demonstrate and evaluate technologies necessary for determining the safety and feasibility of the DBD concept, but without the use or disposal of actual radioactive waste. The overall goal of the DBFT was supported by the following objectives:

- Demonstration of drilling technology and borehole construction to 5,000 m depth in crystalline basement rock with sufficient diameter for cost-effective waste disposal;
- Evaluation of downhole scientific analyses to characterize the thermal-hydrologic-chemical-mechanical (THCM) conditions at a representative location that control waste stability and containment;
- Evaluation of package and seal materials at representative temperature, pressure, salinity, and geochemical conditions;
- Development and testing of engineering methods for test package loading, shielded surface operations, and test package emplacement and retrieval;
- Development and testing of sealing designs and seal emplacement methods; and
- Demonstration of pre-closure and post-closure safety.

The plan for the DBFT (SNL 2014a; SNL 2016a) included siting and drilling two 5,000 m deep boreholes into crystalline basement rock in a geologically stable continental location:

- An initial Characterization Borehole (CB), with approximately an 8.5-in (0.22 m) bottom-hole diameter, to facilitate examination of downhole scientific testing methods. The objective was to identify (a) the critical downhole measurements needed to determine if conditions favorable to long-term isolation of high-activity waste exist at depth and (b) which testing methods were feasible under conditions encountered in a deep borehole.
- A subsequent Field Test Borehole (FTB), with approximately a 17-in (0.43 m) bottom-hole diameter, to facilitate proof-of-concept of engineering activities using surrogate test packages. The objective was to evaluate the feasibility of package emplacement operations by determining performance envelopes for drilling, package handling, and package emplacement and retrieval. In addition, laboratory testing of borehole sealing materials and designs was planned.

Two Requests for Proposal (RFPs) were initiated by DOE-NE to identify potential sites for the DBFT. In response to the first RFP (DOE 2015), a contract was awarded in January 2016, to a team led by Battelle Memorial Institute which included a proposed test site in Pierce County, North Dakota. After efforts to acquire both the initial test site in North Dakota and an alternative proposed site in Spink County, South Dakota were unsuccessful, activities were suspended (Gunter and Freeze 2017).

The experiences in Pierce County, North Dakota and Spink County, South Dakota highlighted the importance of public engagement and support for the DBFT, and that relevant levels of government and other public stakeholders should be involved from the beginning (Gunter and Freeze 2017). Using these lessons learned, DOE-NE issued a new RFP (DOE 2016) which emphasized local, state, and tribal (if applicable) government engagement, as well as public and other stakeholder involvement ahead of proposal submittals and throughout the contract execution phases. The new RFP also allowed for multiple initial awards and multiple phases of contract execution, during which down-selects could be made based on contractor team performance and success with local community acceptance, and to ultimately have one contractor team actually execute the DBFT and drill the Characterization Borehole. In response to the second RFP, four contract awards were announced in December 2016: AECOM for a proposed site in Pecos County, Texas; ENERCON for a proposed site in Quay County, New Mexico; RESPEC for a proposed site in Haakon County, South Dakota; and TerranearPMC for a proposed site in Otero County, New Mexico (Gunter and Freeze 2017).

In May 2017, it was announced that "Due to changes in budget priorities, the Department of Energy does not intend to continue supporting the Deep Borehole Field Test (DBFT) project and has initiated a process to effectively end the project immediately." (DOE 2017)

1.2 Safety Case Overview

The formal concept of a safety case for the long-term disposal of high-activity waste in an engineered facility located in a deep geologic formation was first introduced by the Nuclear Energy Agency (NEA) (NEA 1999). Initial discussion and documentation on the topic continued in NEA (2002), NEA (2004), and IAEA (2006). More recently, there have been a number of international

symposia, conferences, working groups, and summary papers devoted to understanding, developing, and/or summarizing the nature, purpose, context, and elements of safety cases (e.g., NEA 2008; NEA 2009; IAEA 2011; IAEA 2012; NEA 2012; and NEA 2013). In these recent summary and overview reports, it is observed that there is notable convergence in the understanding and development of safety case documents published by national and international organizations. In parallel, DOE-NE has published safety case overviews relevant to geologic disposal in the U.S. (Freeze et al. 2013) and specific to the DBD concept (Arnold et al. 2013, Appendix A; Freeze et al. 2013; Freeze et al. 2016). The following excerpt from NEA (2012, Section 3.1) provides a definition of a safety case that is current and consistent with the aforementioned documents:

The Safety Case is an integration of arguments and evidence that describe, quantify and substantiate the safety of the geological disposal facility and the associated level of confidence. A central part of the safety case is the safety assessment. There are some differences in the use of the term safety assessment across national programs and over time; the definition used in Freeze et al. (2016) and in this report is:

- *Safety Assessment* – An iterative set of assessments for evaluating the performance of a repository system and its potential impact that aims to provide reasonable assurance that the repository system will achieve sufficient safety and meet the relevant requirements for the protection of humans and the environment over a prolonged period. The role of a safety assessment, in a safety case, is (i) to quantify the repository system performance for all selected situations and (ii) to evaluate the level of confidence (taking into account of the identified uncertainties) in the estimated performance of the system (NEA 2013, Section 5.1). This encompasses all aspects that are relevant for the safety of the development, operation and closure of the disposal facility, including qualitative aspects, non-radiological issues, and organizational and managerial aspects (IAEA 2012, Section 4.41).

The scope of this definition has broadened recently to include not just quantitative analyses, but also a broad range of complementary qualitative evidence and arguments that support the reliability of the quantitative analyses (NEA 2013, Section 1). In this report, the quantitative components of a safety assessment are referred to as "pre-closure safety analysis" and "post-closure performance assessment (PA)," the qualitative component is referred to as "confidence enhancement."

A number of elements contribute to, and must be described in, the safety case. A general set of safety case elements for geologic disposal (including DBD) are shown in Figure 1-2. The development of these safety case elements is described in Freeze et al. (2016, Section 1.2); overviews of the key safety elements are provided in the Freeze et al. (2016, Section 1.2.1).

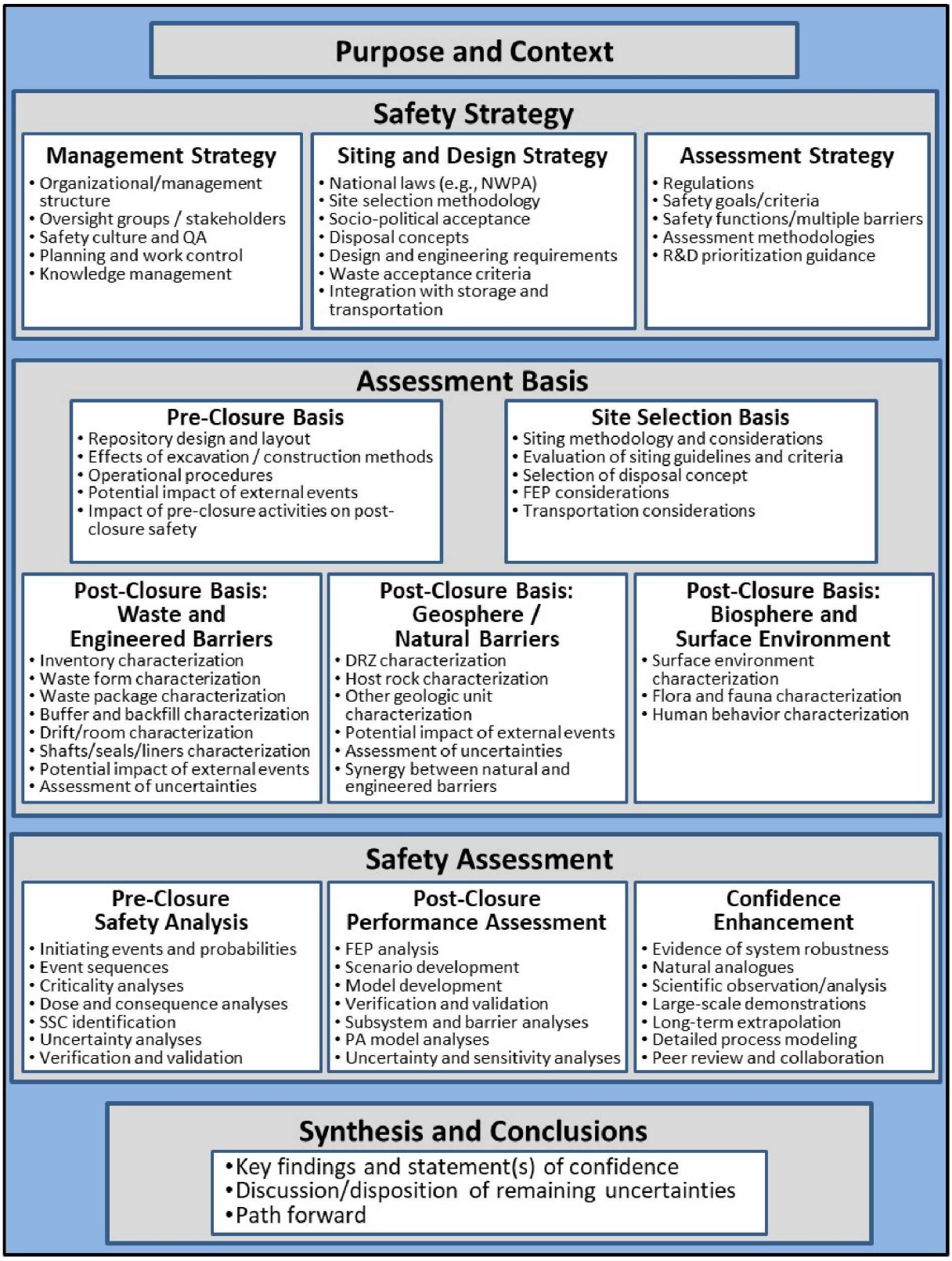

Source: Freeze et al. (2016, Figure 1-2)

Figure 1-2. Key Elements of a Safety Case

1.3 Regulatory Considerations

The safety standards and the implementing regulations governing the management and disposal of radioactive waste in a geologic repository are the fundamental technical requirements that are addressed in a safety case. In the U.S., such standards are promulgated by the U.S. Environmental Protection Agency (EPA) and the U.S. Nuclear Regulatory Commission (NRC). Safety standards and guidance are also available from national programs in other countries and from international organizations (e.g., IAEA 2011).

The current regulatory framework for radioactive waste management in the U.S. focuses on mined geologic repositories and was not intended to be applied to the long-term performance of DBD facilities. Existing general regulations for disposal of high-activity wastes in geologic repositories (10 CFR 60 (NRC) and 40 CFR 191 (EPA)), first promulgated in 1983 and 1985, respectively, remain in effect, and could be applied to disposal of nuclear waste in deep boreholes, as written (EPA 2015). However, these existing regulations would likely be superseded, since they were developed more than 30 years ago and are not consistent with the more recent thinking on regulating geologic disposal concepts that embraces a risk-informed, performance-based approach (NRC 2004), such as that represented in the site-specific regulations for Yucca Mountain (10 CFR 63 (NRC) and 40 CFR 197 (EPA)), first promulgated in 2001 (Arnold et al. 2013, Appendix A).

Nonetheless, it is likely that regulations for a DBD facility would be strongly informed by the current regulations. Therefore, the preliminary safety case framework for DBD is developed based on assumptions about the potential regulatory environment. These assumptions are based on inferences from:

- relevant portions of the existing general standards (10 CFR 60[2] and 40 CFR 191),
- anticipated updates consistent with the risk-informed approach in 10 CFR 63[3] and 40 CFR 197, and
- generic standards that incorporate dose or risk metrics recognized internationally to be important to establishing repository safety (e.g., IAEA 2011; IAEA 2012).

---

[2] 10 CFR 60.2 defines "high-level radioactive waste" as "(1) irradiated reactor fuel, (2) liquid wastes resulting from the operation of the first cycle solvent extraction system, or equivalent, and the concentrated wastes from subsequent extraction cycles, or equivalent, in a facility for reprocessing irradiated reactor fuel, and (3) solids into which such liquid wastes have been converted." This definition is different from the NWPA definition (NWPA 1983, Sec. 2) in that it refers to SNF (part (1) of the 10 CFR 60.2 definition) and HLW (parts (2) and (3) of the 10 CFR 60.2 definition) collectively as high-level radioactive waste.

40 CFR 191.02 defines SNF and HLW separately, and is consistent with the NWPA definition.

[3] 10 CFR 63.2 defines "high-level radioactive waste" as (1) The highly radioactive material resulting from the reprocessing of spent nuclear fuel, including liquid waste produced directly in reprocessing and any solid material derived from such liquid waste that contains fission products in sufficient concentrations; (2) Irradiated reactor fuel; and (3) Other highly radioactive material that the Commission, consistent with existing law, determines by rule requires permanent isolation." This definition is different from the NWPA definition (NWPA 1983, Sec. 2) in that it refers to SNF (part (2) of the 10 CFR 63.2 definition) and HLW (parts (1) and (3) of the 10 CFR 63.2 definition) collectively as high-level radioactive waste.

40 CFR 197.2 defines SNF and HLW separately, and is consistent with the NWPA definition.

Key considerations of the aforementioned regulations that might provide insight to future DBD regulations are summarized in Freeze et al. (2016, Section 2.1).

1.4 Deep Borehole Disposal Reference Case

Normally, a safety case, and associated safety assessment and assessment basis, address a specific site, a well-defined inventory, waste form, and waste package, a specific repository design, specific concept of operations, and an established regulatory environment. However, this level of specificity does not currently exist for the DBD concept or for this preliminary iteration of the DBD safety case. Instead, a DBD reference case for disposal of Cs and Sr capsules (hereafter referred to as the "reference case") in a single borehole is established as a surrogate for site-specific and design-specific information upon which a safety case can be developed. The DBD reference case includes a reference design (disposal concept and surface operations), and information describing the engineered barriers, geosphere and natural barriers, and biosphere.

1.4.1 Disposal Concept

The reference design is based on a disposal concept for DBD of Cs and Sr capsules in crystalline basement. Subsurface features and components of the borehole and host rock, shown in Figure 1-3, include: borehole and casing, waste form (WF), waste package (WP), emplacement zone (EZ) (buffer/backfill/annulus, cement plugs, liner), seal zone (SZ), and upper borehole zone (UBZ). They are described in more detail in Freeze et al. (2016, Section 3.2.2.1) and SNL (2016a, Section 3); a summary is provided below.

The reference disposal concept includes a 5,000-m deep borehole with a bottom-hole (i.e., EZ) diameter of 0.311 m (12.25 in). This design is expected to be achievable in crystalline rocks with currently available commercial drilling technology.

The reference design includes the DOE-managed inventory of 1,335 Cs capsules (containing glass-like CsCl, cooled from a molten pour) and 601 Sr capsules (containing granular, compacted SrF_2 precipitate, chiseled from drying pans) currently stored at the Hanford Waste Encapsulation and Storage Facility (WESF) that are all less than 0.09 m (3.5 in) in diameter (DOE 2014). These capsules contain short-lived ^{90}Sr and ^{137}Cs, and long-lived ^{135}Cs; other radionuclides have decayed away (SNL 2014b).

The waste packages containing the Cs and Sr capsules are placed in the lower EZ portion of the borehole (between 4,466 m and 5,000 m depth). Each carbon steel waste package is assumed to contain 18 Cs or Sr capsules, stacked in 6 layers of 3 capsules (3-packs) each (Figure 1-4). Each waste package would have an outside diameter of 0.219 m (8.625 in) and a total length of 4.76 m, which includes 3.76 m for the 6 layers of capsules, a 0.3-m long fishing neck (to facilitate retrieval during operations), and a 0.7-m-long impact limiter (to minimize damage from drops). With this reference design (other configurations are possible), 108 waste packages would be required to accommodate all of the Cs/Sr capsules (74 for the Cs capsules and 34 for the Sr capsules), and all of the waste packages would fit in a single borehole with an EZ 0.311 m (12.25 in) in diameter and 534 m long (this length includes 10-m long cement plugs above the 40th and 80th waste packages for structural support).

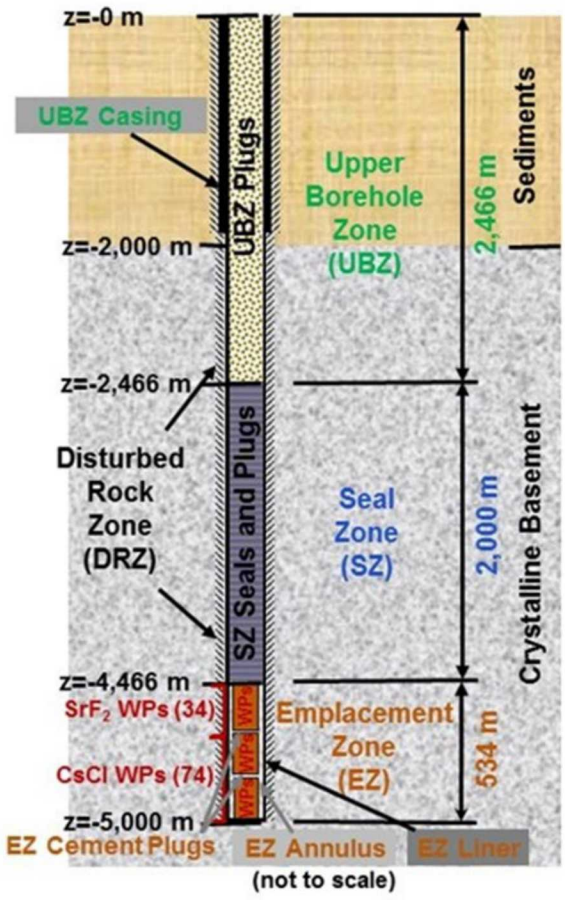

Figure 1-3. Schematic of the Deep Borehole Disposal Concept for Cs/Sr Capsules

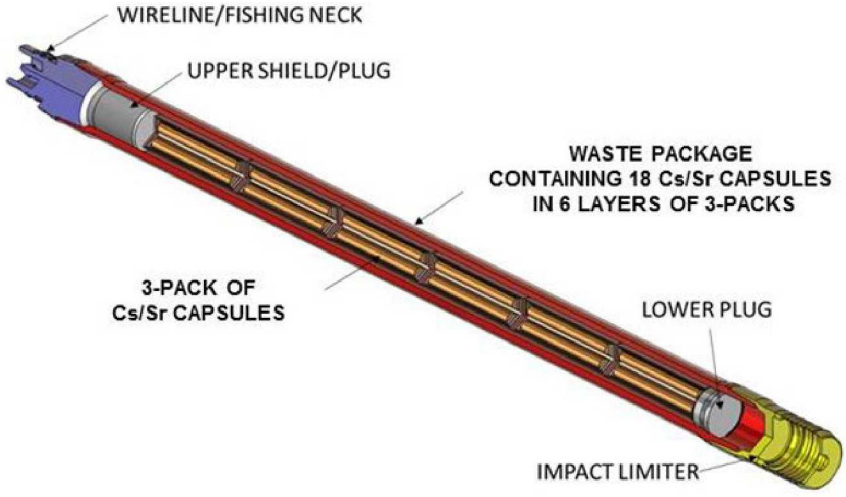

Figure 1-4. Schematic of a Waste Package for Cs/Sr Capsules

A perforated steel liner is assumed to extend the length of the EZ. A temporary guidance casing from the surface will be designed to work in conjunction with the EZ liner to facilitate smooth emplacement of waste packages. The EZ also includes annular spaces between the stacked waste packages and the EZ liner and between the EZ liner and the borehole wall. These annular spaces could be filled with buffer or backfill material. However, for the reference disposal concept, the EZ annular regions are assumed to be filled with high density brine, similar to formation fluid.

The upper portion of the borehole includes the SZ, entirely within the crystalline basement rock, where seals and plugs (bentonite seals, cement plugs, silica sand/crushed rock ballast) will be emplaced directly against borehole wall, and the UBZ, primarily within the sedimentary overburden, where plugs (cement alternating with ballast) will be emplaced against the cemented casing. The SZ is a 2,000-m interval (between 2,466 m and 4,466 m depth). Seals in the SZ are designed to act directly against the disturbed rock zone (DRZ) of the host rock to limit upward radionuclide transport; cement plugs in the SZ would minimize chemical interaction between adjacent seals.

The DBD reference case is further defined by the assessment basis for the subsurface features and components. These include the borehole design (Freeze et al. 2016, Section 4.1.1), wastes and engineered barriers (Freeze et al. 2016, Section 4.2), and generic information and assumptions about crystalline basement rock and the overlying sediments (Freeze et al. 2016, Section 4.3).

1.4.2 Surface and Emplacement Operations

The reference design also includes a concept for surface operations. A wireline waste package emplacement system, depicted in Figure 1-5, was selected as the preferred approach (SNL 2016a, Sections 2.9.2 and 3.4; Peretz and Hardin 2017, Section 1).

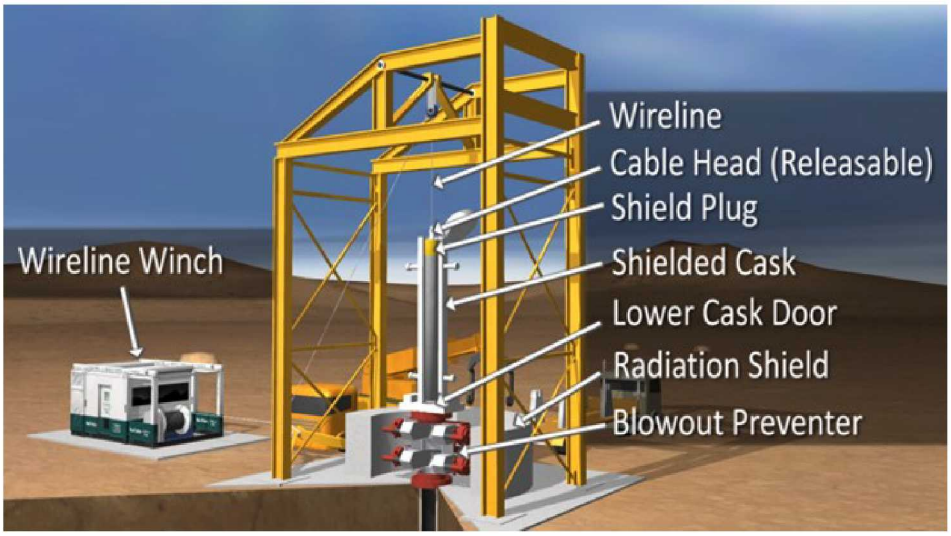

Source: Peretz and Hardin (2017, Figure 3)

Figure 1-5. Components of a Wireline Emplacement System

The reference case includes the following surface operations (Peretz and Hardin 2017, Sections 1.4, 1.5, and 3):

- Waste Package On-Site Receipt – arrival of waste package(s) in transportation cask in a horizontal orientation.
- Waste Package Surface Handling – transfer a waste package from the single-ended transportation cask to a double-ended on-site transfer cask, and move the transfer cask into a vertical orientation over the borehole.
- Waste Package Downhole Emplacement – connect the wireline to the waste package and lower it to the borehole EZ, release and withdraw the wireline.

As waste packages are stacked on each other in the EZ, mechanical loading on the bottom package increases. At intervals of approximately 40 waste packages, a cement plug (see Figure 1-3) is set to transfer load through the casing to the host rock, establishing a new baseline for loading on the next package string (Peretz and Hardin 2017, Section 1.5).

Surface operations are described in more detail in Freeze et al. (2016, Section 4.1.3), SNL (2016a, Section 3), and Peretz and Hardin (2017).

1.5 Summary of New Information and Analyses

Freeze et al. (2016) developed a preliminary, generic safety case of the feasibility of the DBD concept; there is no site, system design studies were just beginning, and the regulatory framework is unclear and lacks focus for this method of disposal. Therefore, at this early phase of DBD concept development, the purpose of this safety case for DBD is to provide a framework to organize and synthesize existing science and identify open issues and information gaps relevant to DBD. Crystalline basement rock is the current focus as a DBD host rock, but other geologies are not excluded.

The feasibility and pre-closure safety of the DBD concept relies on the following characteristics of the design, engineering, and pre-closure operations (SNL 2016a, Sections 1 and 2.1; SNL 2016b):

- **Site Characterization** – Regional and downhole scientific analyses can be performed to adequately characterize the suitability of the heterogeneous subsurface conditions for DBD facility.
- **Deep Drilling** – Drilling a straight, large-diameter borehole to 5,000 m with a 0.43 m (17 in) bottom-hole diameter is likely to be achievable in crystalline basement rock.
- **Site Operations** – The facilities and components for surface activities (waste receipt, waste package surface handling) and downhole activities (waste package emplacement and retrieval, borehole sealing and plugging) can be safely engineered and operated, with consideration of the potential impacts of off-normal events.

Characteristics and conditions of the DBD concept that are favorable to long-term isolation of radioactive waste from the accessible environment include (Freeze et al. 2016, Sections 5 and 6; SNL 2016a, Section 2.1):

- **Great Depth of Disposal** – DBD safety relies on emplacing wastes in competent crystalline rock well below the extent of naturally circulating groundwater. In DBD, waste would be situated at 3 to 5 km depth in low-permeability granite or schist, so the radionuclide migration path distance would be an order of magnitude greater than for mined repositories, which are typically proposed at depths of approximately 500 m.
- **Isolation and Long Residence Time of Deep Groundwater** – Recent studies have shown groundwater deeper than 2 km in the Precambrian basement to have been isolated from the atmosphere for greater than one billion years (e.g., Holland et al. 2013; Gascoyne 2004). The origin and residence time of deep groundwater can be estimated using environmental tracers with long half-lives (e.g., ^{36}Cl, ^{81}Kr, ^{4}He, $^{234}U/^{238}U$ ratio). In addition, deep groundwaters are typically concentrated chloride brines with densities that range from 2.5% greater than pure water (seawater) to more than 30% greater than pure water (Park et al. 2009; Phillips et al. 1981). High salinity at depth can be indicative of isolation from shallower water.

- **Density Stratification of Brine at Depth** – Density stratification of brine tends to limit the effects from future perturbations to hydrologic conditions such as climate change, or from early thermal convection in the borehole due to heat production from ^{137}Cs and ^{90}Sr decay. The density gradient (fresh water near the surface, concentrated brine at depth) is stabilizing and inhibits vertical flow or mixing. The simple existence of concentrated chloride brines in the crystalline basement is a general indicator of great age, especially when no evaporites are present in the geologic setting. Absence of overpressured conditions at depth (so that in situ pressure cannot drive flow towards the surface) is also expected at favorable locations for DBD.
- **Low Permeability of Crystalline Host Rock** – Bulk permeability of deep crystalline rocks is generally low and decreases with depth (Freeze et al. 2016, Section 4.3.2.1 and Figure 4-7).
- **High-Likelihood of Slow Diffusion-Dominated Radionuclide Transport** – Movement in groundwater is practically the only significant pathway for migration of radionuclides from a deep borehole to the accessible environment. If the groundwater has not moved for millions of years (i.e. minimal advection due to low permeability and low regional hydraulic head gradient), then transport is limited to the mechanism of aqueous diffusion, a slow process.
- **Geochemically-Reducing Conditions at Depth** – Reducing conditions in the deep subsurface tend to limit the solubility and enhance the sorption of many radionuclides, further reducing mobility in groundwater.
- **Low Permeability and High Sorption Capacity of Seal Materials** – The low permeability of seal materials (bentonite and cement) inhibits vertical fluid flux and radionuclide transport up the borehole; the high sorption capacity of the bentonite also limits and/or delays radionuclide transport (Freeze et al. 2016, Section 4.2.6). Seals are primarily needed during the first few hundred years of maximum decay heat production in the borehole. Further seal performance is desirable until re-establishment of the natural salinity gradient (density stratification), which tends to oppose upward flow; this period is assumed to be approximately 1,000 years.
- **Multi-Barrier Design** – The safety of a DBD system includes contributions from natural barriers (deep, isolated low permeability host rock) and engineered barriers (multiple, redundant sealing intervals and materials). Although not required for post-closure safety under currently analyzed scenarios, longer-lived, engineered waste forms and/or waste packages would further contribute to waste isolation and multi-barrier capability.

These characteristics of the DBD concept are considered in the preliminary DBD safety case as part of the assessment basis (Freeze et al. 2016, Section 4) and are evaluated as part of the safety assessments (pre-closure safety analysis, post closure PA, confidence enhancement) (Freeze et al. 2016, Section 5).

While the preliminary information and evidence suggests that DBD is a viable concept, a number of open issues requiring further evaluation and/or research exist (Freeze et al. 2016, Section 6.4). This report provides additional information and analyses that further augments the DBD safety case and/or addresses some of the open issues. The new information includes:

- Pre-Closure Basis and Safety Analysis (Section 2)
  - An updated approach for pre-closure radiological assessment of DBD site operations (from Hardin et al. 2017) and an expanded scope of the pre-closure assessment basis and safety analysis (from Peretz and Hardin 2017 and Hardin et al. 2019). The previous pre-closure safety analysis (Freeze et al. 2016, Section 5.1; SNL 2016a, Appendix A and B) was limited to consideration of hazards and event sequences associated only with the wireline emplacement activity. The expanded analysis considers DBD site operations in greater detail, including a number of activities from waste package receipt to borehole closure.
- Post-Closure Basis and Performance Assessment (Section 3)
  - Additional post-closure PA analysis of a disturbed scenario that includes a waste package "stuck" in the crystalline basement above the EZ near a hypothetical borehole-intersecting fracture. The disturbed scenario builds upon previously documented undisturbed (nominal) scenario simulations (Freeze et al. 2016, Section 5.2).
- Confidence Enhancement (Section 4)
  - Identification of downhole testing methods to characterize groundwater isolation/residence time, density stratification, and geochemical conditions at depth.
  - Hydrologic modeling of density stratification of brine at depth.
  - Review of borehole sealing materials and technologies.

2 PRE-CLOSURE BASIS AND SAFETY ANALYSIS

The pre-closure assessment basis includes a description of the surface and subsurface facilities (i.e., the borehole) and their operation for use in a quantitative pre-closure safety analysis. Freeze et al. (2016, Section 4.1) provides specific pre-closure basis information for the Cs/Sr capsule DBD reference case and reference design, including:

- DBD site design and layout (surface facilities, borehole, and engineered barriers)
- Borehole drilling and construction requirements
- DBD site operations (surface facility operations, waste package surface handling, waste package downhole emplacement, borehole sealing and plugging, and facility closure)
- Potential impacts of off-normal events (dropping a waste package, retrieval of a waste package stuck in upper portion of borehole, pre-closure breach of a waste package) and/or external/disruptive events (flooding and extreme weather, seismicity, sabotage) on pre-closure safety
- Potential impacts of pre-closure activities and components on post-closure safety (e.g., waste package stuck in borehole and abandoned, hydrogen (H_2) gas generation from metal corrosion, efficacy of borehole seals and plugs)

This pre-closure basis information, quantitative with uncertainty where possible, supported a pre-closure safety analysis that was limited to consideration of accident hazards and accident event sequences associated with wireline emplacement of Cs/Sr capsule waste packages (Freeze et al. 2016, Section 5.1; SNL 2016a, Appendix A and B).

More recently, an updated approach for pre-closure radiological assessment of DBD operations was developed (Hardin et al. 2017) and the scope of the pre-closure assessment basis and safety analysis was expanded (Peretz and Hardin 2017; Hardin et al. 2019). The expanded pre-closure safety assessment seeks to improve the conceptual design for DBD, by considering risks associated with the full range of waste handling and emplacement operations. It is intended that, by describing and analyzing disposal operations in detail from waste package receipt to borehole closure, additional active and passive safety functions and operational controls can be identified and incorporated in the design. Specific activities included:

- Development of a probabilistic risk assessment (PRA) methodology for the pre-closure radiological safety assessment (Hardin et al. 2017), consistent with the approach required by 10 CFR 63, and generally consistent with the pre-closure safety analysis (PCSA) for a Yucca Mountain repository (BSC 2008a; BSC 2008b). The approach is also consistent with the requirements at 10 CFR 60.
- Expanded identification of activity sequences and risk factors for disposal operations (Peretz and Hardin 2017).
- Implementation of the PRA-based pre-closure safety assessment model (fault trees, event trees, and probability estimates) to calculate results, and the sensitivity of results to key input probability values (Hardin et al. 2019).
- Identification of improvements in the DBD conceptual design documented previously in SNL (2016a).

2.1 Pre-Closure Basis

The PRA methodology adopted for the DBD PCSA is modeled after 10 CFR 63, because that rule (and 10 CFR 60) is a modern approach deemed appropriate by the NRC for licensing radioactive waste disposal. The only real-world application of these regulations for pre-closure operational safety is found in the Yucca Mountain Safety Analysis Report (DOE 2008), and the complementary Safety Evaluation Report (NRC 2015).

The DBD PCSA approach involves describing DBD operations, identifying end states and initiating events ("top events"), constructing fault trees for initiating events, estimating event probabilities, characterizing radiological consequences from failed end states, constructing event trees and summing probabilities for all outcomes (Hardin et al. 2017, Section 5). This approach follows the Yucca Mountain PCSA approach (BSC 2008a; DOE 2008) for scoping and design, but is simplified in the formulation and presentation of event trees and fault trees because the scale of this assessment is much smaller than for the Yucca Mountain PCSA (Hardin et al. 2019, Section 3). Specific elements of the DBD PCSA include (Hardin et al. 2017, Section 3; Hardin et al. 2019, Section 1):

- Process flow diagram (PFD) – Describes the structures, systems, and components (SSCs) and activity sequences associated with normal operations. A simplified PFD for DBD operations is presented in Section 2.2.
- Master logic diagram (MLD) – Top-down structure showing what initiating events, or groups of similar initiating events, could contribute to radiological consequences. A top-level MLD for DBD operations, and MLDs for internal events from specific activity sequences, are presented in Section 2.2.
- Event trees – Describe normal and off-normal operations for activity sequences with the potential for release of radioactive material (i.e., from waste package breach) or worker exposure (i.e., from loss of shielding). Each event tree identifies the top events, and the end states associated with success or failure of the top events.
- Fault trees – Quantify failure probabilities for top events from the event trees. Fault trees are structured as having a top event (stated as a positive outcome) that is made up of casual events and basic events (negatives such as equipment malfunction, human error, etc.); the top event probability is based on Boolean logic and basic event probabilities.

The DBD PCSA thus consists of a set of event trees, each consisting of a number of top events and end states, with failure probabilities for each end state assigned through fault tree analysis. Calculation of the overall probability of successfully completing a borehole disposal campaign is based on the aggregation of the probabilities from each of the various activity sequences and possible end states.

For this preliminary DBD PCSA, initiating events considered included internal events that are initiated within the waste package receipt / handling / emplacement system. External initiating events (e.g., seismic, extreme weather, external fire) were not addressed as part of the base case calculation, but a scoping analysis of external seismic events was performed.

The present application of the DBD PCSA is intended to provide insights that improve the conceptual design for DBD, and not to estimate radiological exposure or dose for comparison to regulatory limits. Accordingly, radiological consequences are abstracted in a way that assigns relative levels of possible exposure or dose without quantification (e.g., as consequence categories A, B, etc.) (Hardin et al. 2019, Section 3).

2.2 Pre-Closure Safety Analysis

The process for receiving, handling, and emplacing waste packages, and completing the disposal borehole, is described in detail in Hardin et al. (2019). To support the DBD PCSA it was diagrammed as a series of activity sequences and nodes, as shown in the PFD in Figure 2-1. Node A represents the starting point; Sequence 1 (borehole qualification) must be completed prior to moving the loaded transfer cask into position over the wellhead station. Sequences 2 through 8 proceed in linear fashion. A decision point is shown after Sequence 8. If a string of about 40 waste packages has been placed, Sequences 9 and 10 are used to place a cement interval plug. Otherwise, the process flow returns to Node A and emplacement activities for the next waste package begin. A second decision point follows setting of the cement interval plug; if space remains in the borehole EZ the flow again returns to Node A. If the EZ has been filled, the borehole is closed under Sequence 11.

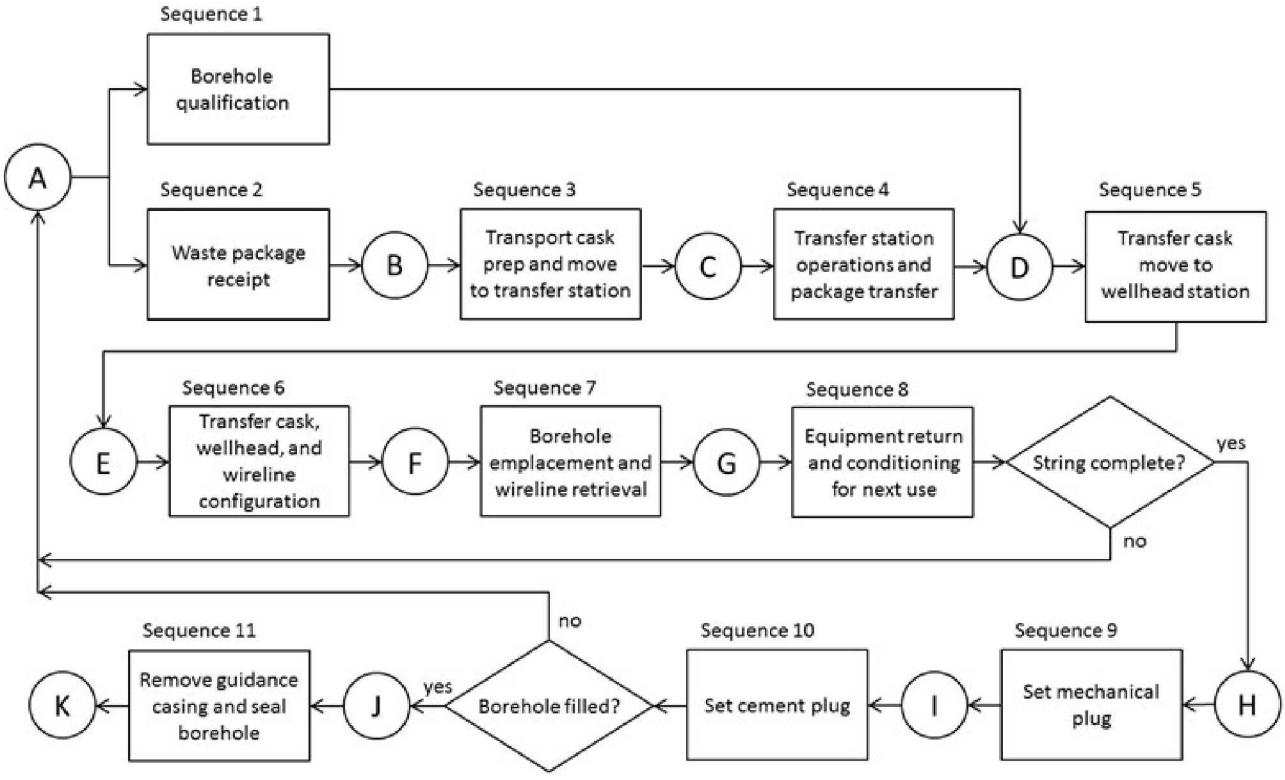

Source: Hardin et al. (2019, Figure 5-1)

Figure 2-1. Simplified Process Flow Diagram

Each of the activity sequences identified in Figure 2-1 is described in detail in Hardin et al. (2019, Section 6). The activity sequences are connected by nodes (Hardin et al. 2019, Section 5). Each node correlates to a fixed set of conditions, as described in Table 2-1 below. The overall sequence begins at Node A, and the logic flow returns to Node A for each subsequent package placement. Emplacement and closure of an individual borehole terminates at Node K.

Table 2-1. Status at Each Process Flow Diagram Node

Node	Status
A	Ready to initiate next emplacement sequence.
B	Sealed transportation cask trailer properly placed on borehole site.
C	Transportation cask and waste package on cradle #1, ready to transfer package.
D	Transfer cask and waste package ready to be moved to wellhead station.
E	Transfer cask and waste package ready for wellhead and wireline configuration.
F	Waste package and wellhead ready for package emplacement in borehole.
G	Waste package emplaced in borehole, wireline retrieved, and wellhead closed.
H	Package string emplacement complete, ready to set interval plug.
I	Mechanical plug set, ready to set cement plug.
J	Borehole filled, ready for borehole closure.
K	Borehole sealed and equipment moved off borehole.

Source: Hardin et al. (2019, Table 5-1)

To produce a MLD, a hazard analysis was performed to identify initiating (top) events for each of the activity sequences (further defined by activity steps, as described in Hardin et al. (2019, Section 6)) based on seven hazard categories associated with the following DBD site operations (Hardin et al. 2019, Section 7.2):

- *Lift*, generally referring to a lift of a cask containing a waste package or a lift of other objects with the potential for dropping that object on a cask containing a waste package.
- *Cask cradle roll*, in which a cask containing a waste package is moved horizontally on a track-mounted cradle.
- *Cask shield plug manipulation*, in which changes are made to shield configurations at the end of a cask containing a waste package.
- *Interface shield slide manipulation*, in which the sliding portion of the interface shield is moved, potentially changing the shield interface between cask and interface shield or the passage from cask to cask.
- *Waste package latch mechanism manipulation or waste package movement*, in which a non-wireline latch mechanism is attached to, removed from, or used to move a waste package.

- *Wellhead system operations*, referring to activities that orient a transfer cask over a wellhead station (either the wellhead flange or the lower plug removal station), that connect the transfer cask to the wellhead flange, or that connect the package in the cask or other downhole equipment to the wireline.
- *Wireline operations*, addressing sequences in which the waste package is lowered into an open borehole, the wireline and tool string are retrieved from an open borehole, or qualification or other equipment is run down and up a borehole over an uncovered emplaced waste package.

A mapping of the seven hazard categories, which are associated with processes internal to the engineered systems for waste handling and emplacement (i.e., internal events), to the 11 activity sequences from Figure 2-1 is summarized in Table 2-2, based on an analysis documented in Hardin et al. (2019, Appendix A). In Table 2-2, seven activity sequences are identified as possibly encountering hazard categories. These activity sequences (or more specifically, one or more of the activity steps comprising the sequence) involve radiological material (handling of waste packages) can pose risk to the public via damage to a package and release of radioactive material, or risk to workers resulting from direct exposure to radiation. The other four activity sequences either do not involve handling of radioactive materials, or are common actions that pose no significant radiological risk. These activity sequences were not selected for further analysis.

Table 2-2. Correlation of Hazard Categories with Activity Sequences

No.	Sequence	Hazard Categories Encountered
1	Borehole qualification	Wellhead system, Wireline
2	Waste package receipt	(not selected for radiological hazard analysis)
3	Transportation cask preparation and move to transfer station	Lift, Cask cradle roll, Cask shield plug
4	Transfer station operations	Cask cradle roll, Cask shield plug, Interface shield slide, Waste package latch or move
5	Transfer cask move to wellhead	Lift, Wellhead system
6	Cask, package, wellhead and wireline configuration	Cask shield plug, Waste package latch or move, Wellhead system, Wireline
7	Emplacement, release, and wireline retrieval	Waste package latch or move, Wellhead system, Wireline
8	Prepare equipment for use	(not selected for radiological hazard analysis)
9	Set mechanical interval plug	Wellhead system, Wireline (coiled tubing)
10	Set cement interval plug	(not selected for radiological hazard analysis)
11	Remove guidance casing and seal borehole	(not selected for radiological hazard analysis)

Source: Peretz and Hardin (2017, Table 16)

The resulting MLDs identify selected "top" initiating events for each activity sequence, by hazard category (Hardin et al. 2019, Section 8). A top-level MLD is shown in Figure 2-2. MLDs showing events for seven selected activity sequences are presented in Hardin et al. (2019, Figures 8-2 through 8-8).

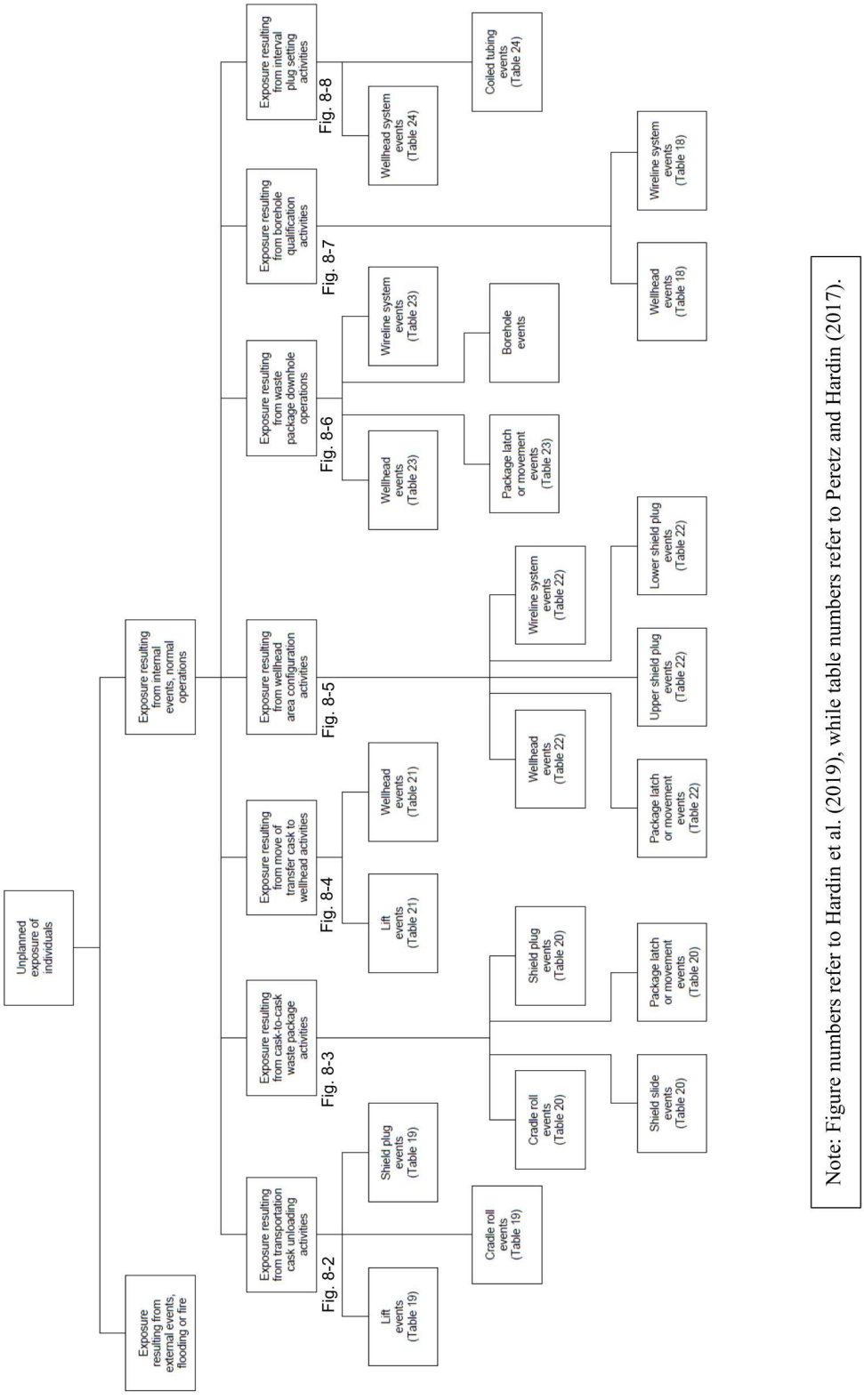

Source: Hardin et al. (2019, Figure 8-1)

Figure 2-2. Top-Level Master Logic Diagram

Based on the MLDs and activity sequence steps, event trees were developed to describe normal and off-normal operations for each of the seven activity sequences with the potential for release of radioactive material (i.e., from waste package breach) or worker exposure (i.e., from loss of shielding) (Hardin et al. 2019, Section 9). Each event tree identifies the top events, and the end states associated with success or failure of the top events. Numerical quantification of dose or radiological release consequences is not attempted. Instead, the radiological consequence associated with each end state is binned into general categories as shown in Table 2-3.

Table 2-3. General Consequence Categories

Category	Consequence
A	Success (normal operations)
B	Loss of shielding and minor worker exposure
C	Loss of shielding and moderate worker exposure
D	Loss of shielding with potential damage or displacement of waste package, but low potential for release of radioactive material
E	Loss of shielding with potential damage or displacement of waste package, and credible, significant potential for release of radioactive material
F	Downhole waste package impact with low likelihood of package breach
G	Downhole waste package impact with quantified probability of package breach

Source: Hardin et al. (2019, Table 9-1)

Event trees for the seven selected activity sequences are presented in Hardin et al. (2019, Figures 9-1 through 9-7). Each event tree has one or more top events and one or more end states (corresponding to a consequence category).

Using the PRA approach, fault trees were developed (using SAPHIRE software (Smith et al. 2012)) to quantify failure probabilities for all top events on each of the seven event trees. The resulting fault trees and failure probabilities are presented in Hardin et al. (2019, Figures 10-1 through 10-43). Failure probabilities are typical for equipment performance and human performance with similar processes. However, at this preliminary stage of design, many of the input values represent design goals rather than a specific performance analysis for an as-designed system.

As described in Hardin et al. (2019, Section 10), all failure probabilities are for a single emplacement sequence (e.g., per waste package). In the case of Activity Sequence 9, set mechanical interval plug, the probabilities are for a single performance of that sequence (e.g., per plug). It should be noted that the interval plug (associated with the EZ cement plug) sequence is performed at a different rate than the package emplacement sequence; if there are 40 packages between EZ cement plugs, the interval plug sequence is performed once after every 40 emplacement sequences. Overall calculations for the entire borehole (e.g., 108 packages, 2 cement plugs) are addressed later.

The DBD PCSA thus consists of a set of event trees, each consisting of a number of top events and end states, with failure probabilities for each end state assigned through fault tree analysis. Calculation of the overall probability of successfully completing a borehole disposal campaign is based on the aggregation of the probabilities of success and failure from all of the end states from each of the seven activity sequence event trees.

Each end state probability (and the contribution to an assigned consequence category) is calculated from the product of fault tree probabilities for the branching that leads to that end state. After the consequence category probabilities are calculated for an event tree, category information is aggregated to obtain the total probability for each category, and category information is then aggregated across all event trees to obtain the DBD PCSA model results (Hardin et al. 2019, Section 11).

The aggregated probabilities for "base case" assumptions for each of the different consequence categories are shown in Table 2-4. For Categories B through G it is the probability of failure, for Category A it is the probability of success (e.g., $1 - p_{fail}$). Per string probabilities are based on 40 WPs in a string.

Table 2-4. Aggregated Probabilities at Stages in the DBD Process

Consequence Category		Probability (per WP)	Probability (per string)	Probability (per EZ plug)	Probability [a] (per borehole)
A	Success	0.99956	0.98237	0.99996	0.954
B	WP loss of shielding, minor worker exposure	2.43E-04	9.66E-03	-	2.59E-02
C	WP loss of shielding, moderate worker exposure	7.70E-05	3.08E-03	-	8.28E-03
D	WP damage during surface handling, low potential for breach and radionuclide release	1.10E-11	4.40E-10	-	1.19E-09
E	WP damage during surface handling, high potential for breach and radionuclide release	4.20E-21	0.00E+00	-	0.00E+00
F	WP damage downhole, low probability of breach and radionuclide release	1.10E-04	4.39E-03	4.20E-05	1.19E-02
G	WP damage downhole, high probability of breach and radionuclide release	4.35E-08	1.74E-06		4.70E-06

[a] Calculated for 108 WPs and 2 EZ plugs

Source: Hardin et al. (2019, Table 11-1)

The probabilities per borehole are based on 108 waste packages and 2 EZ plugs in a borehole. The probability of a successful borehole completion under "base case" assumptions is 95.4%. This per borehole estimate differs from that presented in Hardin et al. (2019, Section 11), which assumed 400 waste packages and 10 plugs per borehole.

The base case analysis (Table 2-4) generally used conservative estimates. A sensitivity analysis was also performed using less conservative estimates to examine the effect of minimizing human errors and increasing the overall reliability of the systems, structures, and components involved (Hardin et al. 2019, Section 11.2). The aggregated probabilities for the sensitivity analysis are shown in Table 2-5.

Table 2-5. Aggregated Probabilities at Stages in the DBD Process, for Sensitivity Analysis

Consequence Category		Probability (per WP)	Probability (per string)	Probability (per EZ plug)	Probability [a] (per borehole)
A	Success	0.9999389	0.9975575	0.9999989	0.994
B	WP loss of shielding, minor worker exposure	3.70E-05	1.48E-03	-	3.99E-03
C	WP loss of shielding, moderate worker exposure	8.27E-06	3.31E-04	-	8.93E-04
D	WP damage during surface handling, low potential for breach and radionuclide release	1.10E-11	4.40E-10	-	1.19E-09
E	WP damage during surface handling, high potential for breach and radionuclide release	2.00E-30	0.00E+00	-	0.00E+00
F	WP damage downhole, low probability of breach and radionuclide release	1.21E-05	4.82E-04	1.11E-06	1.31E-03
G	WP damage downhole, high probability of breach and radionuclide release	9.32E-09	3.73E-07	-	1.01E-06

[a] Calculated for 108 WPs and 2 EZ plugs

Source: Hardin et al. (2019, Table 11-3)

The main change in the sensitivity analysis was to try to achieve off-normal fault tree probabilities on the order of 10^{-6} for the entire event tree, for those activity sequences that dominate DBD system performance. As shown in Table 2-5, the probability of a successful borehole completion rises to 99.4% with these lower failure probabilities.

3 POST-CLOSURE BASIS AND PERFORMANCE ASSESSMENT

The post-closure assessment basis includes a description of the natural and engineered barriers for use in the quantitative post-closure PA. The post-closure technical basis for the Cs/Sr capsule DBD reference case and reference design is divided into three components: waste and engineered barriers; geosphere and natural barriers; and biosphere and surface environment.

Freeze et al. (2016, Section 4.2) provides specific post-closure basis information for the waste and engineered barriers, including:

- Inventory characteristics and quantities (Cs, Sr, and other constituents)
- Waste Form characteristics (CsCl and SrF_2 degradation and solubility)
- Waste Package characteristics (carbon steel corrosion)
- EZ characteristics (buffer/backfill/annulus brine evolution, cement plug degradation, perforated steel liner corrosion)
- SZ characteristics (degradation of bentonite seals, cement plugs, and sand/crushed rock ballast)
- UBZ characteristics (degradation of cement and ballast)
- Potential impacts of external events (climate change, seismicity, igneous activity, human intrusion) on the performance of the engineered barriers

Freeze et al. (2016, Section 4.3) provides specific post-closure basis information for the geosphere and natural barriers, including:

- Crystalline basement host rock characteristics (permeability, porosity, diffusion coefficient, thermal properties, pore fluid chemistry, solubility, sorption)
- DRZ characteristics (extent and properties)
- Overburden characteristics (sedimentary sequence and properties)
- Potential impacts of external events (climate change, glaciation/erosion, seismicity, igneous activity, human intrusion) on the performance of the natural barriers

For this preliminary, generic iteration of the safety case, the biosphere is not yet conceptualized and is not part of the PA model (Freeze et al. 2016, Section 4.4).

This post-closure basis information, quantitative with uncertainty where possible, supported a post-closure PA for the undisturbed (nominal) scenario that included radionuclide transport in the borehole, in the DRZ around the borehole, and in the surrounding rock away from the borehole (Freeze et al. 2016, Section 5.2).

The nominal scenario for DBD of Cs/Sr capsules was developed using a feature, event, and process (FEP) analysis and scenario development methodology (Freeze et al. 2016, Sections 5.2.1 and 5.2.2). The conceptual model was implemented using the Geologic Disposal Safety Assessment (GDSA) framework (Mariner et al. 2016, Section 2.2) for numerical simulations of thermal-hydrology and radionuclide mobilization and transport in a high-performance computing environment. The GDSA framework includes PFLOTRAN (Hammond et al. 2011; Lichtner and Hammond 2012), an open source, massively parallel non-isothermal multi-phase flow and reactive transport code, and DAKOTA (Adams et al. 2013a; Adams et al. 2013b), an analysis package for uncertainty quantification, sensitivity analysis, optimization, and calibration in a parallel computing environment.

In addition to the nominal scenario, Freeze et al. (2016, Section 5.2.2) identified the following other scenarios to be considered in a DBD safety case:

- Defective Engineered Barrier Scenarios
  - defective waste package
  - defective EZ buffer/backfill
  - defective sealing system
- Disturbed Scenarios
  - human intrusion
  - seismic activity
  - igneous event
  - climate change / glaciation

This report examines a disturbed scenario that also captures aspects of a defective sealing system. The disturbed scenario includes a waste package "stuck" in the crystalline basement above the EZ near a hypothetical borehole-intersecting fracture (Figure 3-1). The post-closure basis and PA simulations are described in the following subsections.

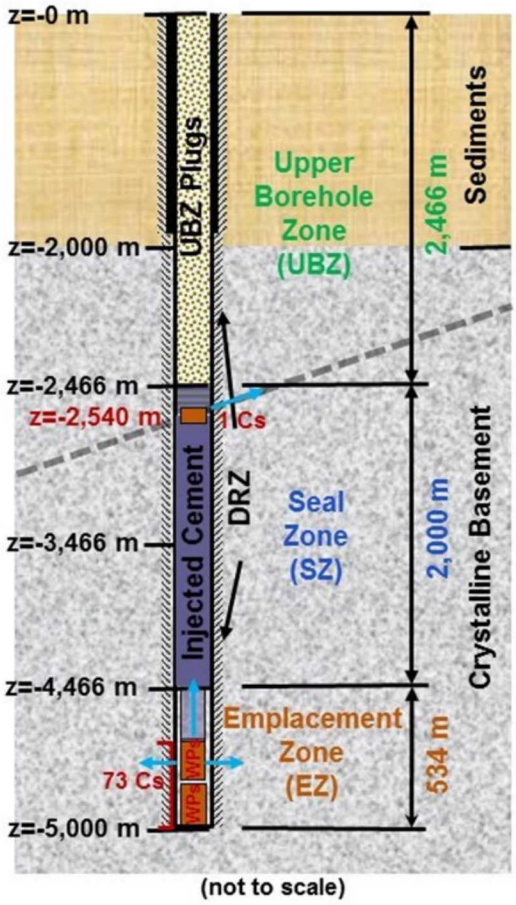

Figure 3-1. Schematic of the Deep Borehole Disposal Disturbed ("Stuck" Package) Scenario

3.1 Post-Closure Basis

The post-closure basis for the disturbed ("stuck" package) scenario derives from the undisturbed (nominal) scenario reference case. Key nominal scenario processes occurring in each of DBD system components, identified through FEP analysis (Freeze et al. 2016, Section 5.2.1), include (Freeze et al. 2016, Sections 5.2.2 and 5.2.3):

- Radionuclide inventory (^{135}Cs, ^{137}Cs, ^{90}Sr) that derives from Cs and Sr capsules. Thermal output and radioactivity from the Cs and Sr capsules assumes surface storage/aging until borehole emplacement in 2050.
- Waste forms (solid CsCl and SrF_2) that are assumed to degrade immediately after emplacement and do not perform any function (e.g., gradual dissolution) that would delay radionuclide release or transport. Unlimited solubility of Cs and Sr in groundwater is assumed.
- A 534 m EZ that contains 108 waste packages (74 for the Cs capsules and 34 for the Sr capsules). The cooler Cs waste packages are emplaced first, in the lower portion of the EZ. The waste packages are assumed to maintain structural integrity during surface

handling and emplacement, but are assumed to degrade immediately after sealing (corresponding to a simulated waste package breach time of one year after sealing) and do not perform any function (e.g., gradual corrosion) that would delay radionuclide release or transport.

- A 2,000 m SZ with permeability and porosity consistent with degraded properties of bentonite clay, cement plugs, and/or sand/crushed rock ballast. The overlying UBZ also has permeability and porosity consistent with degraded material properties.
- Sparsely fractured crystalline basement rock with low permeability and porosity and no regional hydraulic head gradient.
- Overlying sediments represented as a single vertically and laterally homogeneous region. This model simplification does not impact the results because radionuclides are not transported beyond the crystalline basement rock in any of the simulations.
- A DRZ around the borehole that is assumed to have an elevated permeability with respect to the adjacent intact basement rock due to changes in stress induced by drilling.
- A temperature gradient with depth, calculated assuming a geothermal heat flux of 60 mW/m^2 at 6,000 m depth and an average annual surface temperature of 10°C. The resulting thermal gradient is ~25°C/km, with ambient temperatures of about 125°C at the top of the EZ and 140°C at the bottom of the EZ.
- The potential for advective and diffusive aqueous-phase transport. Radionuclide mobilization and transport properties are based on geochemically reducing conditions consistent with deep crystalline rock. (Consideration of gas-phase and/or colloidal transport is deferred to a future PA).

Material properties used to represent these DBD system features and processes in the nominal scenario PA simulations are summarized in Table 3-1.

For the disturbed (stuck package) scenario, the following changes are made to the nominal scenario reference case:

- A single Cs waste package is assumed to remain "stuck" in the crystalline basement above the EZ near a borehole-intersecting fracture. As a remedial measure, it is assumed that cement was injected (through the annulus outside the guidance casing) into the SZ below the stuck package. The injected cement is assumed to be more permeable and more porous than the engineered cement plugs. Specific properties of the injected cement are listed in Table 3-1.
- The properties of the borehole-intersecting fracture (Table 3-1) are derived from a porous medium representation of a discrete fracture, as described in Section 3.1.2. The fracture was assumed to have a 30° dip, intersecting the borehole at a depth of 2,540 m (540 m below the base of sedimentary overburden). Two cases were analyzed: one with no regional hydraulic head gradient (as in the nominal scenario), and one with a regional hydraulic head gradient of 0.0001 m/m (see Section 3.1.1), driving flow up dip toward the sediments.

Table 3-1. Numerical Representation of Material Properties in the PA Simulations

Material	Permeability k (m^2)	Porosity ϕ (–)	Tortuosity τ (–)	Effective Diffusion Coeff. D_e [a] (m^2/s)	Thermal Cond. (W/m·°K)	Heat Capacity (J/kg·°K)	Bulk Density ρ_{rock} (kg/m^3)	Sr K_d [b] (L/kg)	Cs K_d [b] (L/kg)
Emplacement Zone									
Waste Package	$1x10^{-16}$	0.43	1.0	$4.30x10^{-10}$	17	500	7850	0	0
EZ Annulus (Brine-Filled)	$1x10^{-12}$	0.99	1.0	$9.90x10^{-10}$	0.58	4192	1100	0	0
Cement Plug	$1x10^{-18}$	0.175	0.175	$3.06x10^{-11}$	1.7	900	2700	0	0
Injected Cement [c]	$1x10^{-16}$	0.25	0.25	$6.25x10^{-11}$	1.7	900	2700	0	0
Seal Zone									
Cement Plug	$1x10^{-18}$	0.175	0.175	$3.06x10^{-11}$	1.7	900	2700	0	0
Bentonite Seal	$1x10^{-18}$	0.45	0.45	$2.03x10^{-10}$	1.3	800	2700	1525	560
Ballast	$1x10^{-14}$	0.20	0.20	$4.00x10^{-11}$	2.0	800	2700	0	0
Host Rock									
Crystalline Rock	$1x10^{-18}$	0.005	0.20	$1.00x10^{-12}$	2.5	880	2700	1.7	22.5
DRZ	$1x10^{-16}$	0.005	0.20	$1.00x10^{-12}$	2.5	880	2700	1.7	22.5
Fracture [c]	$1x10^{-14}$	$8.1x10^{-6}$	123 [d]	$1.00x10^{-12}$	2.5	880	2700	1.7	22.5
Sediments									
Sediments	$1x10^{-15}$	0.20	0.20	$4.00x10^{-11}$	2.0	800	2700	50	120

[a] D_e = free water diffusion coefficient (D_w = $1x10^{-9}$ m^2/s) x tortuosity x porosity

[b] K_d = distribution coefficient (for linear sorption)

[c] Disturbed (stuck package) scenario only

[d] Fracture tortuosity value that results in an appropriate effective diffusion coefficient

Source: Freeze et al. (2016, Table 5-6)

3.1.1 Crystalline Basement Hydraulic Head Gradient

Groundwater flow rate is typically quantified by the Darcy velocity (also referred to as specific discharge), v_D [m/s] [4] (Freeze and Cherry 1979, p. 16):

$$v_D = K\, i \qquad \text{(Equation 3-1)}$$

where:

K = hydraulic conductivity [m/s]
i = hydraulic (head) gradient [m/m]

and (Freeze and Cherry 1979, p. 27):

$$K = (k\, \rho\, g) / \mu \qquad \text{(Equation 3-2)}$$

$$i = \Delta h / \Delta l \qquad \text{(Equation 3-3)}$$

where:

k = permeability [m^2]
ρ = fluid density [kg/m^3]
g = gravitational constant [m/s^2]
μ = fluid viscosity [kg/m-s] = [Pa-s] = [cp]
Δh = head difference [m]
Δl = distance between head measurements [m]

The center-of-mass of a non-reactive solute (e.g., a non-sorbing dissolved radionuclide) moves in flowing groundwater at the groundwater pore velocity, v_x [m/s]. The groundwater pore velocity (also referred to as average linear groundwater velocity) derives from the Darcy velocity and the porosity, ϕ (Freeze and Cherry 1979, p. 389):

$$v_x = v_D / \phi \qquad \text{(Equation 3-4)}$$

The effects of sorption onto the porous medium can be quantified simplistically (i.e., assuming linear sorption) in terms of a retardation factor, R_f (Freeze and Cherry 1979, Equation 9.14):

$$R_f = 1 + (\rho_{rock}\, K_d) / \phi \qquad \text{(Equation 3-5)}$$

where:

ρ_{rock} = rock bulk density [kg/m^3]
K_d = distribution coefficient [L/g] [5]

[4] As specified, the units are internally consistent, but other conventions may be used, with appropriate units conversions. For example, Darcy velocity and groundwater pore velocity are most commonly reported in units of m/yr.

[5] Distribution coefficients are most commonly reported in units of ml/g or L/kg.

For non-reactive solutes, K_d is 0 and R_f is 1. For reactive solutes, K_d is > 0 and R_f is > 1. This leads to the definition of an apparent groundwater velocity, v_a [m/s], that represents the effective velocity of a sorbing radionuclide through the porous medium:

$$v_a = v_x / R_f \qquad \text{(Equation 3-6)}$$

The distance, x [m], traveled by the center-of-mass of a solute (dissolved radionuclide) in time, t [s], is then:

$$x = v_a\, t \qquad \text{(Equation 3-7)}$$

Data on groundwater flow rates and hydraulic heads and gradients in the deep crystalline basement are sparse, largely because the low permeability and poor water quality means that most drilling and resource exploration occurs in shallower units.

Topographic relief is the dominant mechanism for groundwater flow in continental land masses, both in the shallow and deep subsurface. Maximum flow rates of 1 to 10 m/yr develop in deep aquifers, while much smaller seepage rates occur in aquitards (Garven 1995). In the dolomite strata of Appalachian-Illinois basins in Missouri, minimum flow rates of 1 mm/yr occur in the deepest Cambrian shale (Garven 1995).

In the Precambrian Shield in Canada, groundwater flow occurs through both the granitic and metamorphic bedrock and the overburden deposits. The near-surface bedrock (< 400 m depth) has low primary hydraulic conductivity (< 10^{-10} m/s), but zones of localized, relatively high, secondary hydraulic conductivity (10^{-6} to 10^{-8} m/s) and low interconnected porosity (0.1 to 0.001), are associated with a rock-mass fracture system (Farvolden et al. 1988). Flat-lying fracture zones, where present, are the major controls on regional flow. These zones have been encountered at various depths between the surface and at least 1,000 m, with a generalized vertical spacing of 1 to 300 m and a thickness of 10 to 50 m (Farvolden et al. 1988). Within these zones, permeability is highly anisotropic; distinct flow channels in the fracture plane are a controlling feature. The flat-lying fracture zones are associated with steep fault zones that penetrate to great depth and often appear as long lineaments at the surface. These zones also appear to be highly anisotropic, with permeability controlled by both fracture fillings and regional stresses. The spacing of these steep fault zones varies from less than l km to greater than 5 km.

Regional stresses are important in the hydraulic properties of these faults (Farvolden et al. 1988). Where the maximum horizontal compressive stress is normal to the strike, these faults tend to be closed or tight and chemically filled. The opposite has been observed where regional stresses are parallel to the zone. A similar correlation of regional stress and permeability has been noted in work at the Stripa Mine in Sweden.

In the relatively intact rock blocks between major fault zones, the rock is tight. All fractures are chemically filled and, except for the deep semi-horizontal zones of high permeability mentioned above, groundwater flow is minimal and no systematic flow pattern has been measured or observed (Farvolden et al. 1988).

Regional hydraulic head gradients on the order of 0.001 m/m have been reported in deep sedimentary aquifers (Bassett and Bentley 1983, Figure 6; Lobmeyer 1985; Downey and Dinwiddie 1988). Site investigations were performed at Forsmark and Oskarshamn in Sweden in boreholes in fractured granite down to depths of about 1,000 m. These site investigations yielded estimates of groundwater flow rates, transmissivities, and hydraulic head gradients (Nordqvist et al. 2008). Hydraulic gradients, calculated from borehole flow rates, estimated transmissivities, and assumptions about the flow convergence around the borehole, showed a large variation from extremely low gradients (0.0001 m/m) to in several cases seemingly unrealistically high gradients. Most of the calculated gradients were in the interval of 0.01 to 0.1 m/m (Nordqvist et al. 2008).

These calculated hydraulic gradients are local gradients, representative of the naturally flowing fracture(s) in the measured borehole section. However, Nordqvist et al. (2008, Section 8) suggest that, due to various test conditions and interpretation assumptions, these calculated hydraulic gradient values are likely to be too high relative to reasonable topographically-based estimates of the regional hydraulic gradient.

For the purposes of modeling regional flow in the deep crystalline basement, it is necessary to determine a set of parameters (permeability, porosity, and hydraulic head gradient) that produce a representative Darcy velocity (and groundwater pore velocity) for both the intact rock blocks (matrix) and the fracture/fault zones.

A hydraulic head gradient of 0.0001 is assumed for the deep crystalline basement, consistent with the lower end of measured values in the Swedish boreholes. A host rock with matrix permeability of 10^{-18} m^2 and a porosity of 0.005 (Table 3-1) results in a Darcy velocity of 3 x 10^{-8} m/yr and a groundwater pore velocity of 0.006 mm/yr.

3.1.2 Crystalline Basement Fractures

Conceptually, the crystalline host rock is comprised of two entities: matrix and fractures. There are two main approaches for simulating groundwater flow with heat and mass transport in fractured rock: (1) modeling the fluid transport through each individual fracture (i.e., the discrete fracture network (DFN) approach), and (2) modeling the transport regime as an equivalent porous and anisotropic continuum (i.e., the equivalent continuous porous medium (ECPM) approach) (Garven 1995). Mariner et al. (2016, Section 3.1.3.1) provides a discussion of these two approaches; a summary is provided here.

A planar fracture is defined by orientation, location, radius, aperture, and transmissivity. DFNs are networks of two-dimensional (2D) fracture planes distributed in a three-dimensional (3D) domain. DFNs are limited by their inability to simulate heat conduction through the rock matrix (and resulting inability to capture the effects of thermally driven fluid fluxes or to couple chemical processes to thermal processes), and by the availability of computational resources necessary to simulate problems involving high fracture density, large domain size, or multiple unknowns such as, for instance, multiple chemical species. When DFNs become large, simplifications are commonly made, such as modeling flow only in fracture intersections (pipe model); using ECPM representations in all or part of the model domain; breaking the problem into smaller pieces;

simulating only steady state flow regimes; and/or relying on particle tracking instead of solving the set of fully coupled reactive flow and transport equations.

Because of the need to simulate thermally driven fluid fluxes, the ECPM approach was used to represent the borehole-intersecting fracture in the disturbed (stuck waste package) scenario. A single, dipping, discrete fracture plane was derived from a DFN based on the fracture system in the well-characterized Forsmark metagranite (Follin et al. 2014; Joyce et al. 2014; Wang et al. 2014). The fracture plane properties (transmissivity = 1.5 x 10^{-6} m^2/s, aperture = 1.2 x 10^{-4} m) were conservatively chosen to create a relatively permeable feature at depth; for example, fracture transmissivity is at the upper end of values derived from packer tests in shallower deformation zones (~500 m) in the Forsmark metagranite (Follin et al. 2007). However, it is likely that such a permeable feature intersecting the borehole would be identified during site characterization and/or drilling and would result in the borehole being abandoned or relocated.

The discrete fracture plane was mapped to the PFLOTRAN porous medium model domain (see Section 3.2); properties for the porous medium grid cells (anisotropic permeability, porosity) intersected by the fracture were then calculated from the fracture properties (transmissivity, aperture). The resulting borehole-intersecting fracture in the disturbed scenario consists of a "plane" of ECPM grid cells 15 m on a side, and conceptually can be thought of as equivalent to a 15-m thick brittle deformation zone. The fracture/deformation zone has a dip of 30° and intersects the borehole at a depth of 2,540 m.

For the ECPM representation of the "fracture" grid cells, anisotropic permeability[6] depends upon the orientation and transmissivity[7] of the fracture; porosity additionally depends on the fracture aperture. Discrete fracture location, orientation, transmissivity, and aperture were input to a python script called mapDFN, which calculates ECPM anisotropic permeability by rotating the fracture transmissivity tensor into the coordinates of the grid, and ECPM porosity by dividing the length of the grid cell by fracture aperture (see Mariner et al. 2016, Section 3.1.3.1 for details). The resulting ECPM fracture properties, anisotropic permeability = 1 x 10^{-14} m^2, and porosity = 8.1 x 10^{-6}, were implemented in the PFLOTRAN grid and are summarized in Table 3-1.

The ECPM fracture porosity, which is several orders of magnitude smaller than the matrix porosity, creates high groundwater pore (linear) velocities typical of fracture flow. With a hydraulic head gradient of 0.0001 (see Section 3.1.1), these fracture properties result in a Darcy velocity and a groundwater pore velocity in the fracture of 2 x 10^{-4} m/yr and 27 m/yr, respectively.

[6] The ECPM anisotropic permeability, as used in this report, is the permeability in the direction of the fracture (i.e., dipping at 30° relative to the horizontally oriented PFLOTRAN model domain and grid). This directional permeability is produced in PFLOTRAN by separate permeability values in the x, y, and z grid directions.

[7] Transmissivity, T [m^2/s], is equivalent to Kb, where K [m/s] is defined by Equation 3-2 and b [m] is fracture thickness. For T = 1.5 x 10^{-6} m^2/s, b = 15 m, fluid (brine) density ≈ 1000 kg/m^3 and viscosity ≈ 1 x 10^{-3} Pa·s, the corresponding fracture permeability is 1 x 10^{-14} m^2.

3.2 Post-Closure Performance Assessment

3.2.1 Undisturbed (Nominal) Scenario

Nominal scenario PA simulations included a baseline deterministic run (Freeze et al. 2016, Section 5.2.6) and a set of probabilistic realizations (using Latin Hypercube Sampling (LHS) from parameter distributions) to examine the sensitivity and importance of the long-term radionuclide transport to selected processes and parameters (Freeze et al. 2016, Section 5.2.7). Deterministic nominal scenario PA results from PFLOTRAN (described in detail in Freeze et al. 2016, Section 5.2.6) are summarized here, to provide a comparison basis for the new disturbed scenario PA results presented in Section 3.2.2.

The PA model domain for the nominal scenario (Figure 3-2) is 2D axisymmetric with a radius of 923.627 m and a height of 2,534.08 m. The base of the 534.08-m long EZ lies at 5,000 m below the land surface (mbs); the EZ contains 108 4.76-m long waste packages and two 10-m long cement plugs. To minimize peak temperature in the EZ, the cooler Cs waste packages are emplaced in the lower portion of the EZ, where the ambient temperature is higher, overlain by the hotter Sr waste packages. The EZ liner is not modeled. Instead, the entire annular space between the waste packages and the borehole wall DRZ is modeled as a brine-filled EZ annulus.

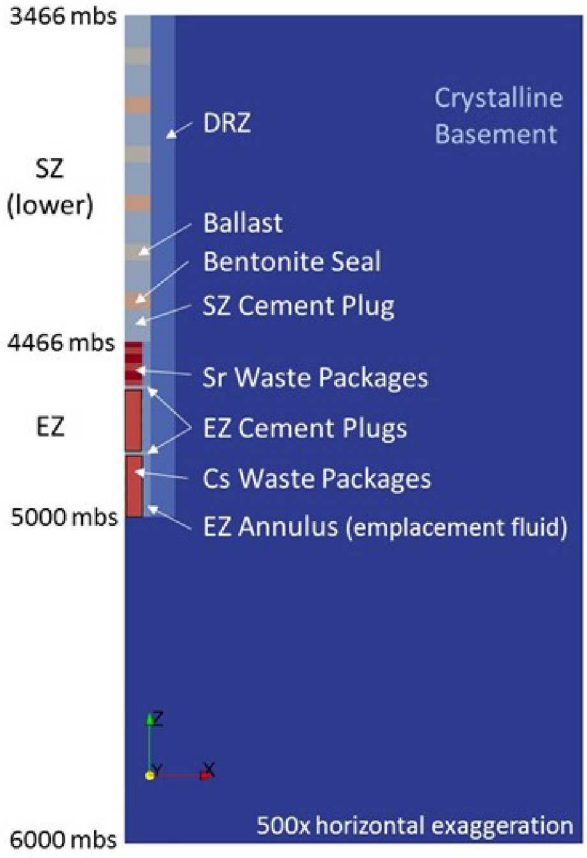

Figure 3-2. A Portion of the DBD PA Model Domain for the Nominal Scenario

The PA model for the nominal scenario includes only the lower portion of the SZ, a 1,000-m interval consisting of alternating lengths of cement, bentonite, and ballast, extending from the top of the uppermost waste package in the EZ to the top of the model domain. Two 100-m-long cement plugs sit at the top and bottom of the lower SZ; five additional cement plugs (each 100-m long) separate alternating 50-m lengths of bentonite seal and ballast material. A DRZ, 0.15 m in width, envelopes the entire length of the borehole.

At the time of waste package breach (one year after sealing), the entire (decayed) inventory of ^{137}Cs, ^{135}Cs, and/or ^{90}Sr in a waste package is assumed to be present in solution within the waste package cell, based on the reference case assumption of unlimited solubility of Cs and Sr in the EZ. Instantaneous dissolution of the entire 18-capsule inventory (in 2050) in a waste package into the void space of the waste package results in a dissolved concentration (source term) of approximately 0.83 mol/L for Cs (from ^{135}Cs and ^{137}Cs) and approximately 0.25 mol/L for Sr (from ^{90}Sr). Unlimited solubility for Cs and Sr is also assumed in the PA model domain beyond the EZ.

Predicted temperatures, fluid fluxes (specific discharge), and radionuclide concentrations for 10,000,000 years were captured at several observation point depths within the model domain, with a focus on the EZ and lowermost SZ cement plug, including the surrounding DRZ.

Temperatures in the EZ, driven by the heat of radioactive decay, peak at ~3 years, reaching 240°C near the midpoint of the EZ. The increase in temperature creates a thermally-driven upward fluid flux that includes effects from fluid thermal expansion (early fluxes of very short duration) and buoyant convection (later fluxes due to buoyancy of the hot fluid, which generally peak at the same time as temperatures, and are relevant to possible radionuclide transport) (SNL 2016a, Section 2.2). The buoyancy-driven flux is largest in the brine-filled EZ annulus of the borehole. However, ~25 m above the top of the EZ, buoyancy-driven vertical specific discharge does not exceed 0.0001 m/yr within the lowermost SZ cement plug or 0.006 m/yr within the surrounding DRZ.

Figure 3-3 shows the concentration of long-lived ^{135}Cs throughout the model domain at 10,000,000 years. The lack of significant buoyancy-driven fluid flux in the SZ is apparent from the negligible ^{135}Cs concentration within the SZ. Even at only ~25 m above the top of the EZ, the concentration of ^{135}Cs never rises above the initial background concentration of 10^{-20} mol/L within the lowermost SZ cement plug or within the surrounding DRZ for the entire simulation duration. Instead, most of the ^{135}Cs remains in the lower part of the EZ, where the 74 waste packages containing the Cs capsules were originally emplaced. The effects of the two 10-m long EZ cement plugs (centered at depths of ~4,805 mbs and ~4,604 mbs) on ^{135}Cs movement are also evident. ^{135}Cs also diffuses laterally through the crystalline host rock away from the EZ. However, after 10,000,000 years, the ^{135}Cs concentration contour of 10^{-15} mol/L has only reached a radius of approximately 20 m beyond the EZ. No ^{135}Cs reaches the biosphere, so there is no dose.

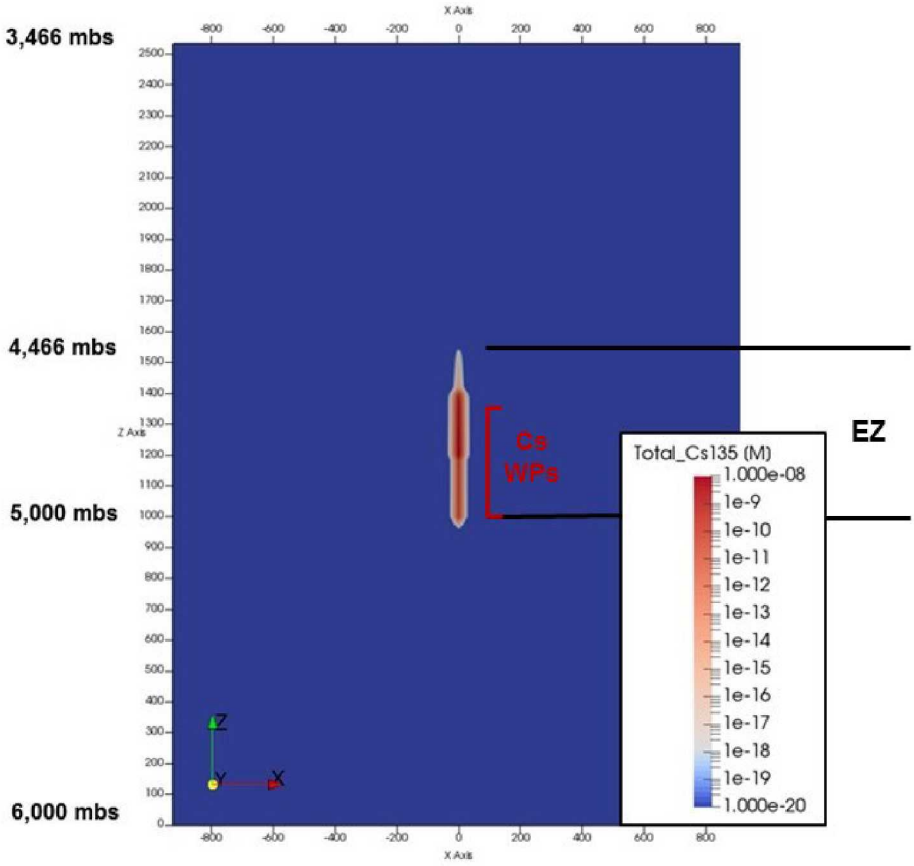

Source: Freeze et al. (2016, Figure 5-8)

Figure 3-3. Dissolved Concentration of ^{135}Cs at 10,000,000 Years for the Nominal Scenario

3.2.2 Disturbed (Stuck Package) Scenario

The disturbed scenario included a waste package "stuck" in the crystalline basement above the EZ near a hypothetical borehole-intersecting fracture. PA simulations included two deterministic runs to examine the sensitivity to the regional head gradient.

The disturbed scenario (Figure 3-4) uses the same reference design, conceptual model, and parameters as the nominal scenario, except for the presence of (1) a hypothetical borehole-intersecting fracture in the crystalline basement above the EZ, (2) a single Cs waste package "stuck" near the borehole-intersecting fracture, and (3) cement injected into the SZ below the stuck package instead of engineered seals and plugs.

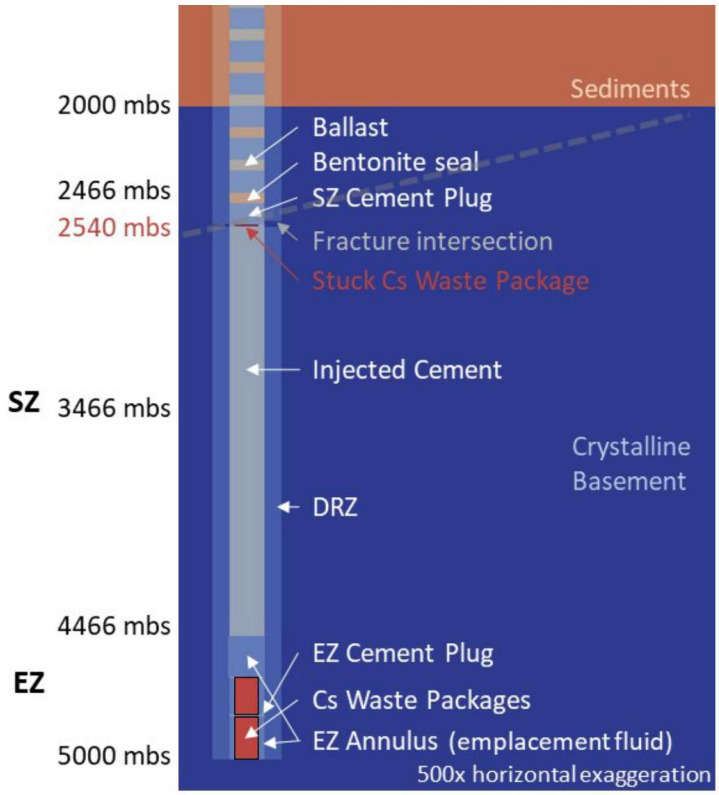

Figure 3-4. A Portion of the DBD PA Model Domain for the Disturbed Scenario

The presence of the fracture/deformation zone necessitated the use of a half-symmetry 3D model domain for the disturbed scenario simulations; the 3D domain is conceptually equivalent to the 2D axisymmetric domain used in the nominal scenario simulations. The 3D model domain is 2,000 m in length (x), 1,000 m in width (y), and 6,000 m in height (z). The half-symmetry (in the y-direction) borehole is centered in x at the front face of the model domain. Refined discretization in x, y, and z at and around the borehole allows definition of individual waste packages (0.11 m radius), the borehole annulus (0.16 m radius), and the DRZ (0.32 m radius). Due to the nature of the vertical refinement at the borehole, it was necessary to choose a single vertical discretization (dz = 5 m) for cells within and around the borehole. As a result, the lengths of cement, bentonite, and ballast regions in the seal (all multiples of 5) were identical to lengths in the 2D axisymmetric grid used in the nominal scenario simulations, and waste packages were slightly longer (5 m as compared to 4.76 m in the 2D grid). Grid cell dimensions increase away from the borehole to 15 m in the x and y dimensions.

Whereas the nominal scenario 2D grid had a vertical z-dimension of 2,534 m (from 6,000 m depth to the top of the lower SZ), the disturbed scenario 3D grid has a vertical z-dimension of 6,000 m (the upper 2,000 m are undifferentiated sediments; the lower 4,000 m are crystalline basement, including the EZ and SZ). As described in Section 3.1.2, the borehole-intersecting fracture was conceptualized as a 15-m thick brittle deformation zone with 30° dip that intersects the borehole at a depth of 2,540 m and has a permeability of 1×10^{-14} m^2 and a porosity of 8.1×10^{-6} (Table 3-1).

For the disturbed scenario, the first 73 Cs waste packages are assumed to be emplaced in the lower portion of the EZ, and the final Cs waste package is assumed to get stuck in the guidance casing during emplacement at the depth of the fracture intersection (2,540 mbs). This location is within the upper SZ, 1,926 m above the top of the EZ and 540 m below the base of the sediments. It is assumed that (1) the stuck waste package cannot be fished, is left in place, and is breached, (2) the SZ seals and plugs below the stuck package are not present, the underlying SZ is instead filled with injected cement to the extent possible (with properties less robust than the engineered cement plugs), and (3) the SZ and UBZ above the stuck waste package are sealed and plugged as planned. Because of the stuck package, the 34 Sr waste packages are not present.

Deterministic simulations were run with PFLOTRAN for two disturbed scenario cases: one with no regional head gradient, and one with a regional head gradient of 0.0001 m/m, driving flow up dip toward the base of the sediments. Figure 3-5 shows the ^{135}Cs concentrations throughout the model domain at 10,000,000 years for each of these cases.

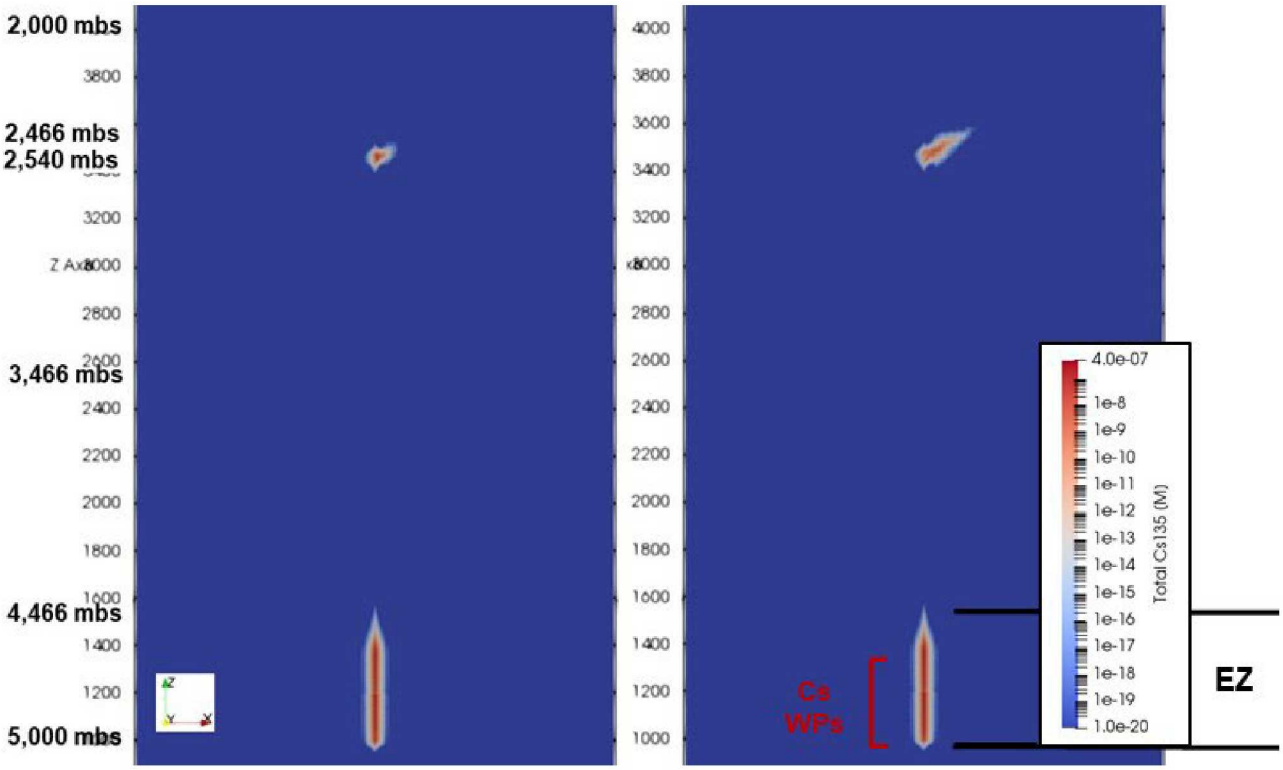

(a) regional gradient = 0 m/m **(b) regional gradient = 0.0001 m/m**

Figure 3-5. Dissolved Concentration of ^{135}Cs at 10,000,000 Years for the Disturbed Scenario

As in the nominal scenario, most of the ^{135}Cs from the first 73 Cs waste packages remains in the lower part of the EZ. For the case with no regional head gradient (Figure 3-5a), a small amount of ^{135}Cs is present in the fracture, due to early-time buoyant convection followed by slow diffusive transport from the single stuck waste package. For the case with a regional head gradient of 0.0001 m/m (Figure 3-5b), ^{135}Cs is advected a distance of approximately 200 m up the fracture over the course of the 10,000,000-year simulation, but is still approximately 400 m below the sediments. This transport distance is consistent with Equation 3-7, which predicts a center-of-mass transport distance for Cs, with a K_d of 22.5 L/kg, of 36 m.

These preliminary disturbed scenario results suggest that, even in the presence of a regional head gradient, long-term advection of radionuclides away from a stuck waste package through a hypothetical borehole-intersecting transmissive fracture, is minimal.

4 CONFIDENCE ENHANCEMENT

In a safety case, confidence enhancement refers to information that provides additional support for the quantitative pre-closure and post-closure safety assessments. It includes qualitative or quantitative evidence, arguments, scientific observations, and/or analyses that were not directly included in the safety assessment models, but that provide additional insights into the robustness, behavior, and evolution of the repository system (Freeze et al. 2016, Section 3.3.3).

Confidence in the DBD concept, supporting the quantitative assessments, derives from the following, summarized in Section 1.5:

Pre-Closure Operations:

- Adequacy of Site Characterization
- Achievability of Deep Drilling
- Safety of Site Operations

Post-Closure Isolation:

- Great Depth of Disposal
- Isolation and Long Residence Time of Deep Groundwater
- Density Stratification of Brine at Depth
- Low Permeability of Crystalline Host Rock
- High-Likelihood of Slow Diffusion-Dominated Radionuclide Transport
- Geochemically-Reducing Conditions at Depth
- Low Permeability and High Sorption Capacity of Seal Materials
- Multi-Barrier Design

Additional confidence enhancement information presented here includes:

- Evidence for isolation and long residence time of deep groundwater (Section 4.1)
- Hydrologic modeling of density stratification of brine at depth (Section 4.2)
- Review of borehole sealing materials and technologies (Section 4.3)

4.1 Evidence for Isolation and Long Residence Time of Deep Groundwater

The robustness of the DBD concept relies in large part on the subsurface hydrogeology and geochemistry, specifically: low permeability and porosity in the host rock; lack of significant vertical connectivity in the DRZ; chemically reducing, high salinity, and density stratified groundwater at depth, and evidence of isolation of deep groundwater. The measurement and confirmation of these heterogeneous properties and conditions poses technical challenges.

A preliminary borehole sampling and testing strategy (SNL 2016b) was developed for key parameters that need to be measured in the 2- to 5-km depth range encompassing the DBD seal and emplacement zones. The testing and sampling strategy has recently been revised (Kuhlman et al. 2019). Key sampling and testing activities that can contribute to better characterization of the subsurface hydrogeology and geochemistry include:

- Sampling and Evaluation While Drilling (Kuhlman et al. 2019, Section 3.12): drilling fluid (mud) logging, coring and core analysis, borehole geophysical logging, single-packer hydraulic testing and sampling, and hydraulic fracturing (mini-frac) tests
- Open Hole Testing and Sampling (Kuhlman et al. 2019, Section 4): flowing fluid electrical conductivity (FFEC) logging, multi-packer hydraulic testing and sampling, hydraulic fracturing stress measurement tests, and injection/withdrawal (push-pull) tracer tests

The testing activities are generally focused on determining (a) geomechanical properties associated with borehole stability that are important during pre-closure drilling and downhole waste emplacement; and/or (b) hydrogeologic properties (e.g., permeability and porosity) that are important to post-closure groundwater flow and radionuclide transport.

The sampling activities are generally focused on geochemical properties that can be indicative of (a) reducing conditions at depth that can limit radionuclide mobility in groundwater, and (b) the origin, residence time, and/or isolation of deep groundwater.

A key challenge, as noted in Freeze et al. (2016, Section 6.4), is collecting evidence for isolation and long residence time of deep groundwater. The origin and residence time of deep groundwater can be estimated from geochemical sampling for chemical composition (e.g., salinity) and environmental tracers with long half-lives (e.g., ^{36}Cl, ^{81}Kr, ^{4}He, $^{234}U/^{238}U$ ratio).

4.1.1 Chemical Composition and Salinity

Fluid compositions depend on mineralogy and geologic history including episodes of marine intrusion and glaciation, but in general, groundwater in the crystalline basement tends to occur in distinct compositional zones correlated with depth (Fritz and Frape 1982; NEDRA 1992; Gascoyne 2004; Kietavainen et al. 2013; DeMaio and Bates 2013):

- Shallow zone (0 – 500 m depth), where groundwater regularly interacts with surface water and has a low total dissolved solids (TDS) (< 30 g/L). Fluids are dilute to brackish with major element compositions dominated by sodium (Na^+), calcium (Ca^{2+}) and bicarbonate (HCO_3^-).
- Intermediate zone (500 – 1,500 m depth), where the transition to higher TDS occurs. Fluids are more saline and evolve toward Na and Ca sulfate (SO_4^{2-}) and chloride (Cl^-) compositions.
- Deep zone (> 1,500 m depth), where fluids have TDS from > 50 g/L to a maximum of about 350 g/L. Deep fluids are typically saline brines of NaCl or $CaCl_2$ composition (with Ca/Na ratio increasing with depth), although magnesium (Mg^{2+}) and/or bromide (Br^-) may be a minor presence (Frape 2015). Densities of deep brines can range from 2.5% greater than pure water (similar to seawater, ρ = 1.025 g/cm^3) to more than 30% greater than pure water (ρ = 1.300 g/cm^3) (Park et al. 2009; Phillips et al. 1981; DeMaio and Bates 2013, Figure 5).

The origins of deep brines can be either (1) allochthonous/paleoseawater – due to recharge from shallower saline water, or (2) autochthonous/paleometeoric water – due to fluid-rock interactions in the deep subsurface. In either case, high salinity at depth can be a general indicator of isolation from shallower groundwater over extended periods of time. Recent studies have shown groundwater deeper than 2 km in the Precambrian basement to have been isolated from the atmosphere for greater than one billion years (e.g., Holland et al. 2013; Gascoyne 2004).

Specific conditions that could lead to allochthonous deep brine include:

- recharge of saline water during periods of marine intrusion (Park et al. 2009)
- evaporative concentration and/or freezing of seawater followed by recharge (e.g. Bottomley et al. 1994)

Hydrologic modeling of high salinity at depth and density stratification of brine under allochthonous conditions is described in Section 4.2.

Specific conditions that could lead to autochthonous deep brine include:

- fluid-rock (e.g., evaporite) interactions that increase dissolved salts (Park et al. 2009)
- fluid-rock (e.g., granite) interactions that incorporate water in hydrous phases (Frape et al. 1984)
- leakage of salt-rich fluid inclusions (Nordstrom and Olsson 1987)
- radiolytic dehydration of subsurface waters (Vovk 1987)

Reaction path modeling of deep brines was used to test the second of these autochthonous conditions. Reaction path calculations were performed using the PHREEQC code (Parkhurst and Appelo 1999) to estimate whether fluid-rock interaction can dehydrate brines, and concentrate salts, by altering granite to more hydrous phases of zeolite and chlorite, and account for the

transition from Na-dominated dilute brines (seawater) to the more concentrated Ca-dominated brines observed at greater depth.

The overall bulk reaction to be modeled is:

Granite + H2O → Hydrous phases + Brine

Granite commonly consists of quartz, potassium feldspar (K-feldspar), and plagioclase feldspar (albite), with smaller amounts of muscovite, biotite, and hornblende. Chlorite and epidote are the most commonly encountered hydrous silicates in deep granites; less common are mica, the zeolite laumontite, and prehnite (Juhlin et al., 1998). Idealized chemical formulae for granite minerals and the hydrous silicates are listed in Table 4-1 and Table 4-2, respectively.

Table 4-1. Primary Granite Minerals

Quartz	SiO_2
K-Feldspar	KAlSi3O8
Plagioclase (Albite)	NaAlSi3O8
Muscovite	$KAl_3Si_3O_{10}(OH)_2$
Biotite[a]	$KMg_3AlSi_3O_{10}(OH)_2$
Hornblende[b]	$NaCa_2(Mg_4Al)(Si_6Al_2)O_{22}(OH)_2$

[a] Phlogopite end-member
[b] Pargasite end-member

Table 4-2. Common Hydrous Silicates in Deep Granite Fractures

Chlorite	$(Mg_5Al)(AlSi_3)O_{10}(OH)_8$
Laumontite	$Ca(AlSi_2O_6)_2 \cdot 4H2O$
Mica	$KAl_2(AlSi_3O_{10})(OH)_2$
Prehnite	$Ca_2Al(AlSi_3O_{10})(OH)_2$
Epidote	$Ca_2Al_3(SiO_4)(Si_2O_7)O(OH)$

For the reaction path calculation, a hypothetical granite was assumed having approximately 20% quartz, 40% K-feldspar, 15% plagioclase (albite), 9% muscovite, 8% biotite, and 8% hornblende by volume. This mineralogic idealization represents a 10 kg (3.8 L) block having a mixture of 33.3 moles quartz; 14.4 moles K-feldspar, 5.7 moles albite, 2.2 moles muscovite, 1.8 moles biotite, and 0.9 moles hornblende. This "granite" is "reacted" with 0.1 L of seawater at 100°C. This is a 38:1 rock-fluid ratio by volume, which is equivalent to a rock with a fluid-filled porosity of ~3%.

In the PHREEQC calculation, the llnl.dat (thermo.com.V8.R6.230) thermodynamic database was used. Biotite and hornblende are approximated in the calculation with end-members phlogopite, $KMg_3AlSi_3O_{10}(OH)_2$, and pargasite, $NaCa_2(Mg_4Al)(Si_6Al_2)O_{22}(OH)_2$. Calcite, gypsum, and kaolinite are allowed to form if saturated. Seawater was used as a generic input fluid with the expectation that the composition of the starting fluid will be evaluated in later studies when better constrained for generic sites, along with more precise considerations of activity coefficients.

The calculation was initially set up to allow dissolution of all granite phases to equilibrium, that is assuming sufficient time and water access to dissolving and precipitating mineral surfaces. This is probably a reasonable assumption given the multi-million-year contact times of most brines with deep granites. The input file was written so that biotite was allowed to dissolve, but not precipitate, which results in chlorite formation. The chlorite composition was set to that of end-member clinochlore 14A, $Mg_5Al_2Si_3O_{10}(OH)_8$, in the llnl.dat database. This was done in the PHREEQC input formalism by sequentially reacting biotite and hornblende with the fluid and the equilibrium phase assemblage described above.

The generalized granite hydrolysis reaction is:

Seawater + 4.98 Quartz + 0.54 Hornblende (Parg.) + 1.29 Muscovite + 0.54 Biotite (Phlog.)
→ 0.57 Albite + 1.83 K-Feldspar + 0.76 Chlorite + 1.06 Laumontite + Brine

This reaction produced a residual Ca-Na-Cl brine with pH ~6.8. There was a net loss H_2O from the fluid, thereby concentrating the dissolved salts and increasing the ionic strength of the solution. In the calculation, almost all of the quartz dissolved; the albite and K-feldspar masses correspondingly increased substantially. In addition to the major alteration phases, minor amounts (< 0.02 moles) of epidote, calcite, and gypsum also formed.

Stoichiometrically, there was an addition of 0.54 moles of H_2O from hornblende dissolution, 0.54 moles from biotite dissolution, and 1.29 moles from muscovite dissolution, followed by a liquid water loss of 7.28 moles by incorporation of H_2O into zeolite (laumontite) and chlorite, resulting in a net loss of 4.9 moles of liquid water from granite hydrolysis. The initial 0.1 L of water (5.6 moles) was reduced to 0.012 L (5.6 – 4.9 = 0.7 moles H_2O), and the dissolved salts concentrated roughly 8-fold, increasing the ionic strength from 0.6 molal to 4.4 molal (Figure 4-1).

For comparison, end-member Canadian Shield brines from Frape et al. (1984), those having highest salt contents of ~240 – 325 g/L, have ionic strengths of 4.5 – 6.2 molal. The fluid Ca/Na ratio calculated for granite hydrolysis is 1.55 (Figure 4-1), which is within the range of Ca/Na ratios measured from Canadian Shield brines, $0.7 < Ca/Na < 3$ by Frape et al. (1984), giving some confidence in the generic granite hydrolysis calculation results. The granite hydrolysis calculations also predict very low Mg, similar to what is observed in the Canadian Shield brines.

Throughout the reaction path, the calculated pH of the fluid remains between 6.8 and 7.1. The concentration of Mg decreases with the extent of granite hydrolysis due to chlorite precipitation which consumes Mg. Calcium increases in solution because the supply of Ca from biotite dissolution exceeds the amount of Ca taken up by laumontite formation. The solution pH is probably controlled by K-feldspar/kaolinite equilibria (e.g., Baccar and Fritz 1993; Smith and Ehrenberg 1989), while albite/K-feldspar probably sets Na/K (Pearson 1987). Increasing the reaction temperature from 100°C to 150°C decreases fluid Ca and Mg levels, but increases fluid K levels. The ionic strength remains roughly the same as at 100°C.

Figure 4-2 shows the change in net rock volume (ΔV), calculated as the volume of minerals formed (e.g., hydrous silicates) minus the volume of minerals dissolved (e.g., biotite, hornblende). The figure shows that the change in net rock volume exceeds the initial water volume (0.1 L, corresponding to an initial pore volume of 100 cm^3) before 0.1 moles of biotite + hornblende has reacted, indicating the expansive nature of the alteration. This result suggests that alteration product accumulation may ultimately limit granite hydrolysis through physical sealing of the small available porosity/permeability.

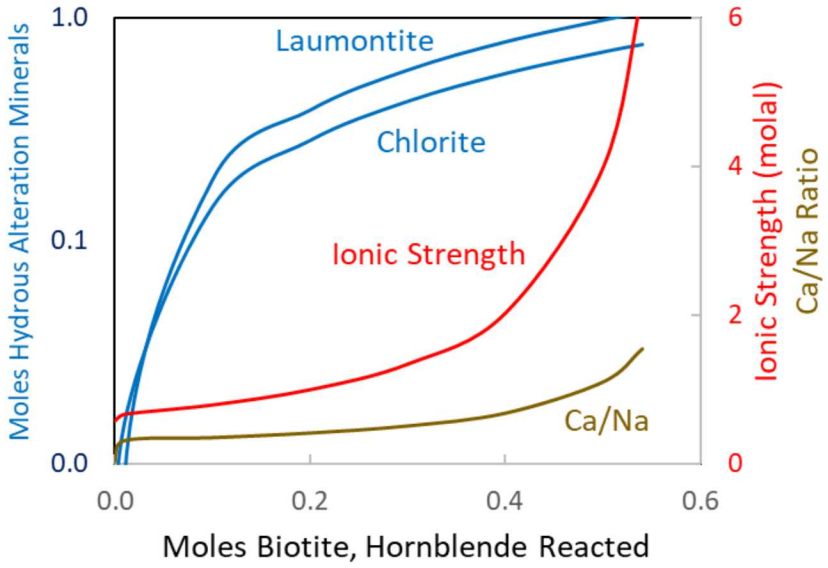

Figure 4-1. Calculated Brine Evolution at 100℃

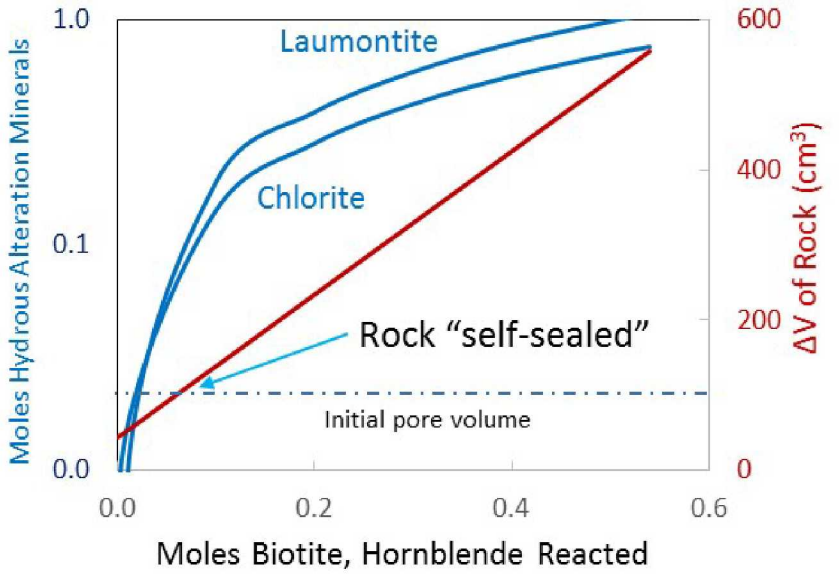

Figure 4-2. Volume Changes from Alteration at 100℃

Some caveats are in order. In the granite hydrolysis calculations, the anorthite component of plagioclase was ignored, primarily because it is so small in granites. Plagioclase in granite is typically low Ca ~An_0 – An_{10} (e.g., Bucher and Stober 2010). But it is potentially important because the anorthite component of plagioclase dissolves non-stoichiometrically (Gardner 1983), and far faster than the albitic end-member, which would increase Ca in the developing brine. Anorthite never dissolves to saturation in the calculations, unlike albite. This means that the endpoint salinities of the granite hydrolysis calculations depend directly on the mass of anorthite put into the calculation.

In near surface environments, anorthite dissolves at least 5 to 10 times faster than the albite component of plagioclase (Clayton 1988; Mast and Drever 1987; Oxburgh et al. 1994). The non-stoichiometry is observed both over relatively short-term lab experiments (< 2,000 hours) and in longer-term watershed studies, and has been proposed to occur in brines in contact with deep granites (Edmunds et al. 1987). Extra Ca is likely produced by accelerated leaching of exsolution intergrowths, dislocations, and/or Ca-rich zonations. Including anorthite in granite hydrolysis calculations increases the final ionic strength, increases the Ca/Na ratio of the fluid, increases the amount of laumontite formed, and decreases calculated chlorite formation.

Another uncertainty in the calculations is activity coefficients in high ionic strength brines (> 1 molal), and the end-point phase assemblage of alteration products, particularly silicates. In higher temperature/pressure aqueous systems, previous studies of crustal fluid-rock reactions (Sassani and Pasteris 1988; Sassani 1992) utilized the approximation of an extended Debye-Huckel activity coefficient approach for such systems. That approach, used here, provides a reasonably accurate approximation based on the true ionic strength of the fluid (which is much lower than the stoichiometric ionic strength due to the high degree of ion complexation in the solution at such conditions). Without consideration of the relevant Pitzer coefficients for these fluids, these approximate results are useful for trends at this point, but accurate prediction of silicate mineral-fluid equilibria remains somewhat uncertain. These first steps at quantification provide a starting point for more explicit and precise evaluations.

Another aspect of the calculation requiring further analysis is Cl/Br ratio. The calculated residual brine has a Cl/Br mass ratio of 286, essentially that of modern seawater and evaporated seawater. This is substantially higher than the Cl/Br ratio observed in deep brines, ~77 – 167, which may be controlled by fluid inclusions or the Cl/Br content of trace minerals. A source of Br, or a mechanism for losing Cl, is needed in the calculation to produce the measured Cl/Br of the deep crustal brines. One possible source of some of the missing Br is leakage from relatively Br-rich fluid inclusions (e.g., Nordstrom et al. 1989; Nordstrom and Olsson 1987). But only “a few thousand mg/L of chloride” are likely to be contributed by fluid inclusions (Nordstrom and Olsson 1987). Another possible explanation is that fluid Cl levels can be decreased by chloride exchange for hydroxyls in the secondary chlorite and zeolite (Bucher and Stober 2002). Yet another theory is that Br levels in the starting brine were higher because the brines were altered through evaporation/freezing before encountering the granites (e.g., Bottomley et al. 1994). Each of these mechanisms could be evaluated in greater detail.

In summary, these reaction path analyses suggest that granite hydrolysis may be capable of removing ~90% of the water from a starting fluid, given sufficient time for reaction, leading to concentrated brine formation with a Ca/Na ratio higher than 1. If this is the case in the subsurface, then isolation of fluids in the deep crystalline basement may be an inherent feature of regions where through-going fracture system flow is absent.

The next steps are to use the reaction path model to work backwards towards a more closely constrained starting fluid chemistry, and to explicitly consider mineral kinetics. The first means establishing the sensitivity of the PHREEQC calculations to input water chemistry, including a more thorough comparison of predicted and observed mineral alteration, and detailed consideration of activity coefficient effects at high ionic strength. Tying the granite hydrolysis reaction to measured mineral dissolution rates should allow order-of-magnitude estimates of the minimum time required for brine formation, and might therefore set constraints on how "old" deep brines actually are.

4.1.2 Environmental Tracers

Environmental tracers, including both isotopic and chemical tracers, can be used to estimate or bound groundwater age (i.e., the average time water molecules in a sample have resided in the subsurface (Bethke and Johnson, 2008) and provenance (i.e., the origin and time history of subsurface hydrogeochemical processes that contributed to the composition and location of the sample). The origin of isotopic tracers may be cosmogenic (production from cosmic radiation in the earth's atmosphere, subsequently introduced into the upper ocean), nucleogenic (production from natural terrestrial nuclear reactions other than cosmic rays), radiogenic (natural production from radioactive decay), and/or anthropogenic (from nuclear bomb tests, technogenic emissions) (Aggarwal et al. 2005, Chapter 3). Nucleogenic and radiogenic isotopes often derive from nuclear processes associated with natural U and/or Th in rock. Chemical tracers include anthropogenic compounds such as manufactured gases, chlorofluorocarbon (CFC) compounds, and sulfur hexafluoride (SF_6) (Bethke and Johnson 2008). In addition to isotopic and chemical tracers, groundwater age and provenance can also be inferred from isotopic ratios, such as those involving one or more stable isotopes (e.g., $\delta^2H/\delta^{18}O$, $^3H/^3He$) or nucleogenic isotopes (e.g., $^{234}U/^{238}U$, $^{87}Sr/^{86}Sr$). Some of the more common environmental tracers are listed in Table 4-3. A detailed discussion of these environmental tracers can be found in Aggarwal et al. (2005), Bethke and Johnson (2008), and IAEA (2013).

Table 4-3. Selected Environmental Tracers

Tracer	Half-Life (yrs)	Groundwater Timescale (yrs)	Dominant Source	Other Source(s)
δ^2H / $\delta^{18}O$	n/a	0.1 – 3	Stable isotopes	
^3H / ^3He	n/a	0.5 – 40	Anthropogenic / Stable	
^{85}Kr	10.72	1 – 40	Anthropogenic (nuc. industry)	
CFCs, SF_6	n/a	1 – 40	Anthropogenic (manufacturing)	
^3H (tritium)	12.3	1 – 50	Anthropogenic (bomb tests)	Cosmogenic Anthropogenic (nuc. industry)
^{32}Si	~150	50 – 1,000	Cosmogenic	
^{39}Ar	269	50 – 1,000	Cosmogenic	
^{14}C	5,730	1,000 – 40,000	Cosmogenic	Anthropogenic (bomb tests) Anthropogenic (nuc. industry)
^4He	Stable	100 – 1,000,000	Nucleogenic	
^{81}Kr	210,000	50,000 – 1,000,000	Cosmogenic	
^{36}Cl	301,000	50,000 – 1,000,000	Cosmogenic	Anthropogenic (bomb tests)
^{234}U / ^{238}U	245,500 / 4,468,000,000	10,000 – 1,000,000	Nucleogenic	
^{129}I	15,700,000	3,000,000 – 80,000,000	Anthropogenic (nuc. industry)	Anthropogenic (bomb tests) Cosmogenic
^{87}Sr / ^{86}Sr	Stable		Radiogenic	

Sources: Aggarwal et al. (2005, Chapter 18, Table 1); Aggarwal et al. (2005, Chapter 3 and Table 2); IAEA (2013, Fig. 1-.3)

Saline fluids at depth have high concentrations of dissolved gases that reflect long exposure to the surrounding rocks in a closed system, including abiogenic H_2 and CH_4 resulting from extensive water/rock reactions, and stable isotopes of noble gases resulting from decay of U, Th, and K naturally occurring in crystalline rock (Holland et al. 2013; Lippmann-Pipke et al. 2011; Kietavainen et al. 2013). Absolute concentrations as well as ratios of radiogenic (^4He, ^{40}Ar), nucleogenic (^{21}Ne, ^{22}Ne), and fissionogenic (^{134}Xe, ^{136}Xe) stable isotopes of noble gases can be used to calculate fracture fluid residence times. Such analyses indicate residence times for deep fluids in the Outokumpu Deep Drill Hole (Fennoscandian Shield) of between 20 million and 50 million years (Kietavainen et al. 2014); residence times for deep (2.4 km) fluids in the Canadian Shield of greater than 1 billion years (Holland et al. 2013); and residence times for fluids from deep (up to 3.3 km) mines in the Witwatersrand Basin (South Africa) of between 1 million and 23 million years (Lippmann et al. 2003).

Additional lines of evidence that point to long fracture fluid residence times in deep cratonic rocks include $\delta^2H/\delta^{18}O$ and $^{87}Sr/^{86}Sr$ ratios indicative of extensive water rock reaction (Kietavainen et al. 2013) or pre-glacial recharge (Gascoyne 2004); and $\delta^{34}S$ and Br/Cl values indicative of seawater or evaporite origin in regions where the most recent marine transgression occurred millions of years ago (Fritz and Frape 1982; Bottomley et al. 1994; Gascoyne 2004).

To support the DBD safety case, the focus is on evidence for isolation and long residence time of deep groundwater; specific applications for identifying "old" groundwaters are discussed in SNL (2016a, Section 2.1) and Freeze et al. (2016, Section 4.3.2.5). The testing and sampling strategy to support DBD (Kuhlman et al. 2019) includes sample collection to determine salinity and brine composition at depth and the presence of longer-lived environmental tracers (e.g., ^{36}Cl, ^{81}Kr, ^{4}He, $^{234}U/^{238}U$ ratio). Specific sample analyses to support these objectives include (Kuhlman et al. 2019, Section 5 and Table 4):

- Major Anions: Br^-, F^-, I^-, SO_4^{2-}, $NO_3^- + NO_2^-$
- Major Cations: Na^+, Ca^{2+}, K^+, Mg^{2+}, $Fe^{2+, 3+}$
- Trace Elements: Al, Sb, As, Ba, Be, Cd, Cr, Co, Pb, Li, Mn, Hg, Mo, Ni, Se, Sr, Ag, Sn, U
- Trace Elements (to compare with concentrations in rock samples/isotopic ratios): Li, Sr, Th, U
- Noble Gases: He, Ne, Ar, and Xe
- Cosmogenic/Anthropogenic Isotopes: ^{3}H, ^{21}Ne, ^{36}Cl, ^{85}Kr, and ^{129}I
- Fission Products Isotopes: ^{36}Cl and ^{129}I
- Radiogenic/Nucleogenic Noble Gas Tracers: ^{3}He, ^{4}He, ^{39}Ar, ^{81}Kr, and ^{129}Xe
- Isotopic Ratios: $^{234}U/^{238}U$, $^{87}Sr/^{86}Sr$, $^{6}Li/^{7}Li$
- Stable Isotopes: $\delta^{18}O$ (oxygen) and $\delta^{2}H$ (deuterium)
- Water Quality Parameters: pH, Eh, temperature, viscosity, salinity, TDS, density/specific gravity

4.2 Hydrologic Modeling of Density Stratification of Brine

As summarized in Section 4.1.1 (and in Freeze et al. 2016, Section 4.3.2.5), groundwater in the crystalline basement tends to occur in distinct compositional zones; shallower fluids are dilute to brackish, whereas the deepest fluids are saline brines. High salinity at depth and density stratification of brine can be indicative of isolation from shallower water.

Park et al. (2009) performed simulations of regional-scale, density-dependent flow and transport over 1,000 years to illustrate how density stratification can inhibit fluid flow at depth and maintain hydraulic isolation of deep basement even when the basement is permeable (highly fractured). In the following subsections, the Park et al. (2009) simulations are extended to longer time periods (1,000,000 years), different basement permeabilities, and to a modified geologic sequence consistent with a DBD site.

4.2.1 Conceptual Model

A schematic illustration of topographically-driven groundwater flow in an unconfined fresh water aquifer with uniform properties is shown in Figure 4-3a. The possible influence of deep brine to reflect or refract flow near the fresh water/brine interface (Park et al. 2009) is shown schematically in Figure 4-3b.

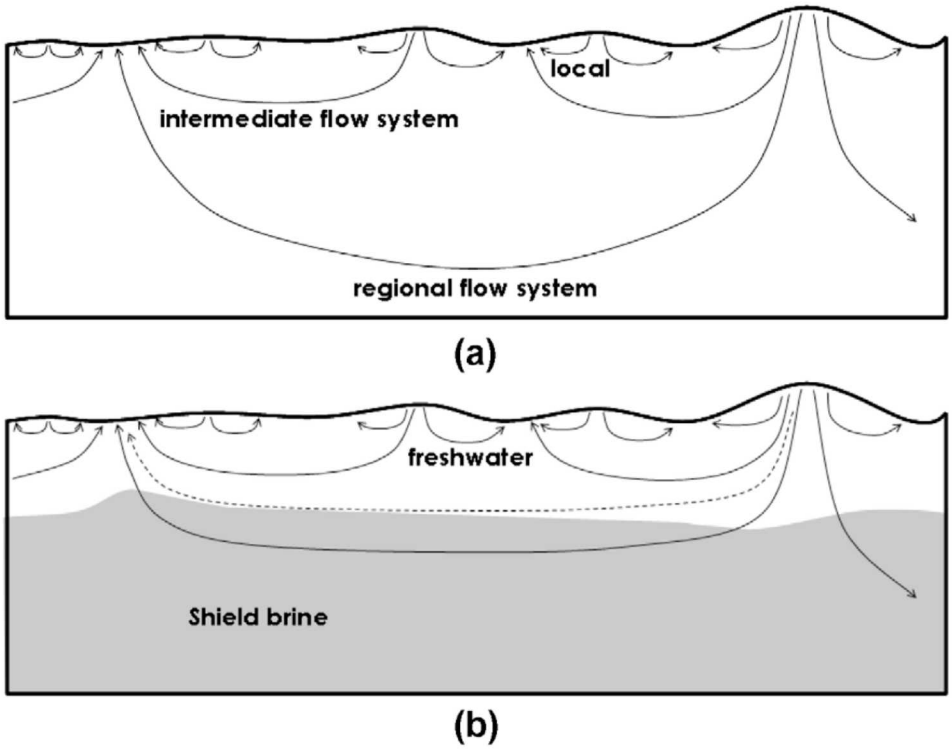

(a) fresh water environment (b) deep (Canadian Shield) brine environment

Source: Park et al. (2009, Fig. 1)

Figure 4-3. Schematic Illustration of the Groundwater Flow

To simulate the potential effects of density stratification of brine, Park et al. (2009) set up a 2D model domain with a specified hydraulic head difference *(*ΔH) of 50 m on the ground surface, representative of topographically-driven regional flow with a hydraulic head gradient of 0.01 (Figure 4-4). The pore water in the domain is initially stratified; a 500-m layer of fresh water (ρ_o = 1.00 g/cm^3) overlies a 2,500-m layer of brine (ρ_b = 1.20 g/cm^3).

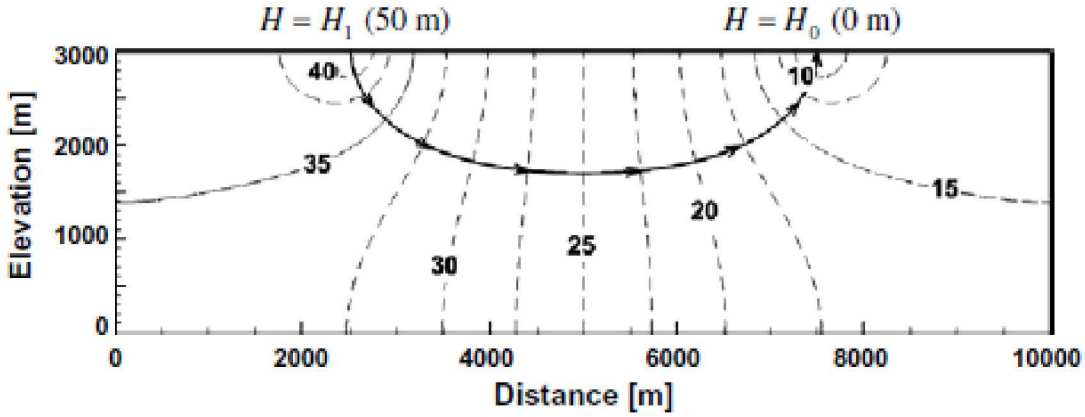

Source: Park et al. (2009, Fig. 6a)

Figure 4-4. Schematic Illustration of Regional-Scale Model Domain and Flow Path

4.2.2 Numerical Implementation

The PFLOTRAN code (see Section 3) was used to perform single-phase, isothermal groundwater flow and non-reactive tracer transport simulations to further explore the effects of density stratification and vertical flow and mixing at depth. In PFLOTRAN, fluid density is calculated as a function of salinity, temperature, and pressure. Salinity is calculated from the concentration of a conservative tracer with the molecular weight of NaCl. For these simulations, the fluid was assumed to be at a constant temperature (25°C) and viscosity (10^{-3} Pa·s).

PFLOTRAN simulations were performed at two model scales. First, a regional-scale model domain was used for comparison with, and extension of, the simulations of Park et al. (2009) (Section 4.2.2.1). Second, a DBD-scale model domain was used to examine density effects at depths expected at a DBD site (Section 4.2.2.2).

4.2.2.1 Regional-Scale Simulations

The PFLOTRAN regional-scale model domain (Figure 4-5) was the same as the 2D domain used by Park et al. (2009), with a horizontal length of 10,000 m and a depth of 3,000 m. The domain was discretized into 10-m by 10-m grid cells to produce a grid 1,000 cells long by 300 cells deep (this discretization is finer than the 100 m by 100 m cells used by Park et al. (2009)).

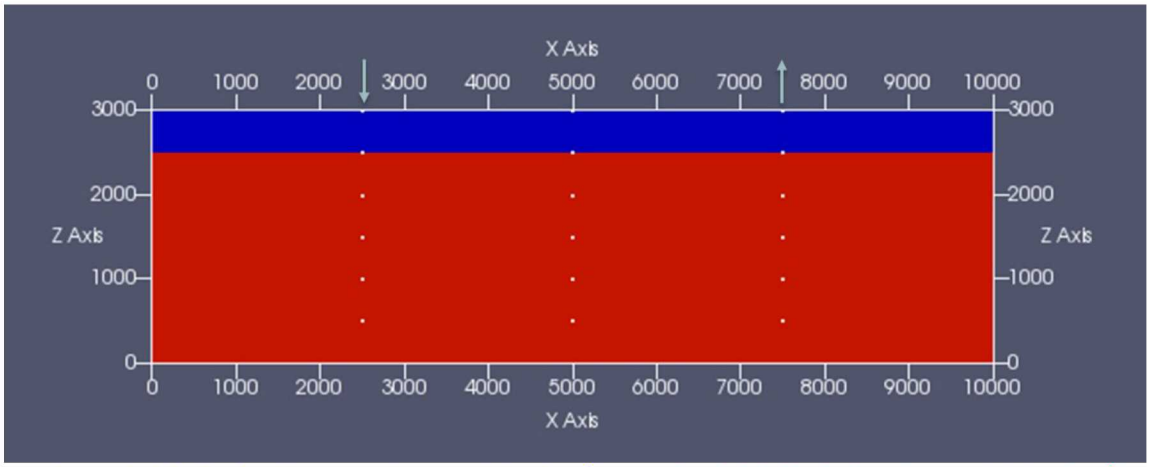

[Blue = initially fresh water ($\rho_o \approx 1.00$ g/cm^3) / Red = initially brine ($\rho_{bo} \approx 1.20$ g/cm^3)]

Figure 4-5. Regional-Scale Model Domain and Initial Salinity Stratification

Initial pressure was calculated as a fresh water hydrostatic gradient. Initial tracer concentration (C_t), representing salinity, was stratified, with fresh water (C_t = 0.029 M, corresponding to $\rho_o \approx$ 1.00 g/cm^3) from 0 to 500 m depth and brine (C_t = 4.45 M, corresponding to $\rho_{bo} \approx$ 1.20 g/cm^3) from 500 to 3,000 m depth. This initial condition does not account for the effect of salinity on pressure, but does account for the effect of pressure on density. The actual chemistry of the brine is not considered in the model.

Tracer concentration is not held constant at any point in the model domain, allowing the salinity to evolve with time as it does in the allochthonous (isolated recharge water) model described by Park et al. (2009). If tracer concentration were held constant at depths from 500 to 3000 m, consistent with the autochthonous (ongoing rock-water interaction) model, the ability of fresh water recharge to penetrate to depths greater than 500 m (and "flush" out brine) would be less than that observed in these simulations.

All model boundaries are no-flow except for two 100-m long regions on the top boundary of the domain. At these locations, constant pressure boundary conditions are applied to establish recharge (from x = 2,450 to 2,550 m) and discharge (from x = 7,450 to 7,550 m). The pressure difference between the two constant pressure boundaries establishes the regional hydraulic head difference (ΔH). A constant concentration (C_t = 0.029 M, representative of fresh water) boundary condition is applied at the recharge boundary. At the discharge boundary, a zero concentration gradient is applied, which allows advection of tracer across the boundary (out of the model domain), but no diffusion.

A set of PFLOTRAN simulations were run for comparison to the regional-scale allochthonous model results of Park et al. (2009). These included:

- Base case simulation, with:
  - homogeneous rock properties: $k = 10^{-14}$ m^2, $\phi = 0.01$
  - initial salinity at depth: $C_t = 4.45$ mol/L, to approximate brine density $\rho_{bo} \approx 1.20$ g/cm^3
  - hydraulic head difference: $\Delta H = 50$ m, corresponding to a hydraulic head gradient of 0.01
- Six one-off simulations, varying:
  - initial salinity at depth: $C_t = 0.029$, 0.68, and 2.3 mol/L at depth, corresponding to $\rho_{bo} \approx 1.00$, 1.03, and 1.10 g/cm^3, respectively
  - hydraulic head difference: $\Delta H = 25$, 100, and 500 m, corresponding to hydraulic head gradients of 0.005, 0.02, and 0.10, respectively

The base case permeability of 10^{-14} m^2 selected by Park et al. (2009) is representative of sedimentary limestone/sandstone or highly fractured crystalline rock (Freeze and Cherry 1979, Table 2.2). However, it expected that overlying sediments would consist of both high and low permeability layers and that the deeper crystalline basement rock would have a lower permeability (Freeze et al. 2016, Section 4.3.2.1). To examine the effect of lower permeability on deep vertical flow and mixing, a parallel set of seven simulations were run with a lower homogeneous permeability ($k = 10^{-15}$ m^2), including the same one-off variations in brine density and hydraulic head difference. The lower permeability of 10^{-15} m^2 is still at the upper end of expected permeabilities in crystalline rock at depth (Freeze et al. 2016, Figure 4-7), but provides a basis for comparison to the set of 10^{-14} m^2 permeability simulations.

All regional-scale PFLOTRAN simulations were run to 1,000,000 years, with maximum 10-year time steps, sufficient to capture the behavior of the transient problem on a geologically relevant time-scale. This is an extension to the duration of simulations of Park et al. (2009), which were only run to 1,000 years. Regional-scale simulation results are presented in Section 4.2.3.1.

4.2.2.2 DBD-Scale Simulation

A single PFLOTRAN simulation with a DBD-scale model domain was also performed. The DBD-scale domain is more representative of depths and rock properties expected at a DBD site location. The DBD-scale domain is similar to the regional-scale model domain of Park et al. (2009), with the following differences:

- the domain is extended to a depth of 5,000 m
- the upper 2,000 m (undifferentiated sediments) have $k = 10^{-15}$ m^2, $\phi = 0.20$, and initial $C_t = 0.029$ mol/L ($\rho_o \approx 1.00$ g/cm^3)
- the lower 3,000 m (crystalline basement) have $k = 10^{-18}$ m^2, $\phi = 0.005$, and initial $C_t = 4.45$ mol/L ($\rho_{bo} \approx 1.20$ g/cm^3)

These hydrogeologic properties are consistent with the DBD reference case (Table 3-1). The DBD-scale model domain is assumed to be isothermal at 25°C, which is a difference from the geothermal gradient in the DBD reference case. DBD-scale simulation results are presented in Section 4.2.3.2.

4.2.3 Model Results

4.2.3.1 Regional-Scale Model Domain

Results from the set of regional-scale PFLOTRAN simulations with a permeability of 10^{-14} m^2 compared well with the allochthonous model results of Park et al. (2009). For illustration, the results of the base case simulations ($k = 10^{-14}$ m^2, $\rho_{bo} \approx 1.20$ g/cm^3, $\Delta H = 50$ m) at 1,000 years for Park et al. (2009) (Figure 4-6) and PFLOTRAN (Figure 4-7a) show a similar density stratification. Base case PFLOTRAN results at 1,000,000 years are shown in Figure 4-7b.

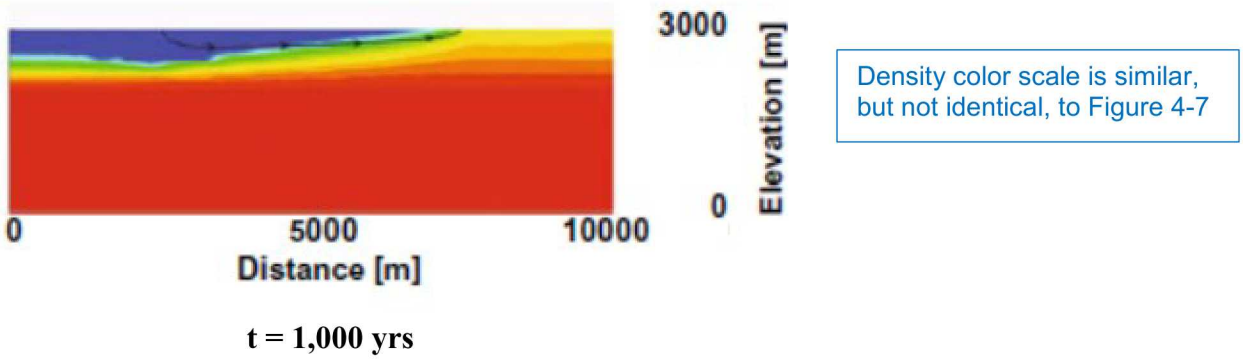

Source: Park et al. (2009, Fig. 7)

Figure 4-6. Park et al. (2009) Base Case ($k = 10^{-14}$ m^2) Model Results (Fluid Density)

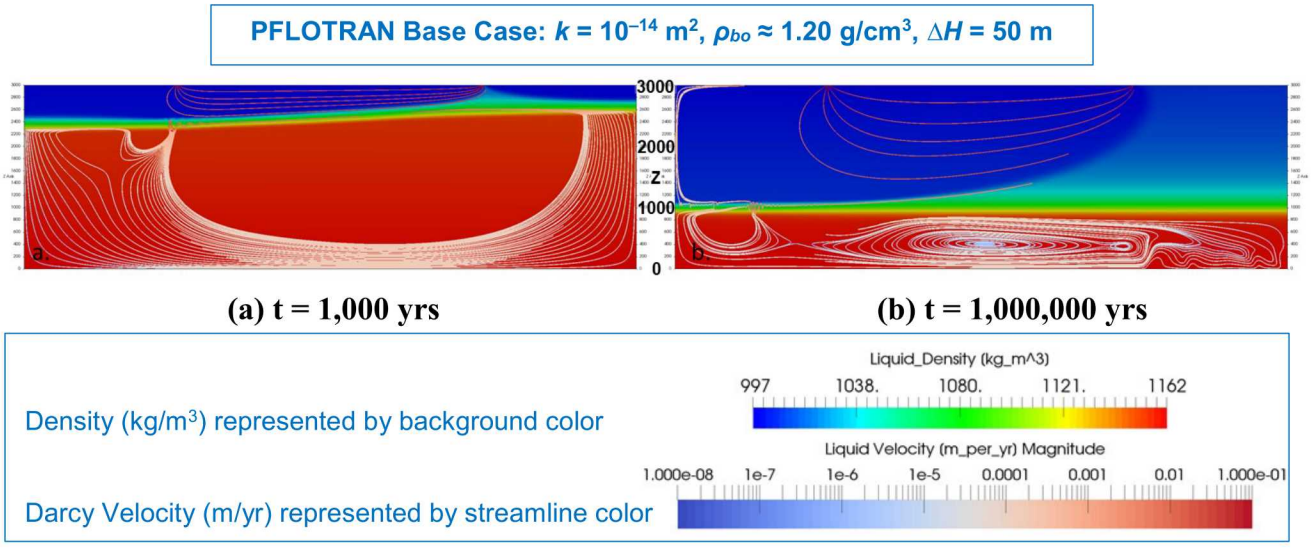

Figure 4-7. PFLOTRAN Base Case ($k = 10^{-14}$ m^2) Model Results (Fluid Density and Darcy Flux)

By 1,000 years in the base case, a flow path from the recharge boundary region to the discharge boundary region is established through the fresh water portion (i.e., above 500 m depth) of the domain (seen best in Figure 4-6). A semi-closed pattern of circulation is established in the deeper (initial brine) portion of the domain (seen best in Figure 4-7a). Although the top surface of the brine is disturbed by flow toward the discharge location, brine persists over most of the domain at depths greater than 500 m. By 1,000,000 years, however, the upper ~1,800 m of the domain has been flushed with fresh water and circulation cells exist below that depth, with almost no mixing between the shallow fresh water and the deep brine (Figure 4-7b). This longer-term behavior was not evident from the short duration simulations of Park et al. (2009).

PFLOTRAN results for the lower permeability base case ($k = 10^{-15}$ m^2, $\rho_{bo} \approx 1.20$ g/cm^3, $\Delta H = 50$ m) are shown in Figure 4-8. As in the $k = 10^{-14}$ m^2 case, a flow path from the recharge boundary region to the discharge boundary region is established through the shallow (≤ 500 m depth) fresh water portion of the domain by 1,000 years, but the semi-closed circulation pattern in the deeper brine has not yet been established (Figure 4-8a). By 1,000,000 years, the effects of the lower permeability are further apparent; only the upper ~800 m of the domain has been flushed with fresh water (Figure 4-8b); as compared to the 1,800 m fresh water flushing depth for the $k = 10^{-14}$ m^2 case (Figure 4-7b). In addition, isolated circulation cells have been established at depth, with almost no mixing into the shallow fresh water.

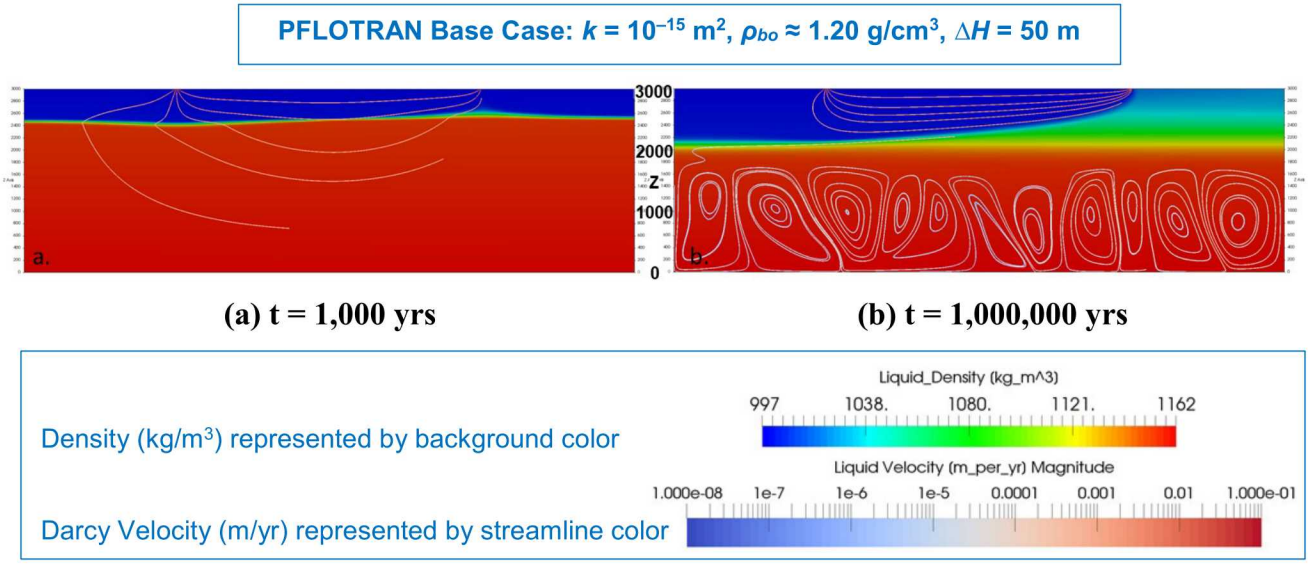

Figure 4-8. PFLOTRAN Base Case ($k = 10^{-15}$ m^2) Model Results (Fluid Density and Darcy Flux)

The base case simulation results for $k = 10^{-14}$ m^2 and $k = 10^{-15}$ m^2 demonstrated density stratification behavior and vertical flow and mixing at depth under simplified hydrogeologic conditions. The one-off simulation results provide further insights into the flow behavior and its sensitivity to regional hydraulic gradient (head difference) and initial brine density (tracer concentration). Selected results from the lower permeability ($k = 10^{-15}$ m^2) one-off simulations are described below.

Figure 4-9 compares 1,000,000-year PFLOTRAN results using 3 different initial brine densities ($\rho_{bo} \approx 1.03$, 1.10, and 1.20 g/cm^3) in the lower permeability case ($k = 10^{-15}$ m^2, $\Delta H = 50$ m). With a homogeneous domain permeability of 10^{-15} m^2, there is very little sensitivity to initial brine density in the first 1,000 years; therefore, a comparison of 1,000-year PFLOTRAN results is not shown. In all cases the flowlines have been established from recharge location to discharge location, but fresh water penetration (brine flushing) below 500 m depth is minimal (similar to the results in Figure 4-8a).

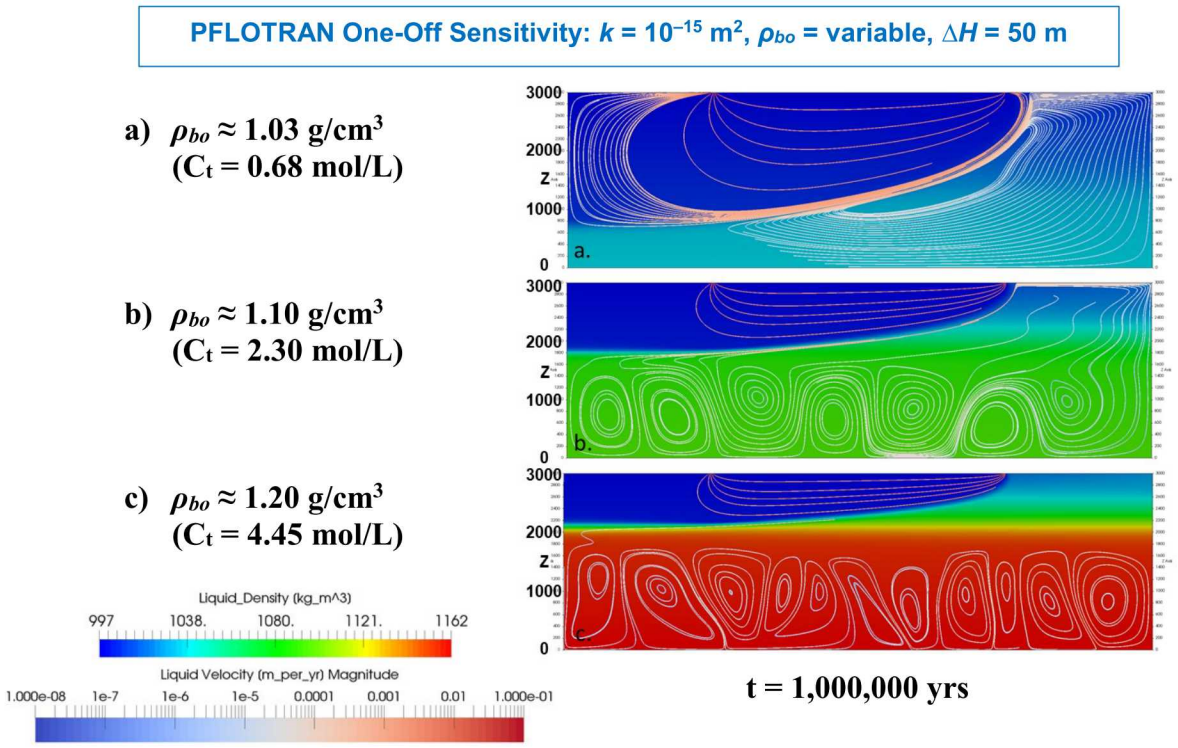

Figure 4-9. PFLOTRAN ($k = 10^{-15}$ m^2) Model Results (Sensitivity to Initial Brine Density)

By 1,000,000 years, the effect of initial brine density is apparent; low-density brine is more easily displaced than high-density brine. With lower-density brine ($\rho_{bo} \approx 1.03$ g/cm^3 ($C_t = 0.68$ M)), fresh water has flushed the brine to a depth of ~2,200 m (Figure 4-9a). With moderate-density brine ($\rho_{bo} \approx 1.10$ g/cm^3 ($C_t = 2.3$ M)), fresh water has flushed the brine to a depth of ~1,100 m (Figure 4-9b). And with the base case higher-density brine ($\rho_{bo} \approx 1.20$ g/cm^3 ($C_t = 4.45$ M)), fresh water has only flushed the brine to a depth of ~800 m (Figure 4-9c). For the cases with denser brine ($\rho_{bo} \geq 1.10$ g/cm^3), a deep circulation system has developed within the brine region.

Figure 4-10 compares 1,000,000-year PFLOTRAN results using 3 hydraulic head differences (ΔH = 25, 50, and 100 m) in the lower permeability case ($k = 10^{-15}$ m^2, $\rho_{bo} \approx 1.20$ g/cm^3). These head differences applied over the 5,000 m distance between recharge and discharge locations result in regional hydraulic head gradients of 0.005, 0.01, and 0.02, respectively. With a homogeneous domain permeability of 10^{-15} m^2, there is very little sensitivity to regional hydraulic gradient in the first 1,000 years; therefore, a comparison of 1,000-year PFLOTRAN results is not shown. In all cases the flowlines have been established from recharge location to discharge location, but fresh water penetration (brine flushing) below 500 m depth is minimal (similar to the results in Figure 4-8a).

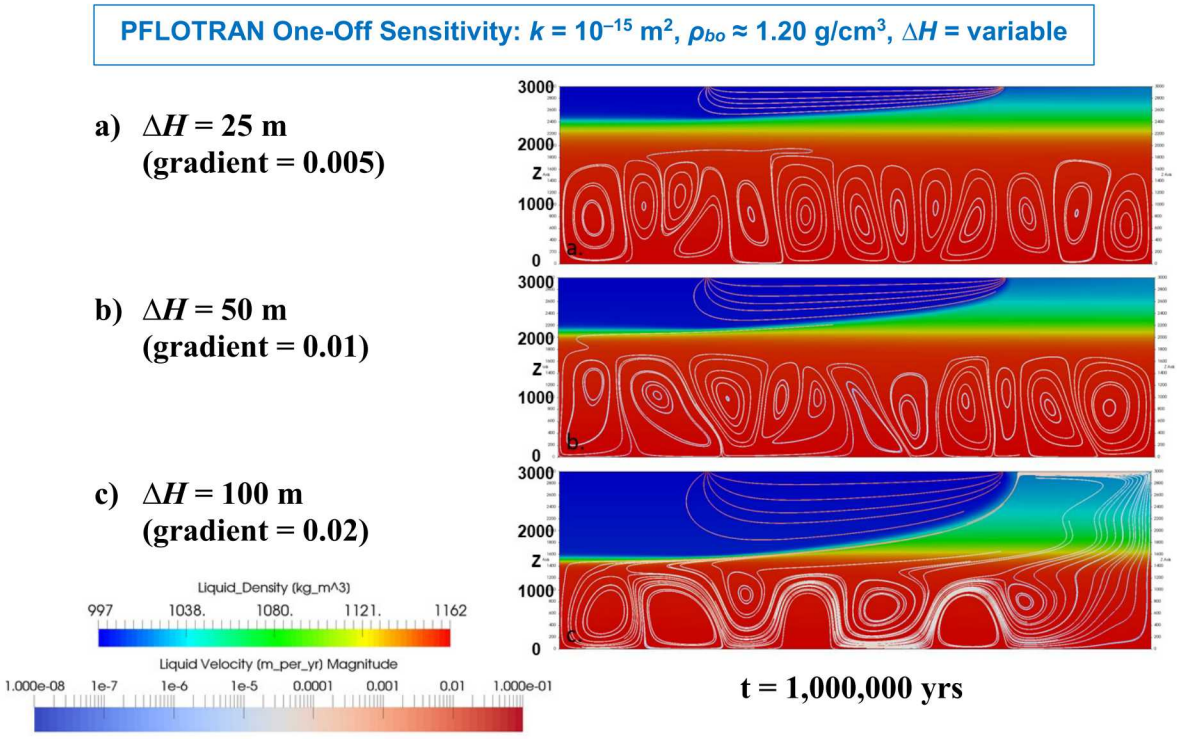

Figure 4-10. PFLOTRAN ($k = 10^{-15}$ m^2) Model Results (Sensitivity to Hydraulic Head Difference)

By 1,000,000 years, the effect of regional hydraulic gradient is apparent; increasing the hydraulic gradient, i, increases the depth to which fresh water recharge circulates. With a relatively small regional gradient (ΔH = 25 m, i = 0.005), fresh water has only flushed the domain to a depth of ~550 m (Figure 4-10a). With the base case ΔH = 50 m (i = 0.01), fresh water has flushed the domain to a depth of ~800 m (Figure 4-10b). And with a larger gradient (ΔH = 100 m, i = 0.02), fresh water has flushed the domain to a depth of ~1,400 m (Figure 4-10c). In all cases, a deep circulation system has been established in the brine region.

With an extremely large regional gradient (ΔH = 500 m, i = 0.1), fresh water flushes the entire domain and flowlines from recharge location to discharge location extend down to 3,000 m depth. However, these results are not shown, as this gradient is much larger than would be appropriate

for a DBD site. For example, the hydraulic gradient assumed for deep crystalline basement is 0.0001 (Section 3.1.1)

Simulations with $k = 10^{-16}$ m^2 and 10^{-18} m^2 were also run; however, simulation results for these lower permeabilities are not shown, as they were nearly identical to the results with $k = 10^{-15}$ m^2.

4.2.3.2 DBD-Scale Model Domain

DBD-scale model results are shown in Figure 4-11. The 2,000-m thickness of overlying undifferentiated sediments have a higher permeability ($k = 10^{-15}$ m^2) than the crystalline basement and an initial density of fresh water ($\rho_o \approx 1.00$ g/cm^3). As a result, flowlines from the fresh water recharge location to the discharge location circulate to the base of the sediments. Darcy fluxes in the sediments are on the order of 10^{-3} m/yr.

Basement permeability ($k = 10^{-18}$ m^2) is sufficiently low that significant advection does not develop in the deep basement brine. Instead, the recharge and discharge boundary conditions drive fluxes in the basement that are 3 to 4 orders of magnitude smaller than fluxes in the sediments, insufficient for significant fresh water flux into the basement. There is a small amount of mixing at the fresh water-brine interface, but no fresh water flushing of brine in basement; with these properties, the density stratification of the brine remains for 1,000,000 years.

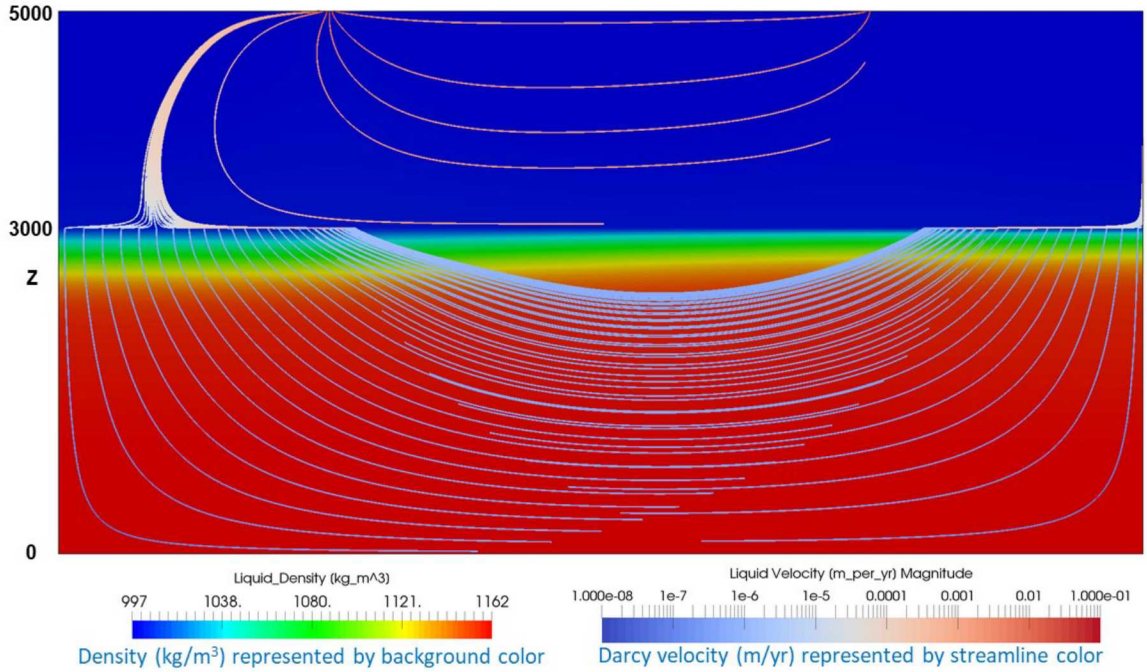

Figure 4-11. PFLOTRAN DBD-Scale Model Results (Fluid Density and Darcy Flux)

Darcy velocities, calculated from Equation 3-1, are ~3 x 10^{-3} m/yr for the fresh water in the sediments and ~4 x 10^{-6} m/yr for the brine in the crystalline basement. These values are consistent with the Darcy velocities in Figure 4-11.

4.3 Borehole Sealing Materials and Technologies

This section sets out the rationale and performance targets for DBD sealing, reviews existing borehole sealing technologies (mainly from the oil, gas and geothermal industries), and evaluates their possible suitability for use in DBD sealing. It also introduces as yet untested methods that have been proposed for DBD sealing and addresses some of the main problems.

4.3.1 Overview

DBD is a multi-barrier disposal concept which relies primarily on the great depth of disposal and the isolation provided by the natural geological and hydrogeochemical environment (see Sections 1.1 and 1.5; Chapman and Gibb 2003; Beswick et al. 2014). This contrasts with the shallower mined repository concepts in which the role of engineered barriers in the overall safety case is greater. If the isolation from the biosphere and surface environment provided by the deep natural barriers is not to be compromised, it is essential that the DBD seals limit and/or delay radionuclide migration from the waste packages in the borehole EZ to the overlying sections of the borehole. This is necessary to prevent any possibility for the borehole itself, or the adjacent DRZ, to provide a transport path to the surface of less resistance than the surrounding geological barrier.

Most DBD designs advocate that the borehole is sealed as short a distance as possible above the topmost waste package in the EZ to maximize the depth of isolation. For the Cs/Sr capsule DBD reference design outlined in Section 1.4, the upper portion of the borehole includes the SZ, where seals and plugs (bentonite seals, cement plugs, silica sand/crushed rock ballast) will be emplaced directly against the borehole wall, and the UBZ, where plugs (cement alternating with ballast) will be emplaced against the cemented casing. The SZ is a 2,000-m interval (between 2,466 m and 4,466 m depth) that directly overlies the top of the EZ. Seals in the SZ are designed to act directly against the DRZ of the crystalline basement host rock to inhibit vertical fluid flux and radionuclide transport up the borehole and through the DRZ. In the UBZ, the exact nature and distribution of seals, plugs, and/or backfill materials is dictated largely by the host geology, and so is site-specific. Seal materials may also contribute to thermal-hydro-chemical conditions that can limit and/or delay radionuclide transport, particularly in the SZ.

As noted in Section 1.5, seals are primarily needed during the first few hundred years of maximum decay heat production in the borehole. After this period, borehole temperatures are expected to return to ambient and there will be little driving force for upward movement of water. Further seal performance is desirable until re-establishment of the natural salinity gradient (density stratification), which tends to oppose upward flow; this period is assumed to be approximately 1,000 years. Seal longevity is discussed further in Section 4.3.2.

In the post-closure PA simulations presented in Section 3, no performance credit is taken for processes in the EZ (e.g., waste form and waste package degradation, sorption in the EZ annulus). However, engineered waste forms, waste packages, and/or EZ annulus fill materials could further contribute to waste isolation and multi-barrier capability. Effective backfilling of the EZ annular regions (between (i) the waste packages and EZ liner, and (ii) the EZ liner and borehole wall) can prevent, or significantly delay, groundwater access to, and subsequent corrosion of, the waste packages. Backfilling of these EZ annular regions could also limit and/or delay migration of

radionuclides and H_2 gas from corrosion (see Freeze et al. 2016, Section 6.4) out of the EZ. This could be achieved through the use of sealing and support matrices (SSMs) deployed along with the waste packages during emplacement in the EZ (Collier et al. 2015a).

While seals, plugs, and backfill in the EZ and UBZ have the potential to further prevent and delay radionuclide release and migration, the remainder of this section is focused on the performance, materials, and emplacement technology of the seals in the SZ.

Many versions of DBD (e.g. Woodward-Clyde 1983; Arnold et al. 2011, Arnold et al. 2013) have looked to utilize the conventional man-made materials and systems developed by the oil and gas industry for sealing the boreholes. Others, recognizing the difficulties faced by these conventional methods, have proposed more innovative, but as yet untested, methods. Among the latter are ceramic plugs (Lowry et al. 2015) and "rock welding" (Gibb et al. 2008; Beswick et al. 2014; Gibb and Travis 2015).

Boreholes for the disposal of radioactive waste differ from hydrocarbon exploration and production wells, geothermal energy wells, and deep geoscientific boreholes in many key respects; not least in their depth-diameter combination and the fact that DBD boreholes are cased over a greater portion of their total depth. Moreover, in contrast to wells which are designed to extract resources or data over a limited period, DBD boreholes are intended to provide long-term isolation for potentially hazardous materials. Consequently, their sealing requirements are significantly different from those of exploration and production wells, although some commonalities may exist with plugging and abandoning exhausted or terminated wells.

4.3.2 Seal Performance Targets

For any borehole sealing technology, seal emplacement must be relatively straightforward and reliable and seal longevity must be consistent with regulatory and/or post-closure performance requirements. Seal materials should be designed to have a low permeability, bond effectively to the surrounding borehole wall and DRZ, and be resistant to thermal, chemical, and mechanical alteration which might degrade seal performance. These key performance targets for DBD sealing materials and technologies are summarized below.

Longevity

Ideally, borehole seals should provide complete and permanent isolation of the EZ, preventing liquids and gases from flowing upwards through the borehole and its associated DRZ more easily than through the surrounding geological barrier. However, for any such upward flow to occur two conditions must exist. Firstly, there must be a driving force for the upward flow. Secondly, the engineered barriers (e.g., seal systems) and natural barriers (e.g., density stratification of brine, see Section 4.2) to flow up the borehole must have been removed or the force must be sufficient to disrupt them.

The most likely (perhaps only) significant force producing upward fluid flow in and around the borehole is buoyant convection driven by the decay heat from the waste in the EZ. Thermal modeling (Gibb et al. 2006; Arnold et al. 2013; Arnold et al. 2014; Travis and Gibb 2015; Freeze

et al. 2016) shows that sufficiently elevated temperatures in and around the EZ would only be sustained for between a few hundred to a few thousand years, after which any thermally-driven buoyant convection would effectively cease. Modeling also suggests that during this period, waste from the EZ would be transported upwards, by advection, by only a few hundred meters, due largely to the low hydraulic conductivities, and hence the overall isolation of the waste would not be threatened, even in the absence of seals.

Natural barriers to upward flow in and around the borehole come from the low permeability of the host rock and the density stratified groundwaters (fresh water near the surface and concentrated brine at depth), both of which are disrupted or perturbed by the drilling of the borehole and activity during the operational phase. Once the latter ceases, the low permeability can be re-created by the sealing materials in the SZ and the regional groundwater density stratification (salinity gradient) will be restored by natural forces.

Assuming the thermally-driven buoyant convection is strong enough to temporarily disrupt the natural barrier in the borehole, a safety case would require that the seals outlast the thermal pulse, which is a function of the time required for the decay heat production to dissipate (and is dependent on the waste inventory). For the Cs/Sr capsule DBD reference case, the time needed for the thermal pulse to subside and buoyant convection to cease is on the order of a few hundred years (Freeze et al. 2016, Figures 5-4 and 5-5). For SNF, where decay heat is largely governed by the same short-lived radionuclides (^{90}Sr and ^{137}Cs), the time scale is on the order of 500 to 1,000 years (Arnold et al. 2013, Section 4.2).

Once the driving force for upward movement of ground water has dissipated, further seal performance is desirable until re-establishment of the natural salinity gradient, which tends to inhibit vertical flow or mixing. Therefore, an additional consideration governing the desired longevity of the borehole seals is the time required for re-establishment of the natural density stratification of groundwater within and around the borehole. This period is assumed to be approximately 1,000 years (Freeze et al. 2016, Section 6.4), with a bounding value of 10,000 years based on a simplified analytical solution (Travis et al. 2017). Numerical modeling work is underway at the University of Sheffield to refine this bounding estimate. It is also worth noting that this time could possibly be reduced by appropriate choice of the closure fluids in the borehole (i.e., having salinity similar to the natural gradient).

Reliability

Sealing emplacement methods must be as reliable as possible and the seals themselves must have as low a risk of failure as is reasonably practicable.

Resistance to Alteration

Borehole seals should be resistant to thermal, chemical, and mechanical alteration under the anticipated range of downhole temperatures, pressures, and geochemical conditions.

Temperature − There are two main contributions to the temperature within the EZ in DBD: the semi-permanent geothermal gradient and the highly transient radioactive decay heat from the

waste. Ambient temperatures due to the natural geothermal gradient are on the order of 140°C at 5,000 m depth (i.e., at the bottom of the EZ) (Section 3.1). Maximum temperatures in the EZ may be as high as 240˚C in the waste package and 200˚C at the borehole wall for Cs/Sr capsule disposal (Freeze et al. 2016, Figure 5-4). However, maximum temperatures in the seals, above the EZ, are likely to be much closer to ambient, on the order of 85˚C at 3,000 m depth.

Pressure − The sealing method and materials used at depths up to 4 km should be capable of performing their functions under hydrostatic pressures of up to 40 MPa, with appropriate safety margins. Also, load stresses from any overlying materials in the borehole could increase the pressure by a few MPa, although this effect can be mitigated through the use of SSM and engineering design (e.g. bridge plugs).

Groundwater Chemistry − Borehole seals must perform in a hostile chemical environment in which the brines present at the depths relevant to DBD (3-5 km) will be dominated by Na, Ca and Cl with the Ca/Na ratio probably increasing with depth. Seals should be able to operate in groundwaters with TDS of at least of 200 g/L.

Resistance to Flow and Transport

As mentioned previously, resistance to flow and transport through the borehole seals is especially important during the first few hundred to few thousand years of thermally-driven buoyant convection, after which slow diffusion is the predominant transport mechanism.

Seal Permeability and Porosity − Low permeability of seal materials (bentonite and cement) inhibits vertical fluid flux and radionuclide advection up the borehole. An overall permeability, taking into consideration degradation processes, of 10^{-18} m^2 is desirable, which should provide a more than adequate safety margin against any escaped radionuclides reaching the surface via the borehole, especially when the natural restoration of the groundwater barriers in and around the borehole is taken into consideration. Low porosity of seal materials corresponds to lower diffusion coefficients.

Seal Sorption − Seal materials may be selected for specific chemical characteristics. For example, the high sorption capacity of bentonite limits and/or delays radionuclide transport. Also, the presence of cement plugs can minimize chemical interaction between adjacent seals.

Disturbed Rock Zone Extent − The DRZ is an unavoidable consequence of drilling deep boreholes, the mechanical effects of which create a zone of fractured rock beyond the borehole wall. Any sealing method proposed for DBD should ideally extend to the DRZ, significantly reducing its permeability or eliminating it altogether, to avoid radionuclides circumventing the engineered seal.

4.3.3 Sealing Systems and Materials

This section discusses sealing systems and materials with potential applicability to all types of DBD designs (e.g., Cs/Sr capsules and SNF). The majority of existing sealing methods in the hydrocarbon and geothermal industries are based on inorganic, man-made, setting materials such as cement and concrete, although other methods utilize swelling materials (e.g. clays) and mechanical packers, resins and asphalt.

Cements

There is a long history of sealing oil and gas and geothermal boreholes with cement, though the great depth of a disposal borehole poses emplacement challenges (Freeze et al. 2016, Appendix D). Cement pastes are usually designed to thicken and set quickly, which causes problems for emplacement in a deep borehole, particularly in DBD, where the high temperatures and elevated pressures accelerate thickening and reduce setting time. Additives can be employed to delay this process, but identifying and optimizing the most appropriate types and quantities are still active areas of research for DBD. To date, organic additives have been demonstrated that can delay grout thickening by at least 4 hours (sufficient for DBD) but no longer than 24 hours, at temperatures up to 140˚C and at elevated pressure (50 MPa) (Collier et al. 2015a; Collier et al. 2015b; Collier et al. 2016). Retardation of thickening time using inorganic additives has also been proven, but they currently do not perform as well as organic materials across the range of elevated temperatures and pressures likely to be experienced in DBD.

A problem for cement-based seals for deep boreholes relates to emplacement: it is very difficult to deliver the cement to where it is needed and to form a good, continuous, seal free from micro-annuli without premature setting and hardening. The cement slurry must be capable of being pumped at depth under high pressure conditions and to fill all the void space. Reverse circulation methods can improve the emplacement process, but significant challenges remain.

The formation of a good bond with the borehole wall rock is essential but very difficult to achieve in practice. Great care must be taken to remove any drilling fluid and wall cake prior to emplacement of the cement due to their chemical incompatibility. The operation to remove the drilling fluid by flushing with chemicals is also problematic and, if not done correctly, can itself lead to poor bonding of the cement to the wall rock.

As the rock formation relaxes, it can strip away water from the cement (forming a “thief” zone) and lead to shrinkage and a loss of water of hydration. Fluid loss additives to minimize this effect are often insufficient and can lead to decreased compressive strengths in the hardened cement paste. Experience gained from geothermal well cementing, which is often characterized by high temperatures and hostile chemical environments (usually acidic), illustrates this problem. Flash setting of cements and a reduction in well lifetime are two of the more serious consequences. Introducing additives to the cement, pre-quenching of the wells, and remedial cementing, while possible (albeit difficult) in geothermal wells, are not really an option in DBD.

With continued research into deep emplacement methods, cement plugs can be a useful component of DBD seal systems.

Bentonite and Other Clay-Based Systems

Bentonite expands in contact with water, has a high surface area, is routinely used to seal oil and gas and geothermal boreholes, and has been extensively studied as an engineered barrier in mined repositories (Freeze et al. 2016, Appendix D). Bentonite (altered volcanic ash with a high content of smectite clay) and other clays are characterized by extremely low permeabilities and self-healing properties, making them good candidates for seal materials. Their ability to expand on contact with water — an advantage when used as a seal — is a disadvantage when it comes to emplacement of the material in a fluid filled borehole. Various methods have been proposed for overcoming this problem when emplacing clay-based materials in boreholes, including those for DBD. The most promising method appears to be that involving emplacement of solid smectite blocks within perforated copper or bronze supercontainers (Pusch et al. 2012). However, this method may not work well in practice for DBD, due to the possibility of the supercontainers becoming jammed because of the small clearances. A different approach could entail the use of a specially developed dump bailer (used in hydrocarbon wells to deploy a measured quantity of cement) to emplace bentonite blocks while keeping them dry. In addition to these emplacement problems, other factors point to clays being a less than optimum choice for use as seal materials in DBD. These include (i) the need to keep the clay hydrated, (ii) the potential for interaction between the smectite clay and groundwater, which may lead to compositional and physical changes, and (iii) chemical interactions between the bentonite and other materials in the borehole, especially cements and metallic materials.

As with cement, continued research into deep emplacement methods for bentonite can make it a viable component of DBD seal systems.

Geopolymers

These are cement derivatives produced by alkali activation of Class C fly ash with a NaOH and sodium silicate solution. These materials are at an early stage of development but show some promise measured against the criteria needed to function as a seal in deep boreholes. However, since they do not solve the DRZ problem, they are unlikely to be useful as the main seal barrier in DBD.

Silicone Rubber

Typically used in conjunction with a cement to form gas-tight, well-bonded, seals in gas wells, these materials show little shrinkage, are temperature resistant up to 300˚C, and are able to withstand a wide range of chemical environments. Another advantage is that they can be used easily with coiled tubing equipment. In view of these properties, silicone rubbers are worthy of further investigation as a component of the DBD seal zone.

Asphalt

The black colored hydrocarbons that constitute asphalt, also known as bitumen, have some useful characteristics for use as sealing materials. They are insoluble in water, colloidal, chemically inert, ductile, and durable (on a geological timescale). Asphalts also exhibit thermo-plastic behavior and can soften in the temperature range 35˚C to 80˚C. On the downside, accurate emplacement of asphalt-based seals could be challenging in deep boreholes. Also, organic acids leaching from the asphalt might complicate predictions of long-term radionuclide transport because of their ability to form aqueous complexes with some cationic radionuclides.

Crushed Rock

Crushed rock has been used as a seal in hydrocarbon wells, often in conjunction with other granular materials such as sand and clay, and has been advocated as a possible seal in investigation boreholes for mined repositories and for DBD (Pusch et al. 2012). While emplacement is relatively simple, ensuring a complete and continuous seal free of voids is not so. For this reason, crushed rock is unlikely to be a suitable choice for the main seals in DBD.

Sandaband®

This is a proprietary mineral-based sealing system consisting of a dry mixture of barite and bentonite with up to 75% of fine silica sand. When mixed with water, viscosifiers and dispersants, it behaves as a Bingham fluid allowing it to be pumped to where it is required but then behaving like a solid when stationary. The ability to deform when the applied stress exceeds its yield strength gives this material a self-healing property which is useful in a sealing context. Other promising properties of this material include low permeability, resistance to shrinkage and fracture, and thermodynamic stability. Also, it is chemically inert and is expected to have good durability. On the negative side, emplacement is difficult (it must be kept isolated from other fluids in the borehole), it contains organic additives, there is limited documented evidence of its use in boreholes.

Ceramic Seals

One of the more promising methods that have been proposed for sealing DBD involves the use of ceramic plugs. A ceramic plug is emplaced within the borehole seal zone, and expands upon ignition through a thermite reaction. The properties of these seals should be superior to those of cement-based seals in terms of durability and reduced permeability. It has been suggested that ceramic seals might penetrate into the DRZ, although this is likely to be only for a few millimeters at most and requires experimental validation. Ceramic-based seals show promise for use in a multiple-material-based seal zone and warrant further R&D.

Rock Welding

Rock welding uses downhole electric heating to partially melt and recrystallize crushed granite backfill and wall rock of the borehole into a "weld" similar in makeup to the native crystalline rock (Gibb et al. 2008; Gibb and Travis 2015). Rock welding can create a seal for DBD as strong and durable as the undisturbed host rock and eliminate the DRZ by annealing shut any radially extensive flow paths. A research program is underway at the University of Sheffield to investigate and develop rock welding and has already demonstrated that the concept is viable on the laboratory scale. However, further work is required to scale up the method for DBD and downhole trials, optimization and testing need to be undertaken.

DRZ Minimization

As noted in Section 4.3.2, any sealing method for DBD should ideally extend to the DRZ, reducing its permeability and/or vertical connectivity. The generic DBD design (Section 1.4.1), proposes emplacing the SZ materials directly against the host rock and DRZ for this purpose. However, with the exception of rock welding, and to a lesser extent ceramic seals, none of the materials described above are specifically designed to significantly penetrate into, or otherwise reduce, the permeability of the DRZ. Therefore, continued research is warranted into sealing emplacement methods and material properties that might minimize the DRZ effects.

More work is also needed to further investigate the nature and extent of the change in permeability arising from the DRZ. It is possible that relaxation and stress relief, if largely confined to crystal boundaries in the crystalline host rock, would not impair the effective seal to a degree that would be of serious concern. However, until this is proven it has to be assumed that the DRZ is a possible conduit for upward flow of fluids.

5 SYNTHESIS AND CONCLUSIONS

Freeze et al. (2016) developed a preliminary, generic safety case of the feasibility of the DBD concept; there is no site, system design studies were just beginning, and the regulatory framework is unclear and lacks focus for this method of disposal. Therefore, at this early phase of DBD concept development, the purpose of this safety case for DBD is to provide a framework to organize and synthesize existing science and identify open issues and information gaps relevant to DBD.

Confidence in the DBD concept derives from the following, summarized in Section 1.5:

Pre-Closure Operations:

- Adequacy of Site Characterization
- Achievability of Deep Drilling
- Safety of Site Operations

Post-Closure Isolation:

- Great Depth of Disposal
- Isolation and Long Residence Time of Deep Groundwater
- Density Stratification of Brine at Depth
- Low Permeability of Crystalline Host Rock
- High-Likelihood of Slow Diffusion-Dominated Radionuclide Transport
- Geochemically-Reducing Conditions at Depth
- Low Permeability and High Sorption Capacity of Seal Materials
- Multi-Barrier Design

Open issues requiring further evaluation and/or research were listed in Freeze et al. (2016, Section 6.4). This report provides additional information and analyses that address some of the open issues and further augments the DBD safety case. Specific open issues addressed include:

- **Operational Feasibility** – The pre-closure radiological assessment approach was updated and the scope of the pre-closure assessment basis and safety analysis was expanded (Section 2). The previous pre-closure safety analysis (Freeze et al. 2016, Section 5.1; SNL 2016a, Appendix A and B) was limited to consideration of hazards and event sequences associated only with the wireline emplacement activity. The expanded analysis considers DBD site operations in greater detail, including a number of activities from waste package receipt to borehole closure.

- **Operational Failures** – The post-closure consequences of an operational failure (package breach subsequent to a waste package becoming stuck above the EZ) were examined through a post-closure PA analysis of a disturbed scenario (Section 3). The disturbed scenario includes a waste package "stuck" in the crystalline basement above the EZ near a hypothetical borehole-intersecting fracture. The disturbed scenario builds upon previously documented undisturbed (nominal) scenario simulations (Freeze et al. 2016, Section 5.2).
- **Characterization of the Heterogeneous Subsurface Conditions** – The robustness of the DBD concept relies in large part on the subsurface hydrogeology and geochemistry, specifically: low permeability and porosity in the host rock; lack of significant vertical connectivity in the DRZ; chemically reducing, high salinity, and density stratified groundwater at depth, and evidence of isolation of deep groundwater. The measurement and confirmation of these spatially heterogeneous properties and conditions poses technical challenges.

  Section 4.1 identifies key testing and sampling activities that can contribute to better characterization of the subsurface hydrogeology and geochemistry. Testing activities are generally focused on determining geomechanical and hydrogeologic properties at depth. Sampling is generally focused on chemical composition and environmental tracers that can provide evidence for isolation and long residence time of deep groundwater.

  Section 4.2 describes simulations of density-dependent flow and transport to illustrate how density stratification can inhibit fluid flow at depth and maintain hydraulic isolation of the deep basement. High salinity at depth and density stratification of brine can be indicative of isolation from shallower water.
- **Robustness of Seals** – Seals are primarily needed during the first few hundred years of maximum decay heat production in the borehole. After this period, borehole temperatures are expected to return to ambient and there will be little driving force for upward movement of water. Further seal performance is desirable until re-establishment of the natural salinity gradient (density stratification), which tends to oppose upward flow; this period is assumed to be approximately 1,000 years. Section 4.3 provides a review of borehole sealing materials and technologies with capability to achieve these requirements.

The pre-closure basis and safety analyses, post-closure basis and PAs, and confidence enhancement information documented in Freeze et al. (2016) and augmented in this report collectively suggest that the DBD concept is a viable approach for safe disposal of radioactive wastes. The PCSA (Section 2.2) indicates a probability of successful borehole completion of greater than 99%. The post-closure PA model results (Section 3.2) for both the nominal and disturbed (stuck package) scenarios suggest that there is minimal radionuclide migration away from the EZ and zero dose for 10,000,000 years, at which time long-lived ^{135}Cs has almost completely decayed away.

Key results contributing to long-term isolation of radioactive waste from the accessible environment include:

- Waste emplacement is deep; between 4,466 and 5,000 m depth in low-permeability crystalline basement rock with limited interaction with shallower groundwater.
- Radionuclide mobility is limited due to geochemically reducing conditions in the deep subsurface that enhances solubility and sorption.
- For the nominal scenario, borehole seals can be engineered to maintain their physical integrity as permeability barriers, at least for a few hundred years, which is the time period of thermally-induced upward groundwater flow from decay heat. Long-term radionuclide movement is limited to slow diffusive transport.
- For the disturbed scenario, long-term advection of radionuclides away from a stuck waste package through a hypothetical borehole-intersecting transmissive fracture, driven by a regional head gradient in the crystalline basement, is still minimal.
- No performance credit is taken for the waste forms or waste packages. Robust waste forms and/or waste packages would further limit and/or delay radionuclide migration.

These results suggest that a favorable safety case can be developed for DBD of Cs/Sr capsules.

This research was performed as part of the DBFT. Based on revised DOE priorities in mid-2017, the DBFT and other research related to a DBD option were discontinued; ongoing work and documentation were closed out by the end of FY 2017. This report was initiated as part of the DBFT and documented as an incomplete draft at the end of FY 2017. The report was finalized by Sandia in FY2018 without DOE funding, subsequent to the termination of the DBFT, and published in FY2019.

6 REFERENCES

10 CFR Part 60. *Disposal of High-Level Radioactive Wastes in Geologic Repositories*. Readily available. (46 FR 13971/13980, February 25, 1981 (Subparts A-D) and 48 FR 28194/28217, June 21, 1983 (Subparts E-H))

10 CFR Part 63. *Disposal of High-Level Radioactive Wastes in a Geologic Repository at Yucca Mountain, Nevada*. Readily available. (66 FR 55732/55792, November 2, 2001)

40 CFR Part 191. *Environmental Radiation Protection Standards for Management and Disposal of Spent Nuclear Fuel, High-Level and Transuranic Radioactive Wastes*. Readily available. (50 FR 38084, September 19, 1985)

40 CFR Part 197. *Public Health and Environmental Radiation Protection Standards for Yucca Mountain, Nevada*. Readily available. (66 FR 32074/32132, June 13, 2001)

Adams, B.M., M.S. Ebeida, M.S. Eldred, J.D. Jakeman, L.P. Swiler, W.J. Bohnhoff, K.R. Dalbey, J.P. Eddy, K.T. Hu, D.M. Vigil, L.E. Baumann, and P.D. Hough 2013a. *DAKOTA, a Multilevel Parallel Object-Oriented Framework for Design Optimization, Parameter Estimation, Uncertainty Quantification, and Sensitivity Analysis, Version 5.3.1+ User's Manual*. SAND2010-2183, Updated May 22, 2013. Sandia National Laboratories, Albuquerque, NM. (http://dakota.sandia.gov/)

Adams, B.M., M.S. Ebeida, M.S. Eldred, J.D. Jakeman, L.P. Swiler, W.J. Bohnhoff, K.R. Dalbey, J.P. Eddy, K.T. Hu, D.M. Vigil, L.E. Baumann, and P.D. Hough 2013b. *DAKOTA, a Multilevel Parallel Object-Oriented Framework for Design Optimization, Parameter Estimation, Uncertainty Quantification, and Sensitivity Analysis, Version 5.3.1+ Theory Manual*. SAND2011-9106, Updated May 22, 2013. Sandia National Laboratories, Albuquerque, NM. (http://dakota.sandia.gov/)

Aggarwal, P.K., J.R. Gat, and K.F.O. Froelich, eds. 2005. *Isotopes in the Water Cycle: Past, Present and Future of a Developing Science*. Springer, Dordrecht, Netherlands.

Arnold, B.W., P.V. Brady, S.J. Bauer, C. Herrick, S. Pye, and J. Finger 2011. *Reference Design and Operations for Deep Borehole Disposal of High-Level Radioactive Waste.* SAND2011-6749. Sandia National Laboratories, Albuquerque, NM.

Arnold, B.W., P. Brady, S. Altman, P. Vaughn, D. Nielson, J. Lee, F. Gibb, P. Mariner, K. Travis, W. Halsey, J. Beswick, and J. Tillman 2012. *Research, Development, and Demonstration Roadmap for Deep Borehole Disposal.* FCRD-USED-2012-000269, SAND2012-8527P. Sandia National Laboratories, Albuquerque, NM.

Arnold, B.W., P. Brady, S. Altman, P. Vaughn, D. Nielson, J. Lee, F. Gibb, P. Mariner, K. Travis, W. Halsey, J. Beswick, and J. Tillman 2013. *Deep Borehole Disposal Research: Demonstration Site Selection Guidelines, Borehole Seals Design, and RD&D Needs.* FCRD-USED-2013-000409, SAND2013-9490P. Sandia National Laboratories, Albuquerque, NM.

Arnold, B.W., P. Brady, M. Sutton, K. Travis, R. MacKinnon, F. Gibb, and H. Greenberg 2014. *Deep Borehole Disposal Research: Geological Data Evaluation, Alternative Waste Forms, and Borehole Seals.* FCRD-USED-2014-000332, SAND2014-17430R. Sandia National Laboratories, Albuquerque, NM.

Baccar, M.B. and B. Fritz 1993. "Geochemical modelling of sandstone diagenesis and its consequences on the evolution of porosity". *Applied Geochemistry*, *8*, pp. 285-295.

Bassett, R.L. and M.E. Bentley 1983. *Deep Brine Aquifers in the Palo Duro Basin: Regional Flow and Geochemical Constraints*. Report of Investigations No. 130, Bureau of Economic Geology, University of Texas at Austin, Austin, TX.

Beswick, J., F.G.F. Gibb, and K.P. Travis 2014. *Deep borehole disposal of nuclear waste: engineering challenges* in Energy, 167 (EN2), Proceedings of the Institution of Civil Engineers, Paper 1300016, pp. 47-66.

Bethke, C.M. and T.M. Johnson 2008. "Groundwater Age and Groundwater Age Dating". *Annual Review of Earth and Planetary Sciences 36,* pp. 121-152.

Bottomley, D.J., D.C. Gregoire, and K.G. Raven 1994. "Saline groundwaters and brines in the Canadian Shield - geochemical and isotopic evidence for a residual evaporite brine component". *Geochimica Et Cosmochimica Acta, 58(5)*, 1483-1498. doi: 10.1016/0016-7037(94)90551-7

Brady, P.V., B.W. Arnold, G.A. Freeze, P.N. Swift, S.J. Bauer, J.L. Kanney, R.P. Rechard, J.S. Stein, 2009. *Deep Borehole Disposal of High-Level Radioactive Waste.* SAND2009-4401. Sandia National Laboratories, Albuquerque, NM.

Brady, P.V., B.W. Arnold, R.J. MacKinnon, E.L. Hardin, D.C. Sassani, K.L. Kuhlman, and G.A. Freeze 2015. *Research Needs for Deep Boreholes.* SAND2015-20803C. In Proceedings of the 15th International High-Level Radioactive Waste Management Conference, April 12-16, Charleston, SC.

BSC (Bechtel-SAIC Co.) 2008a. *Receipt Facility Event Sequence Development Analysis.* 200-PSA-RF00-00100-000-00A. February, 2008. U.S. Department of Energy, Office of Civilian Radioactive Waste Management.

BSC (Bechtel-SAIC Co.) 2008b. *Receipt Facility Reliability and Event Sequence Categorization Analysis.* 200-PSA-RF00-00200-000-00A. February, 2008. U.S. Department of Energy, Office of Civilian Radioactive Waste Management.

Bucher, K. and I. Stober 2002. "Water-rock reaction experiments with Black Forest gneiss and granite". *Water-Rock Interaction,* pp. 61-95. Springer, Dordrecht.

Bucher, K. and I. Stober 2010. "Fluids in the upper continental crust". *Geofluids*, *10*, pp. 241-253.

Chapman, N. and F.G.F Gibb 2003. A truly final waste management solution – is very deep borehole disposal a realistic option for HLW or fissile material? *Radwaste Solutions, 10(4)*, pp. 26-35.

Clayton, J.L. 1988. "Some observations on the stoichiometry of feldspar hydrolysis in granitic soil". *Journal of Environmental Quality*, *17*, pp. 153-157.

Collier, N.C., K.P. Travis, F.G.F Gibb, and N.B. Milestone 2015a. *Cementitious grouts for disposal of nuclear wasteforms in deep boreholes*. In Proceedings of the 15th International High-Level Radioactive Waste Management Conference, April 12-16, Charleston, SC.

Collier, N.C., K.P. Travis, F.G.F Gibb, and N.B. Milestone 2015b. *Characteristics of cementitious paste for use in deep borehole disposal of spent fuel and high-level wasteforms*. In Scientific Basis for Nuclear Waste Management XXXVIII, Materials Research Society Symposium Proceedings, 1744. http://dx.doi.org/10.1557/opl.2015.314.

Collier, N.C., N.B. Milestone, K.P. Travis, and F.G.F. Gibb 2016. The effect of organic retarders on grout thickening and setting during deep borehole disposal of high-level radioactive waste. *Progress in Nuclear Energy, 90*, pp. 19-26.

DeMaio, W. and E. Bates 2013. *Salinity and Density in Deep Boreholes*. *UROP Report: October 29, 2013*. Massachusetts Institute of Technology, Department of Nuclear Science and Engineering.

Downey, J.S. and G.A. Dinwiddie 1988. *The Regional Aquifer System Underlying the Northern Great Plains in Parts of Montana, North Dakota, South Dakota, and Wyoming - Summary*. Professional Paper 1402-A. United States Geological Survey, Washington, DC.

DOE (U.S. Department of Energy) 2008. *Yucca Mountain Repository License Application: Safety Analysis Report*. DOE/RW-0573, Revision 0. http://www.nrc.gov/waste/hlw-disposal/yucca-lic-app/yucca-lic-app-safety-report.html#1.

DOE (U.S. Department of Energy) 2014. *Assessment of Disposal Options for DOE-Managed High-Level Radioactive Waste and Spent Nuclear Fuel*. U.S. Department of Energy, Washington, DC.

DOE (U.S. Department of Energy) 2015. *Request for Proposal (RFP) – Deep Borehole Field Test: Site and Characterization Borehole Investigations*. Solicitation Number DE-SOL-0008071, U.S. Department of Energy Idaho Operations Office, Idaho Falls, ID.

DOE (U.S. Department of Energy) 2016. *Request for Proposal (RFP) – Deep Borehole Field Test: Characterization Borehole Investigations*. Solicitation Number DE-SOL-0010181, US Department of Energy Idaho Operations Office, Idaho Falls, ID.

DOE (U.S. Department of Energy) 2017. *Studying the Feasibility of Deep Boreholes*. https://www.energy.gov/under-secretary-science-and-energy/articles/studying-feasibility-deep-boreholes

Edmunds, W.M., R.L.F Kay, D.L. Miles, and J.M. Cook 1987. "The origin of saline groundwaters in the Carnmenellis granite, Cornwall (UK): Further evidence from minor and trace elements". *Saline Water and Gases in Crystalline Rocks. Geological Association of Canada Special Paper*, *33*, pp. 127-143.

EPA (U.S. Environmental Protection Agency) 2015. *EPA's Environmental Radiation Protection Standards for SNF, HLW, and TRU Waste: Applicability of 40 CFR Part 191 to Deep Boreholes*. Presentation by U.S. Environmental Protection Agency to U.S. Nuclear Waste Technical Review Board International Technical Workshop on Deep Borehole Disposal of Radioactive Waste, Washington, DC, October 20-21, 2015.

Farvolden, R.N., O. Pfannkuch, R. Pearson, and P. Fritz. 1988. "Region 12, Precambrian Shield". *The Geology of North America Vol. O-2, Hydrogeology,* pp. 101-114. Geological Society of America, Boulder, CO.

Follin, S., J. Levén, L. Hartley, P. Jackson, S. Joyce, D. Roberts, and B. Swift 2007. *Hydrogeological Characterization and Modelling of Deformation Zones and Fracture Domains, Forsmark Modelling Stage 2.2*. SKB R-07-48, Svensk Kärnbränslehantering AB, Stockholm, Sweden.

Follin, S., L. Hartley, I. Rhen, P. Jackson, S. Joyce, D. Roberts, and B. Swift 2014. "A methodology to constrain the parameters of a hydrogeological discrete fracture network model for sparsely fractured crystalline rock, exemplified by data from the proposed high-level nuclear waste repository site at Forsmark, Sweden". *Hydrogeology Journal, 22(2)*, pp. 313-331.

Frape, S., P. Fritz, and R.T. McNutt 1984. Water-rock interaction and chemistry of groundwaters from the Canadian Shield. *Geochimica et Cosmochimica Acta 48*, pp. 1617-1627.

Frape, S. 2015. *Geochemistry of Fluids at Depth, Panel#5*. Presentation to U.S. Nuclear Waste Technical Review Board International Technical Workshop on Deep Borehole Disposal of Radioactive Waste, Washington, DC, October 20-21, 2015.

Freeze, R.A. and J.A. Cherry 1979. *Groundwater*. Prentice-Hall, Inc., Englewood Cliffs, NJ.

Freeze, G., C.D. Leigh, S.D. Sevougian, and M. Gross 2012. *A Safety Framework for Disposal of Heat-Generating Waste in Salt: Annotated Outline*. FCRD-USED-2012-000431, SAND2012-10797P. Sandia National Laboratories, Albuquerque, NM.

Freeze, G., M. Voegele, P. Vaughn, J. Prouty, W.M. Nutt, E. Hardin, and S.D. Sevougian 2013. *Generic Deep Geologic Disposal Safety Case*. FCRD-UFD-2012-000146 Rev. 1, SAND2013-0974P. Sandia National Laboratories, Albuquerque, NM.

Freeze, G., E. Stein, L. Price, R. MacKinnon, and J. Tillman 2016. *Deep Borehole Disposal Safety Analysis*. FCRD-UFD-2016-000075 Rev. 0, SAND2016-10949R. Sandia National Laboratories, Albuquerque, NM.

Fritz, P. and S.K. Frape 1982. "Saline groundwaters in the Canadian Shield a 1st overview". *Chemical Geology, 36*, 179-190. doi: 10.1016/0009-2541(82)90045-6

Gardner, L.R. 1983. "Mechanics and kinetics of incongruent feldspar dissolution". *Geology*, *11*, pp. 418-421.

Garven, G. 1995. "Continental Scale Groundwater Flow and Geologic Processes". *Annu. Rev. Earth Planet. Sci. 23*, pp. 89-117.

Gascoyne, M. 2004. "Hydrogeochemistry, groundwater ages and sources of salts in a granitic batholith on the Canadian Shield, southeastern Manitoba". *Applied Geochemistry, V.19*, pp. 519-560.

Gibb, F.G.F., K.P. Travis, N.A. McTaggart, and D. Burley 2006. Modelling temperature distribution around very deep borehole disposals of HLW. *Nuclear Technology, 163*, pp. 62-73.

Gibb, F.G.F., K.P. Travis, N.A. McTaggart, and D. Burley 2008. A model for heat flow in deep borehole disposals of high-level nuclear waste. *Journal of Geophysical Research, 113(5)*, B05201, doi: 10.1029/2007JB005081.

Gibb, F.G.F. and K.P. Travis 2015. *Sealing deep borehole disposals of radioactive waste by "rock welding"*. In Proceedings of the 15th International High-Level Radioactive Waste Management Conference, April 12-16, Charleston, SC.

Gunter, T. and G. Freeze 2017. *Deep Borehole Disposal Research in the United States*. In Proceedings of the WM2017 Conference, March 5-9, Phoenix, AZ.

Hammond, G.E., P.C. Lichtner, C. Lu, and R.T. Mills. 2011. "PFLOTRAN: Reactive Flow and Transport Code for Use on Laptops to Leadership-Class Supercomputers", in F. Zhang, G.T. Yeh, and J. Parker (ed.) *Groundwater Reactive Transport Models.* Bentham Science Publishers.

Hardin, E., J. Su, and F. Peretz 2017. *Methodology for Radiological Risk Assessment of Deep Borehole Disposal Operations.* SFWD-SFWST-2017-000105 Rev. 0, SAND2017-3281R. Sandia National Laboratories, Albuquerque, NM.

Hardin E.L., A. Clark, J. Su, and F. Peretz 2019. *Preclosure Risk Assessment for Deep Borehole Disposal.* SAND2019-1827. Sandia National Laboratories, Albuquerque, NM.

Holland, G., B.S. Lollar, L. Li, G. Lacrampe-Couloume, G.F. Slater, and C.J. Ballentine 2013. "Deep fracture fluids isolated in the crust since the Precambrian era". *Nature, 497*(7449), 357-+. doi: 10.1038/nature12127

IAEA (International Atomic Energy Agency) 2006. *Geologic Disposal of Radioactive Waste, Safety Requirements*. IAEA Safety Standards Series No. WS-R-4, IAEA, Vienna, Austria.

IAEA (International Atomic Energy Agency) 2011. *Disposal of Radioactive Waste, Specific Safety Requirements*. IAEA Safety Standards Series No. SSR-5, IAEA, Vienna, Austria.

IAEA (International Atomic Energy Agency) 2012. *The Safety Case and Safety Assessment for the Disposal of Radioactive Waste, Specific Safety Guide*. IAEA Safety Standards Series No. SSG-23, IAEA, Vienna, Austria.

IAEA (International Atomic Energy Agency) 2013. *Isotope Methods for Dating Old Groundwater*. STI/PUB/1587, IAEA, Vienna, Austria.

Joyce, S., L. Hartley, D. Applegate, J. Hoek, and P. Jackson 2014. "Multi-scale groundwater flow modeling during temperate climate conditions for the safety assessment of the proposed high-level nuclear waste repository site at Forsmark, Sweden". *Hydrogeology Journal, 22(6)*, pp.1233-1249.

Juhlin, C., T. Wallroth, J. Smellie, T. Eliasson, C. Ljunggren, B. Leijon, and J. Beswick 1998. *The Very Deep Hole Concept: geoscientific appraisal of conditions at great depth*. SKB Report TR 98–05. Svensk Kärnbränslehantering AB, Stockholm, Sweden.

Kietavainen, R., L. Ahonen, I.T. Kukkonen, N. Hendriksson, M. Nyyssonen, and M. Itavaara 2013. "Characterisation and isotopic evolution of saline waters of the Outokumpu Deep Drill Hole, Finland - Implications for water origin and deep terrestrial biosphere". *Applied Geochemistry, 32*, 37-51. doi: 10.1016/j.apgeochem.2012.10.013

Kietavainen, R., L. Ahonen, I. T. Kukkonen, S. Niedermann, and T. Wiersberg 2014. "Noble gas residence times of saline waters within crystalline bedrock, Outokumpu Deep Drill Hole, Finland". *Geochimica Et Cosmochimica Acta, 145*, 159-174. doi: 10.1016/j.gca.2014.09.012

Kuhlman, K.L., E.L. Hardin, and M.J. Rigali 2019. *Deep Borehole Laboratory and Borehole Testing Strategy: Generic Drilling and Testing Plan.* SAND2019-1896. Sandia National Laboratories, Albuquerque, NM.

Lichtner, P.C. and G.E. Hammond 2012. *Quick Reference Guide: PFLOTRAN 2.0 (LA-CC-09-047) Multiphase-Multicomponent-Multiscale Massively Parallel Reactive Transport Code.* DRAFT LA-UR-06-7048. December 8, 2012. Los Alamos National Laboratory, Los Alamos, NM.

Lippmann, J., M. Stute, T. Torgersen, D.P. Moser, J.A. Hall, L. Lin, M. Borcsik, R.E.S. Bellamy, and T.C. Onstott 2003. "Dating ultra-deep mine waters with noble gases and Cl-36, Witwatersrand Basin, South Africa". *Geochimica Et Cosmochimica Acta, 67(23)*, 4597-4619. doi: 10.1016/s0016-7037(03)00414-9

Lippmann-Pipke, J., B.S. Lollar, S. Niedermann, N.A. Stroncik, R. Naumann, E. van Heerden, and T.C. Onstott 2011. "Neon identifies two billion year old fluid component in Kaapvaal Craton". *Chemical Geology, 283(3-4),* 287-296. doi: 10.1016/j.chemgeo.2011.01.028

Lobmeyer, D.H. 1985. *Freshwater Heads and Ground-Water Temperatures in Aquifers of the Northern Great Plains in Parts of Montana, North Dakota, South Dakota, and Wyoming.* Professional Paper 1402-D. United States Geological Survey, Washington, D.C.

Lowry, W., S. Dunn, and K. Coates 2015. *High performance ceramic plugs for borehole sealing*. In Proceedings of the 15th International High-Level Radioactive Waste Management Conference, April 12-16, Charleston, SC.

Mariner, P.E., E.R. Stein, J.M. Frederick, S.D. Sevougian, G.E. Hammond, and D.G. Fascitelli 2016. *Advances in Geologic Disposal System Modeling and Application to Crystalline Rock.* SAND2016-9610R, FCRD-UFD-2016-000440. Sandia National Laboratories, Albuquerque, NM.

Mast, M.A. and J.I. Drever 1987. "The effect of oxalate on the dissolution rates of oligoclase and tremolite". *Geochimica et Cosmochimica Acta*, *51*, pp. 2559-2568.

NAS (National Academy of Sciences) 1957. *The Disposal of Radioactive Waste on Land*. http://www.nap.edu/openbook.php?record_id=10294

NEA (Nuclear Energy Agency) 1999. *Confidence in the Long-term Safety of Deep Geological Repositories: Its Development and Communication*. Organisation for Economic Co-operation and Development, Nuclear Energy Agency, Paris, France.

NEA (Nuclear Energy Agency) 2002. *Establishing and Communicating Confidence in the Safety of Deep Geologic Disposal: Approaches and Arguments*. Organisation for Economic Co-operation and Development, Nuclear Energy Agency, Paris, France.

NEA (Nuclear Energy Agency) 2004. *Post-Closure Safety Case for Geological Repositories, Nature and Purpose.* NEA Report No. 3679. Organisation for Economic Co-operation and Development, Nuclear Energy Agency, Paris, France.

NEA (Nuclear Energy Agency) 2008. *Safety Cases for Deep Geological Disposal of Radioactive Waste: Where Do We Stand? Symposium Proceedings Paris, France, 23-25 January 2007*, NEA Report No. 6319. Organisation for Economic Co-operation and Development, Nuclear Energy Agency, Paris, France.

NEA (Nuclear Energy Agency) 2009. *International Experiences in Safety Case for Geological Repositories (INTESC)*, NEA Report No. 6251. Organisation for Economic Co-operation and Development, Nuclear Energy Agency, Paris, France.

NEA (Nuclear Energy Agency) 2012. *Methods for Safety Assessment of Geological Disposal Facilities for Radioactive Waste: Outcomes of the NEA MeSA Initiative.* NEA No. 6923. Organisation for Economic Co-operation and Development, Nuclear Energy Agency, Paris, France.

NEA (Nuclear Energy Agency) 2013. *The Nature and Purpose of the Post-Closure Safety Cases for Geological Repositories*, NEA/RWM/R(2013)1, Organisation for Economic Co-operation and Development, Nuclear Energy Agency, Paris, France.

NEDRA (Scientific Industrial Company on Superdeep Drilling and Comprehensive Investigation of the Earth's Interior) 1992. *Characterization of Crystalline Rocks in Deep Boreholes. The Kola, Krivoy Rog and Tyrnauz Boreholes*. 92-39. Svensk Kärnbränslehantering AB (SKB), Stockholm, Sweden.

Nordqvist, R., E. Gustafsson, P. Andersson, and P. Thur 2008. *Groundwater flow and hydraulic gradients in fractures and fracture zones at Forsmark and Oskarshamn*. SKB R-08-103, Svensk Kärnbränslehantering AB, Stockholm, Sweden.

Nordstrom, D.K. and T. Olsson 1987. "Fluid inclusions as a source of dissolved salts in deep granitic groundwaters". *Saline Water and Gases in Crystalline Rocks. Geological Association of Canada Special Paper*, *33*, pp. 111-119.

Nordstrom, D.K., J.W. Ball, R.J. Donahoe, and D. Whittemore 1989. "Groundwater chemistry and water-rock interactions at Stripa". *Geochimica et Cosmochimica Acta*, *53*, pp. 1727-1740.

NRC (U.S. Nuclear Regulatory Commission) 2004. *Update of the Risk-Informed Regulation Implementation Plan*. SECY-04-0068. April 23, 2004.

NRC (U.S. Nuclear Regulatory Commission) 2015. *Safety Evaluation Report Related to Disposal of High-Level Radioactive Wastes in a Geologic Repository at Yucca Mountain, Nevada, Volume 2: Repository Safety Before Permanent Closure.* NUREG-1949 Volume 2. Office of Nuclear Material Safety and Safeguards, U.S. Nuclear Regulatory Commission, Washington, DC.

NWPA (Nuclear Waste Policy Act) 1983. *Public Law 97-425; 96 Stat. 2201, as amended by Public Law 100-203, Title I. December 22, 1987*.

NWTRB (U.S. Nuclear Waste Technical Review Board) 2016. *Technical Evaluation of the U.S. Department of Energy Deep Borehole Disposal Research and Development Program.* Report to the U.S. Congress and the Secretary of Energy. U.S. Nuclear Waste Technical Review Board, January 2016.

Oxburgh, R., J.I. Drever, and Y.T. Sun 1994. "Mechanism of plagioclase dissolution in acid solution at 25 C". *Geochimica et Cosmochimica Acta*, *58*, pp. 661-669.

Park, Y.J., E.A. Sudicky, and J.F. Sykes 2009. “Effects of shield brine on the safe disposal of waste in deep geologic environments”. *Advances in Water Resources, 32*(8), 1352-1358. doi: 10.1016/j.advwatres.2009.06.003

Parkhurst, D.L. and C.A.J. Appelo 1999. *User's guide to PHREEQC (Version 2): A computer program for speciation, batch-reaction, one-dimensional transport, and inverse geochemical calculations*. Water-Resources Investigations Report 99-4259. United States Geological Survey.

Pearson Jr., F.J. 1987. “Models of mineral controls on the composition of saline groundwaters of the Canadian Shield”. *Saline Water and Gases in Crystalline Rocks. Geological Association of Canada Special Paper*, *33*, pp. 39-51.

Peretz, F. and E. Hardin 2017. *Hazard Analysis for Radiological Risk from Deep Borehole Disposal Operations.* SFWD-SFWST-2017-000109, ORNL/SR-2017/252. Oak Ridge National Laboratory, Oak Ridge, TN.

Phillips, S.L., A. Igbene, J.A. Fair, H. Ozbek and M. Tavana 1981. *A Technical Databook for Geothermal Energy Utilization*. LBL-12810. Lawrence Berkeley Laboratory, Berkeley, CA.

Pusch, R., G. Ramqvist, J. Kasbohm, S. Knutsson, and M.H. Mohammed 2012. The concept of highly radioactive waste (HLW) in very deep boreholes in a new perspective. *Journal of Earth Sciences and Geotechnical Engineering, 2(3)*, pp. 1-24.

Sassani, D.C. 1992. “Petrologic and Thermodynamic Investigation of the Aqueous Transport of Platinum-Group Elements During Alteration of Mafic Instrusive Rocks”. Ph.D. Thesis, Washington University, St. Louis, MO.

Sassani, D.C. and J.D. Pasteris 1988. “Preliminary investigation of alteration in a basal section of the southern Duluth Complex, Minnesota, and the effects on sulfide and oxide mineralization”. *North American Conference on Tectonic Control of Ore Deposits and Vertical and Horizontal Extent of Ore Systems,* pp. 280-291.

Smith, J.T. and S.N. Ehrenberg 1989. "Correlation of carbon dioxide abundance with temperature in clastic hydrocarbon reservoirs: relationship to inorganic chemical equilibrium." *Marine and Petroleum Geology 6*, No. 2, pp. 129-135.

Smith, C., J. Knudsen, T. Wood and K. Kvarfordt 2012. *SAPHIRE 8. Computer Software. Version 1.0*. Idaho National Laboratory and the U.S. Nuclear Regulatory Commission.

SNL (Sandia National Laboratories) 2014a. *Project Plan: Deep Borehole Field Test.* FCRD-UFD-2014-000592, Rev. 0, SAND2014-18559R. Sandia National Laboratories, Albuquerque, NM.

SNL (Sandia National Laboratories) 2014b. *Evaluation of Options for Permanent Geologic Disposal of Used Nuclear Fuel and High-Level Radioactive Waste Inventory in Support of a Comprehensive National Nuclear Fuel Cycle Strategy.* FCRD-UFD-2013-000371, Rev. 1, SAND2014-0187P/SAND2014-0189P. Sandia National Laboratories, Albuquerque, NM.

SNL (Sandia National Laboratories) 2016a. *Deep Borehole Field Test Conceptual Design Report.* FCRD-UFD-2016-000070, Rev. 1, SAND2016-10246R. Sandia National Laboratories, Albuquerque, NM.

SNL (Sandia National Laboratories) 2016b. *Deep Borehole Field Test Laboratory and Borehole Testing Strategy.* FCRD-UFD-2016-000072, SAND2016-9235R. Sandia National Laboratories, Albuquerque, NM.

Travis, K.P, F.G.F. Gibb, and D. Burley 2017. *Determining salinity recharge time for deep borehole disposal*. In Proceedings of Waste Management 2017 Conference. March 5-9. Phoenix Arizona.

Travis, K.P. and F.G.F. Gibb 2015. *Deep geological boreholes: a suitable disposal route for the Hanford Cs/Sr capsules*. In Proceedings of the 15th International High-Level Radioactive Waste Management Conference, April 12-16, Charleston, SC.

Vovk, I.F. 1987. "Radiolytic salt enrichment and brines in the crystalline basement of the East European Platform". *Saline Water and Gases in Crystalline Rocks. Geological Association of Canada Special Paper*, *33*, pp. 197-210.

Wang, Y., E. Matteo, J. Rutqvist, J. Davis, L. Zheng, J. Houseworth, J. Birkholzer, T. Dittrich, C.W. Gable, S. Karra, N. Makedonska, S. Chu, D. Harp, S.L. Painter, P. Reimus, F.V. Perry, P. Zhao, J.B. Begg, M. Zavarin, S.J. Tumey, Z.R. Dai, A.B. Kersting, J. Jerden, K.E. Frey, J.M. Copple, and W. Ebert 2014. *Used Fuel Disposal in Crystalline Rocks: Status and FY14 Progress*. FCRD-UFD-2014-000060, SAND2014-17992R. Sandia National Laboratories, Albuquerque, NM.

Woodward-Clyde Consultants 1983. *Very Deep Hole Systems Engineering Studies*. Office of Nuclear Waste Isolation (ONWI), Columbus, OH.

DISTRIBUTION

1	MS0736	Evaristo Bonano	8840
1	MS0736	Peter Swift	8840
1	MS0736	Patrick Brady	8840
1	MS0747	David Sassani	8842
1	MS0779	Carlos Lopez	8842
1	MS0747	Geoff Freeze	8843
1	MS0747	Ernest Hardin	8844
1	MS0747	Kris Kuhlman	8844
1	MS0747	Robert MacKinnon	8844
1	MS0747	Emily Stein	8844
1	MS0899	Technical Library	9536 (electronic copy)


Sandia National Laboratories